Fracture and permeability characteristics of thermally degraded concrete.

Louay Abdel-Razek Aboul-Nour

Civil Engineering

1988

Abstract

This study has been motivated by the premature and accelerated corrosion of bridge decks in the Eastern Province region of Saudi Arabia, where chloride profiles have indicated severe gradients of chloride ions. What has been perplexing is the rapid breakdown of the concrete structure, leading to very high levels of chloride ingress. One of the main causes leading to this rapid breakdown of concrete resistance to chloride ingress is due to the Thermal Incompatibility of Concrete Constituents (TICC) phenomenon. In this effect, diurnal and seasonal temperature changes lead to internal stresses and subsequent microcraking in the concrete expansion of aggregate and paste.

The influence of TICC on concrete deterioration was obtained by studying variation in fracture toughness, permeability, and flexural strength of thermally cycled specimens. Also flexural strength tests and coefficients of thermal expansion of Riyadh aggregate and its concrete were determined. The cycling itself consisted of heating specimens to 80 C for six hours, followed by cooling to room temperature for another six hours. Several variables were considered, including influence of aggregate type, mix design, specimen prestress, alternate wetting and drying, and admixtures such as latex and superplasticezers. In addition, permeability characteristics of naturally cycled concrete were also studied.

Results show that although strength is insensitive to TICC cracking at first, there is an immediate loss of resistance to permeability and fracture toughness, indicating the greater relevance of the latter parameters of TICC characterization of concrete rather than strength. Other interesting results include severe detrimental effect of TICC on initially stressed specimens and the beneficial influence of admixtures in reducing the adverse TICC effect.

Fracture and Permeability Characteristics Of Thermally Degraded Concrete

by

Louay Abdel-Razek Aboul-Nour

A Thesis Presented to the

FACULTY OF THE COLLEGE OF GRADUATE STUDIES

KING FAHD UNIVERSITY OF PETROLEUM & MINERALS

DHAHRAN, SAUDI ARABIA

In Partial Fulfillment of the
Requirements for the Degree of

MASTER OF SCIENCE

In

CIVIL ENGINEERING

June, 1988

Order Number 1355698

Fracture and permeability characteristics of thermally degraded concrete

Aboul-Nour, Louay Abdel-Razek, M.S.

King Fahd University of Petroleum and Minerals (Saudi Arabia), 1988

U·M·I
300 N. Zeeb Rd.
Ann Arbor, MI 48106

FRACTURE AND PERMEABILITY CHARACTERISTICS OF THERMALLY DEGRADED CONCRETE

BY

LOUAY ABDEL-RAZEK ABOUL-NOUR

A Thesis Presented to the

FACULTY OF THE COLLEGE OF GRADUATE STUDIES

KING FAHD UNIVERSITY OF PETROLEUM & MINERALS

DHAHRAN, SAUDI ARABIA

In Partial Fulfillment of the
Requirements for the Degree of

MASTER OF SCIENCE

In

CIVIL ENGINEERING

JUNE 1988

KING FAHD UNIVERSITY OF PETROLEUM AND MINERALS

DHAHRAN, SAUDI ARABIA

This thesis, written by Mr. LOUAY ABDEL-RAZEK ABOUL-NOUR under the direction of his Thesis Committee, and approved by its chairman and members, has been presented to and accepted by the Dean of the College of Graduate Studies, in partial fulfillment of the requirements for the degree of MASTER of SCIENCE in CIVIL ENGINEERING

Abdullah Al-Zahi

Dean, College of Graduate Studies

M. J. Abdulaimani

for Civil Eng. Department Chairman

THESIS COMMITTEE

Dr. M.H. Baluch, Chairman

Dr. A.K. Azad, Co-Chairman

Dr. M. Al-Mandil, Member

بسم الله الرحمن الرحيم

وقل رب زدني علما

Dedicated to my

BELOVED PARENTS,

AYMAN and HANAN

ACKNOWLEDGEMENT

May all praise and thanks (first and last) be to ALLAH, the Almighty, with whose gracious help it was possible to accomplish this work.

I greatly owe my success (in more than words can express) to my beloved parents, brother, and sister for their patience, encouragement, and continuous prayers.

Acknowledgement is due to the Civil Engineering Department of King Fahd University of Petroleum and Minerals (KFUPM) for its facilities and support provided for the completion of this research. Also, I would like to extend my appreciations to King Abdul Aziz City of Science and Technology (KACST), in particular the "National Bridge Deck Cracking Project" for its financial support.

I am deeply indebted to, and gratefully thank Dr. M.H. Baluch, thesis committee chairman, for his frequent attention, advice, and guidance. Truely it was a great pleasurable experience to have been associated with him on this research.

My thanks and appreciations extend to both Dr. A.K. Azad, thesis committee co-chairman, and Dr. M.Y. Al-Mandil, thesis committee member, for their valuable assistance, comments, and suggestions during this study.

I wish to thank the Civil Engineering Department faculty, staff, and laboratory technicians whom have provided moral aid and academic assistance.

I am grateful to staff members of, the Mechanical Work Shop of the Mechanical Engineering Department, the Central Library for their supply of needed information, the Data Processing Center (DPC) and the Computer Graphics Center (CGC) for their allowance in using their well developed computer facilities.

Last, but for sure not least, I am sincerely grateful to all my collegues and friends whom have surrounded me with an Islamic atmosphere during my pleasent stay in Dhahran, Saudi Arabia.

TABLE OF CONTENTS

4. EXPERIMENTAL METHODOLOGY

LIST OF TABLES

LIST OF FIGURES

LIST OF PLATES

THESIS ABSTRACT

Name of Student : ABOUL NOUR, LOUAY ABDEL RAZEK
Title of Study : FRACTURE AND PERMEABILITY CHARACTERISTICS OF THERMALLY DEGRADED CONCRETE
Major Field : Civil Engineering (STRUCTURES)
Date of Degree : June 1988

This study has been motivated by the premature and accelerated corrosion of bridge decks in the Eastern Province region of Saudi Arabia, where chloride profiles have indicated severe gradients of chloride ions. What has been perplexing is the rapid breakdown of the concrete structure, leading to very high levels of chloride ingress. One of the main causes leading to this rapid breakdown of concrete resistance to chloride ingress is due to the Thermal Incompatibility of Concrete Constituents (TICC) phenomenon. In this effect, diurnal and seasonal temperature changes lead to internal stresses and subsequent microcracking in the concrete as a consequence of incompatible coefficients of thermal expansion of aggregate and paste.

The influence of TICC on concrete deterioration was obtained by studying variation in fracture toughness, permeability, and flexural strength of thermally cycled specimens. Also flexural strength tests and coefficients of thermal expansion of Riyadh aggregate and its concrete were determined. The cycling itself consisted of heating specimens to 80 C for six hours, followed by cooling to room temperature for another six hours. Several variables were considered, including influence of aggregate type, mix design, specimen prestress, alternate wetting and drying, and admixtures such as latex and superplasticizers. In addition, permeability characteristics of naturally cycled concrete were also studied.

Results show that although strength is insensitive to TICC cracking at first, there is an immediate loss of resistance to permeability and fracture toughness, indicating the greater relevance of the latter parameters for TICC characterization of concrete rather than strength. Other interesting results include severe detrimental effect of TICC on initially stressed specimens and the benificial influence of admixtures in reducing the adverse TICC effect.

MASTER OF SCIENCE DEGREE

KING FAHD UNIVERSITY OF PETROLEUM AND MINERALS
Dhahran, Saudi Arabia

June 1988

خلاصـــة الرسالة

اســـــم الطالـــب : لـــؤي عبد الرازق أبو النـــــور

عنوان الدراســـــة : خصائص الكسر والنفاذية للخرسانة المتدهورة حراريا

التخصـــــــــص : هندســـــة مدنيـــــة (منشـــآت)

تاريـــخ الشـــهادة : يونيـــــو ١٩٨٨م

تولدت هذه الدراسة عند ظهور تآكل سريع في أسقف أغلب كباري المنطقـــــة الشرقية بالمملكة العربية السعودية ، حيث أن نسب أيون الكلوريد الدخيلـــة تشير الى تكسر سريع للمنشأ الخرساني . أحد أهم الأسباب المؤدية الى ذلـــك الانهيار السريع لمقاومة الخرسانة ضد أملاح الكلوريد الدخيلة تكمن في ظاهـرة عدم تواؤم الخصائص الحرارية للمكونات المختلفة للخرسانـــــــة . ويرى أن الاختلافات الحرارية اليومية والموسمية تؤدي الى تزايد اجهادات الشـــــد الداخلية ومن ثم تتولد شقوق مجهرية دقيقة تزداد في النمو نتيجة اختـــلاف في الخصائص الحرارية لكل من الركام والمونة المتصلبة .

تم دراسة تأثير اختلاف الخصائص الحرارية لمكونات الخرسانة على تلـــف وتدهور حالة الخرسانة السليمة عن طريق مقارنة نتائج اختبارات صلابة المـادة لمقاومة الكسر والنفاذية وقوة الثني لعينات خرسانية خضعت لتغيرات دوريـــة حرارية بواسطة الأفران المعملية ، وهي عبارة عن تسخين العينات لمـــدة ست ساعات حتى ٨٠ درجة مئوية ، ثم تبريدها حتى ٢٧ درجة مئوية لمدة ست ساعـــات أخرى . وقد أخذ في الاعتبار متغيرات متعددة منها : تأثير نوع الركـــام ، تصميم الخلطة ، عينات سابقة الاجهاد ، الغمر والتجفيف الدوري للعينـــات ، اضافة مزيج كيميائي للخلطة مثل (اللثي و الملدنات الممتازة) . اضافة الـى ذلك فقد تم دراسة خصائص النفاذية لخرسانة خضعت لتغيرات دورية حراريـــــة طبيعية .

وقد أشارت النتائج الى فقدان فوري لكل من مقاومة النفاذية ، ومقاومـــة الصلابة ضد الكسر ، بالرغم من قلة حساسية اختبارات القوة على الخرسانـــــة المتدهورة نتيجة عدم تواؤم الخواص الحرارية لمكوناتها . وتظهر النتائـــج انعدام حساسية اختبارات القوة الى ظاهرة التكسر الناتـــــج عن عدم تواؤم الخصائص الحرارية لمكونات الخرسانة ، الا أنه يوجد فقدان فوري في المقاومـة النفاذية والصلابة ضد الكسر . وذلك يعني أن كلا من اختباري النفاذية والصلابة ضد الكسر يوضحان تأييدا لظاهرة عدم تواؤم الخصائص الحرارية لمكونـــــات الخرسانة أكثر مما توضحه اختبارت القوة . وهناك نتائج أخرى هامة تتضمـــن التأثير الضار جدا لظاهرة التكسر الناتج عن عدم تواؤم الخصائص الحراريـــة لمكونات الخرسانة على العينات السابقة الاجهاد ، بالاضافة الى التأثير الطيب الناتج عن اضافة المزيج الكيميائي للخلطة في تقليل ذلك التأثير الضار لتلك الظاهرة .

درجة الماجستير في العلوم

جامعـة الملك فهد للبترول والمعـادن
الظهران ـ المملكة العربية السعودية

يونيـــو ١٩٨٨م

INTRODUCTION

1.1 General

Recently the issue of concrete durability in the Middle-East has rapidly popularized due to the fact that numerous structures of various types have witnessed positive signs of failure before reaching their expected service life (maintenance-free life). The deterioration mechanism of such structures is very complicated and complex in nature. Various unfavourable conditions occur simultaneously and act together to highly accelerate the deterioration process. Such unfavourable conditions may be divided into three different categories according to their source {1-3}.

1. Low quality workmanship practices :

The vast majority of decayed structures were completed twenty to forty years ago. At that time concrete practices were new in the Arabian peninsula and just starting. Accordingly novice unexperienced workmanship produced poor quality concretes. Mainly careless mixing, placing, and vibration of concrete was the cause. This unfavourable condition as of now is playing a significantly reduced role. Gain in workmanship experience through new concrete technology provided day after day has rendered this effect to a minimum.

2. Poor local concrete materials :

Local concrete materials available in the Middle-East are of extremely poor quality. Generally strength, thermal, elastic and surface properties of local aggregates along with durability resistance are below standards.

Coarse aggregates are basically limestone in origin and geologically young in nature, and hence characterised by having low strength, high permeability and high impurity content of deleterious substances. Fine aggregates in the form of dune sands are uniformly graded and also show high impurity content of deleterious matter. The mixing water itself contains an increased amount of salt concentration which is harmful to concrete.

3. Severe environmental and climatic conditions

The surrounding environment generally affects the substructures, whereas superstructures are mostly affected by climate. The Middle-East's environment is of maximum severity for high chloride and there is also high sulphate salt concentration within foundation soils. Salty water table level becomes another factor near coastal regions. The climate of the area is extremely dry and arid in character. Large daily and seasonal temperature variations occur frequently. Humidity in coastal vicinities elevates to saturation levels quite often in summer.

The later conditions combine to form a so called thermal degradation of concrete which is considered to be the main driving force of the damaging process within the structure. Recorded observations revealed most deteriorated structures to be those under severe exposure to direct sun-light such as bridge decks, airport runways, roadway pavements, etc.

The climate in the peninsula is so severe that ambient temperature changes of 20-25 degree Celsius and seasonal changes of 40-50 degree Celsius are normally exhibited. However for concrete exposed to direct sun-light, daily temperature changes may elevate up to 50 degree Celsius and seasonal changes up to 70 degree Celsius.

As mentioned previously, the geological configuration of local aggregate rocks is limestone predominant, calcareous in nature containing a considerable amount of calcite. Calcite has a very low coefficient of thermal expansion (CTE) as compared to that of hardened cement paste present in the concrete matrix. Coefficient of thermal expansion of limestone aggregates range from $0.9x10^{-6}$ to $12.2x10^{-6}$ per degree Celsius while that of hardened cement paste is much higher, ranging from $11.0x10^{-6}$ to $20.0x10^{-6}$ per degree Celsius {4-6}. Often, the CTE of hardened cement paste is 10 to 20 times that of some limestone aggregates.

Large differences in coefficient of thermal expansion along with high temperature variations cause high internal stresses to build up at the aggregate-cement interface. In most cases it is enough to break the adhesion bond between aggregate and hardened paste. In addition, cracks are also initiated in the hardened mortar within the matrix.

On thermal cycling, micro cracking spreads throughout the material, decreasing its overall soundness. The material exhibits decrease in strength and increase in permeability, thereby increasing the risk and vulnerability to faster rates of degradation. Chloride and sulphate ingress increases, leading to corrosion and rusting of steel that expands in volume and subsequently leads to debonding of concrete reinforcement. Bigger and wider cracks are produced and finally reach the external concrete surface.

Due to such collective unfavourable conditions, there has been a great need to define new strict concrete code practices that accomodate for the regional situation rather than utilising foreign codes that were not designed with the needs of the local region in mind. Special provisions should be followed and kept in mind during material selection, concrete mixing, placing, vibrating, and curing, taking into consideration the importance and function of the structure and its location with regard to the surrounding environment and the prevailing climatic conditions.

1.2 Literature Review

The concept of thermal incompatibility of concrete components (TICC) has been looked into over the past twenty years by many researchers {7-10}. Most researchers believe that TICC is the major initiating cause of rapid deterioration {11-16}. TICC led researchers to investigate the problem from various points of view. Some concentrated their efforts in determination of CTE of different minerals, aggregates, hardened cement mortars, and concretes {17-24}. Others tried to simulate the problem by casting concrete using various types of aggregates, cycling the concrete thermally and then subjecting it to strength and durability tests {25-29}.

The concrete durability problem in the Middle-East triggered researchers to direct their interests and efforts towards determination of the various reasons behind the rapid structural deterioration in the area. Extensive information was collected about the peninsulas' environment and climate {30-34}. Protective measures were suggested such as using sweet water in concrete mixing, high sulphate resistant cement (type V) for concretes in contact with foundation soil, coating reinforcment bars to prevent corrosion, air entraining the concrete and adherence to special hot weather concrete regulations {35-36}. The use of admixtures such as superplasticisers and latex helps in

decreasing the water cement ratio, hence increasing the strength and enhancing the workability. Such corrective provisions presented only a marginal improvement. The overall problem is of a more involved nature and related to thermal incompatability of concrete components.

The failure mechanism described by Venecanin {37} indicates that both rise and drop in temperature of concrete add to the damage induced by TICC phenomenon. During heating of concrete, the hardened cement paste expands more than the aggregate, leading to tensile stresses at the aggregate surface exceeding the bond strength which in turn causes bond failure of the aggregate particle. During cooling, the hardened cement paste contracts more than the aggregate, leading to tensile stresses in the hardened paste and compressive stresses in the aggregate and causing mico crack initiation in the hardened paste (Plate 1.1).

Few researchers claim that factors such as hot climate, cement hydration, drying shrinkage, presence of salts, moisture movements, severe exposures and aggregate cement reaction are of greater signifigance than TICC {38-39}. They state that most of the Middle-East limestones are geologically young and coarsely crystaline with low elastic modulii thus they can resist higher stresses and bond failures are rare. Also most of the cracking is attributed to reinforcement rusting.

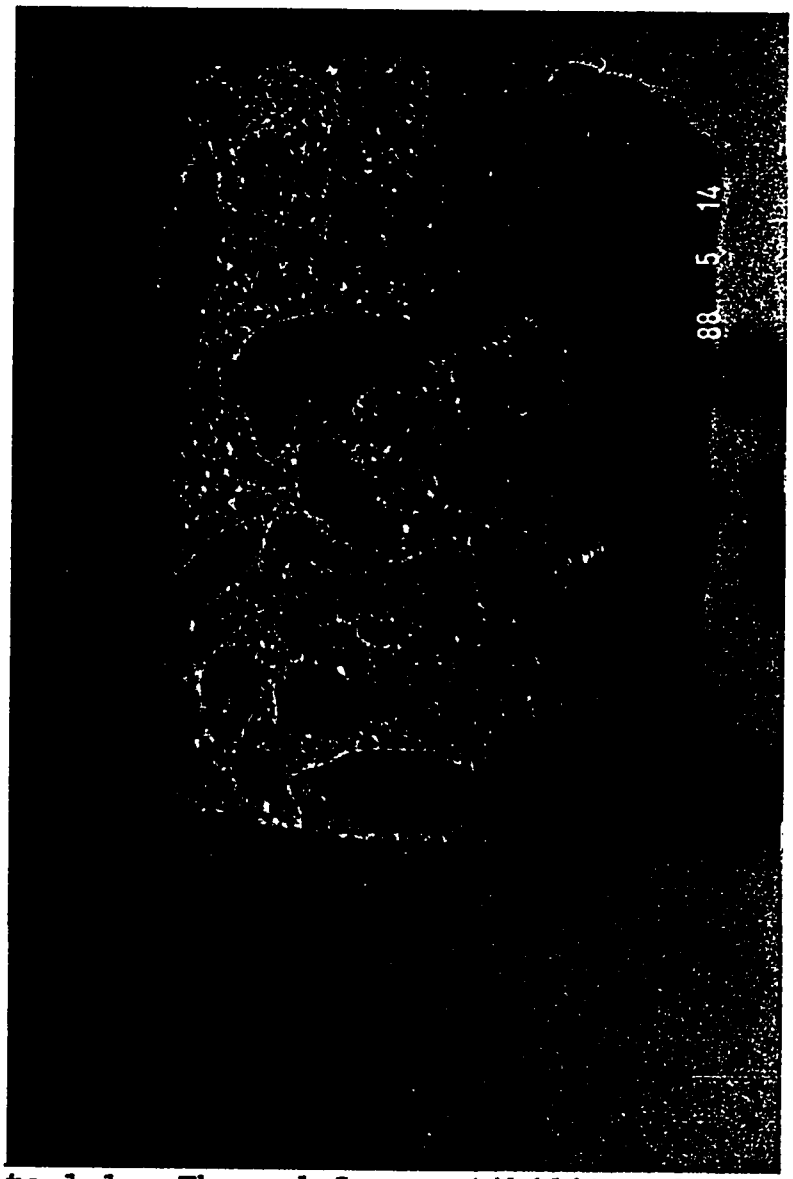

Plate 1.1 : Thermal Incompatibility of Concrete Components (TICC).

It is also believed that micro cracks have a tendency to be healed by calcium hydroxide. Definitely all these factors contribute one way or another and affect the durability of the material, but Venecanin {40-41} has presented a theoretical model to show that TICC is the main driving force of damage, especially when the degree of TICC is of a high order.

1.3 Scope and Scheme of Work

This thesis tends to evaluate various concretes exposed to simulated thermal cycling by measuring fracture parameters and permeability values. A total of eight different concrete groups were investigated taking into consideration the variables shown in the chart (Fig. 1.1). The only criterion used was to achieve good quality concrete that maintained a slump of three inches.

A reference concrete group was fabricated using Abu-Hadriyah aggregate, having a coarse/fine aggregate ratio of 1.5, no admixture, no support restraint and no wet/dry cycle. Local aggregates used in the mix were varied and two more groups were made using Riyadh and Jabal Dhahran aggregate. Another two groups were made using two types of admixtures, superplasticizer and latex. The coarse/fine aggregate mix proportion was decreased to 0.5 producing a sixth group.

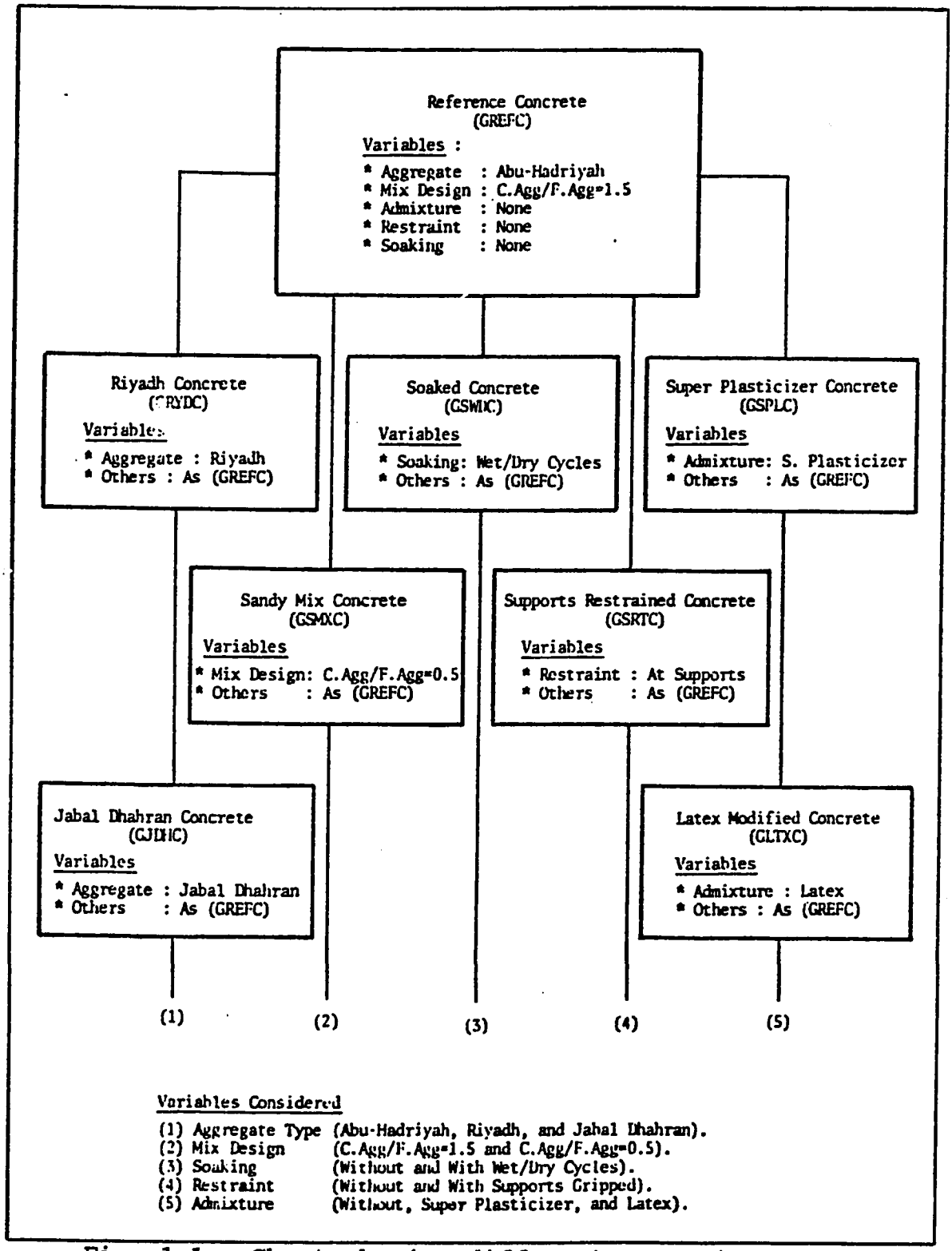

Fig. 1.1 : Chart showing different concrete groups and variables considered

Groups seven and eight were the same as the reference concrete but one was subjected to support restraint during thermal cycling while the other received a single wet/dry cycle within every thermal cycle.

The study consisted mainly of two phases. The first phase delt with the determination of fracture parameters such as the rate of energy release G_C {42-44}. It is well defined and known that fracture parameters such as critical stress intensity factor K_{IC} and critical rate of energy release G_{IC} are material properties. Fracture parameters are sensitive to pre-existing flaws and micro-cracks. Any change in the microstructure integrity or soundness may be detected through the variation of the rate of energy release G_C value. Fracture specimens were specially designed to be slender beams with a mid span notch immersed half way through the beam depth to assure an opening mode type I fracture failure. Cylinders were cast for compressive strength determination. All beam groups received thermal cycling and were tested for fracture toughness G_C. Some beams were tested after no cycling, while others received 45,90, and 120 cycles. Cycling was extended in three groups up to 180 cycles and in one case to 210 cycles. Modulii of rupture of all specimens were determined.

The second phase took into consideration the permeability values of the same concrete groups cast. Due to thermal cycling, micro cracking may spread through out the material. In early stages of thermal cycling, the material might not lose a considerable amount of strength but it may becomes vulnerable to other forms of degradation attack. With micro cracking leading to increased permeability, chloride and sulphate ingress would increase, speeding up the corrossion process. Subsequently, the bars undergo volumetric expansion due to the formation of ferrous and ferric oxides that accumulate on the bars surroundings. Consequently, the concrete matrix is over stressed and cracking occurs in the concrete at the bar surface, decreasing the bond strength of the reinforcement. These volume changes reach high levels where cracking reaches the concrete external surfaces, exposing the reinforcement to direct environmental attack.

Measuring permeability would also present a fairly good idea about the level of micro cracking occuring within the material. Cubes along with cylinders were cast for the previosly mentioned groups. Some cubes would be tested for permeability directly after they have achieved their full strength (ie. after 28 days of water tank lab curing). Other cube specimens would undergo thermal cycling and would be tested for permeability after 45,90, and 120 heat/cool cycles. All cylinders would be tested for compression.

Some cores would be drilled from reinforced concrete panels exposed to natural thermal cycling for a duration of two and a half years and tested for permeability and compared to referenced non cycled concrete for sake of comparison. Also, the coefficient of thermal expansion CTE of local aggregates such as Riyadh, Abu-Hadriyah, and Jabal Dahran would be determined if not readily available in literature {45}.

1.4 Objectives

1. Examine the fracture characteristics of various thermally degraded concretes.
2. Investigate the change of permeability in the same group of thermally degraded concretes as in item 1, together with concrete exposed to natural cycling.
3. Determine the coefficient of thermal expansion of some local aggregates such as Abu-Hadriyah, Jabal Dhahran, and Riyadh aggregate (if not available in literature {45}).
4. Interpret findings in view of certain known case studies involving bridge decks in the Eastern Province region, and develop some recommendations for local concreting practices to suit the regions' prevailing environmental and climatic conditions.

BASIC THEORY FOR FRACTURE MEASUREMENTS

2.1 General

Fracture mechanics has evolved recently over the past sixty years. As a discipline, it is still new and fields of research are very wide. The concept of fracture mechanics has been developed lately, although numerous recorded fracture failures have occured more than a century ago {46}.

2.1.1 Historical Background

In the Middle-Ages after metal working improvement, the application of metals in structures multiplied profoundly. Unexpected failures were exhibited and structures in some cases were found performing unsatisfactorily under normal prevailing conditions designed for.

In the nineteenth century, metals were widely used in the fabrication of railway transporting means. At that time lots of railway accidents resulted in high levels of casualties. Most of the accidents were a result of derailing caused by fracture of wheels, axles, or rails. Rarely were these accidents due to poor design, but gradually it was realised that material deficiencies as pre-existing flaws could initiate cracks and fractures that lead to failure.

The objective then was to produce better materials by reducing pre-existing flaws through implementing better

production methods, accordingly enhancing the metals' structural performance. This would consequently lower the risk of failure to more acceptable levels than before.

Another series of accidents occured after the introduction of weld designs. Fracture failures struck many ships, bridges, and other structures {47}. It was noticed that the failures often occured under conditions of low service stress which seemed to be unexplainable. Extensive investigations revealed that flaws and stress concentrations were the cause. Fracture of steel elements was brittle, accompanied by little plastic deformation.

2.1.2 Fracture Mechanics Evolution

After the second World War high strength materials invaded the markets and were widely used for weight savings. Also stress analysis methods were developed to determine local stresses. Accordingly design safety factors were reduced, resulting in further weight saving but increasing the vulnerability to fracture failures. Structures designed in high strength materials have low margin of safety. Service stresses along with an aggressive environment may sometimes be high enough to induce cracks particularly if pre-existing flaws and high stress concentrations are present.

High strength materials have low crack resistance (fracture toughness) and the residual strength in presence of cracks is low. When small cracks exist, high strength material structures may fail at stresses below the service stresses designed for.

The occurence of low stress fracture in such materials induced the development of Fracture Mechanics. Conventional design criteria are based on strength, stability, and durability but do not take into consideration the presence of cracks. Therefore for some cases the conventional design methods are inadequate, insufficient, and do not serve their cause. After two decades of development Fracture Mechanics has become a very beneficiary tool for high strength material design.

2.2 Fracture Within Structures

The concept of fracture in structures is a very serious problem which conventional design criteria has failed to solve. In the fracture mechanics philosophy structures are considered safe if stress intensities at pre-existing material defficiencies are well below critical fracture levels when subjected to extreme service loads. Only by satisfying the above condition, conventional design methods become sound to implement and apply. Once this condition is violated, the cracks begin to propagate and deterioration picks up inertia until failure is reached. The main aim is to assure low levels of internal stress intensities at material pre-existing flaws to prevent the initial trigger of deterioration.

2.2.1 Crack Propagation

Consider a structural element possessing a crack. Due to repetitive loading along with aggressive environmental attack, the crack will grow with time. The longer the crack the higher the induced stress intensity, therefore the rate of crack propagation increases with time and may be represented by the ascending curve shown (Fig. 2.1). The presence of the crack reduces the strength of the structure, and as long as the crack grows the residual strength simultaneously decreases (Fig. 2.2).

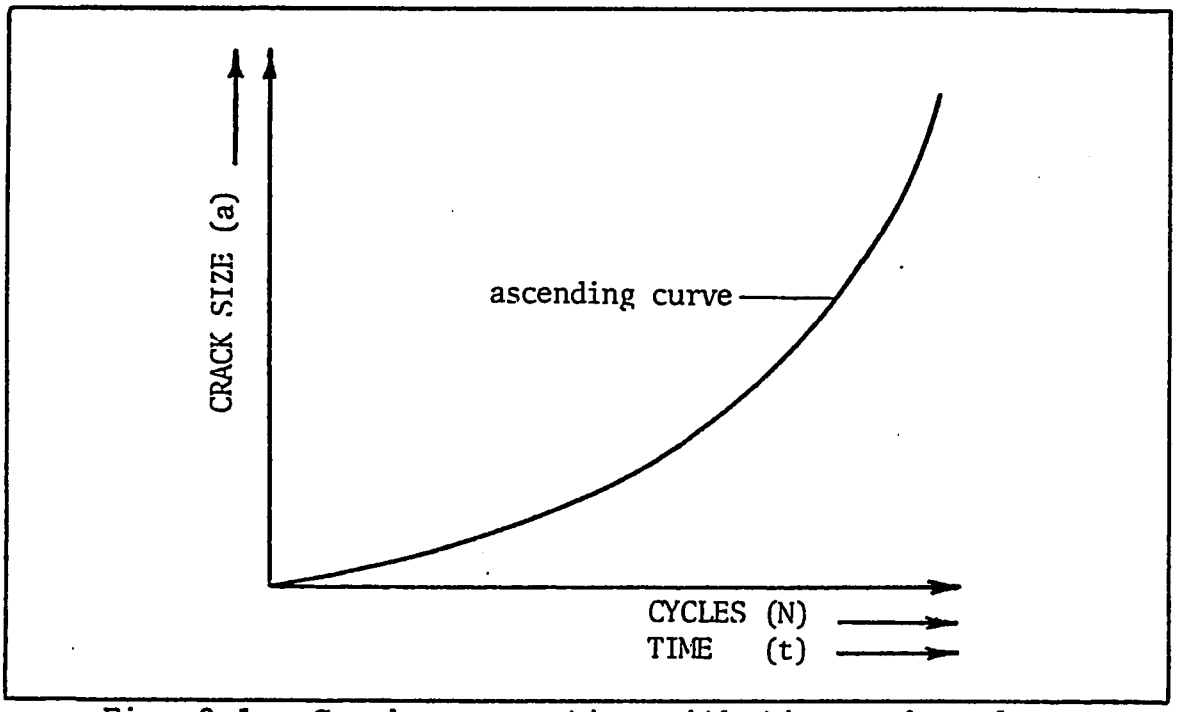

Fig. 2.1 : Crack propagation with time and cycles

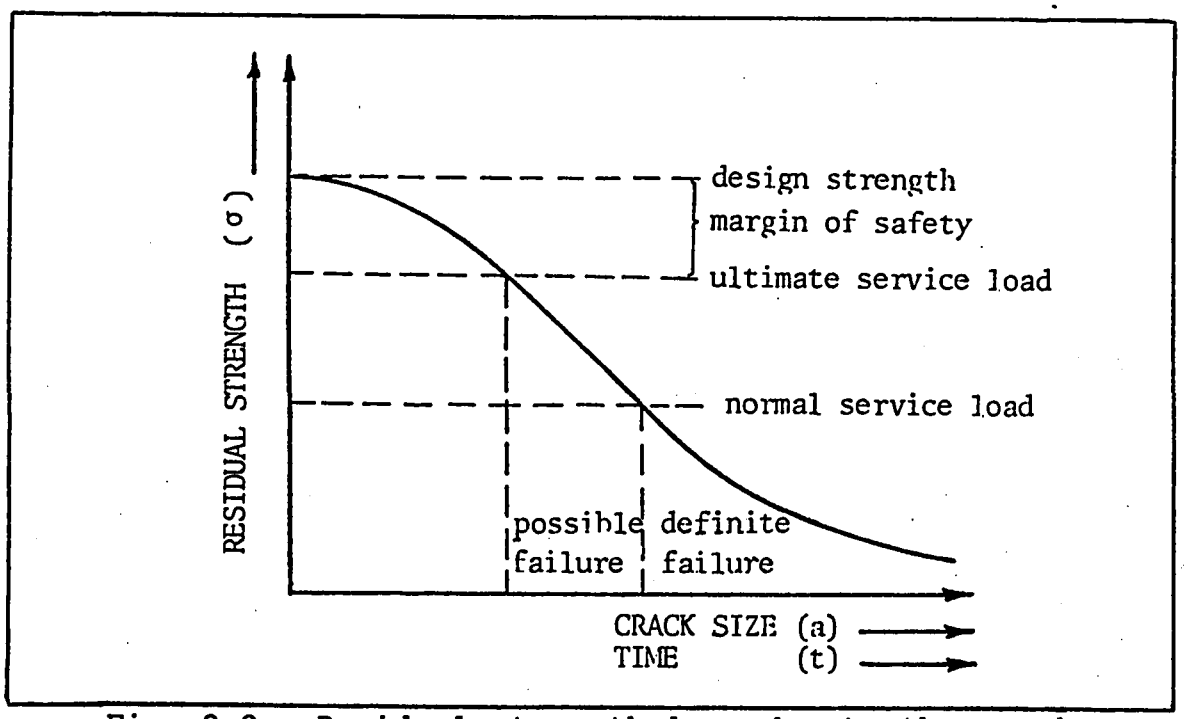

Fig. 2.2 : Residual strength loss due to the crack propagation

2.2.2 Deterioration and Failure Phenomenum

As the decreasing residual strength phenomenon caused by crack propagation proceeds, the margin of safety decreases and the structure becomes highly liable to sudden fracture failure. Actually the residual strength keeps decreasing until the maximum ultimate load the cracked structure can carry is reduced to the vicinity of the normal service loads. Then fracture failure directly occurs once the new ultimate strength is reached or exceeded (Fig. 2.2).

2.2.3 Importance of Fracture Mechanics

Many structures are designed to carry high service loads that are enough to initiate cracks, especially when pre-existing flaws and stress concentrations are present. Consequently designs should anticipate any cracking possibility. Designer engineers should maintain the probability of failure to low acceptable levels during the structures' whole service life.

For safety ensurance, prediction of how fast the crack grows and how quick the residual strength decreases are the objectives of Fracture Mechanics. Literally it is essential to define the residual strength as a function of crack size, the critical crack size to be tolerated under expected service loads, the time of crack growth from an initial size to the critical size, the permissible size of pre-existing

flaws, and how often should the structure be checked and inspected for cracks.

2.2.4 Modes of Fracture

Any crack in a solid can be stressed in three different modes (Fig. 2.3). Generally structures are stressed in all three modes but usually a single mode type is dominant.

Mode I (Opening Mode)

Normal stresses result in an opening mode where the displacement of the crack surfaces are perpendicular to the crack plane (Fig. 2.3a). The fracture portion of this study deals only with Mode Type I cracking.

Mode II (Sliding Mode)

In-plane shear produces a sliding mode where the displacement of the crack surfaces are in the crack plane and perpendicular to the crack leading edge (Fig. 2.3b).

Mode III (Tearing Mode)

Out-of-plane shear causes a sliding mode where the displacement of the crack surfaces are in the crack plane and parallel to the crack leading edge (Fig. 2.3c).

Fig. 2.3a

Mode I :
Opening mode

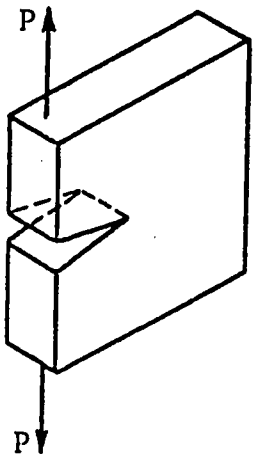

Fig. 2.3b

Mode II :
Sliding mode

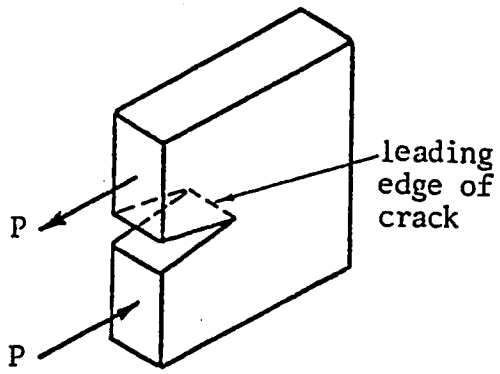

Fig. 2.3c

Mode III :
Tearing mode

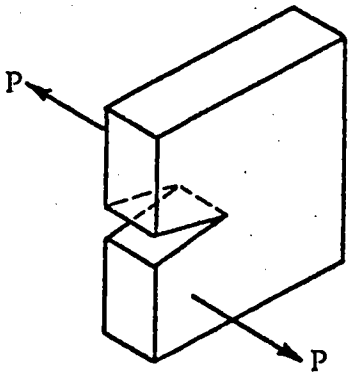

Fig. 2.3 : Modes of fracture

2.3 Linear Elastic Fracture Mechanics (LEFM) Criteria

Since high strength materials have a low fracture toughness, they may successfully be treated by Linear Elastic Fracture Mechanics (LEFM). The concept is based on the elastic stress field equations in the vicinity of the crack tip. Both the stress (K_C) and energy (G_C) criteria are developed by linear elastic fracture mechanics, where the size of the crack tip plastic zone is small compared to the crack size. Throughout the presented work, linear elastic fracture mechanics approach will be used and in particular the energy approach (Gurney Approach) {48}.

In cases where the crack tip plastic zone is of an appreciable size, corrections need to be made using either small scale yielding models e.g. Dugdale-Barenblatt {49} or general yielding models {50} of Elasto-Plastic Fracture Mechanics (EPFM). For low strength materials that have high fracture toughnesses, a large crack tip plastic zone compared to the crack size exists. Wells {51-52} developed a new criterion for such cases of low strength materials based on a crack opening displacement (COD) concept. Basically it states that crack propagates when a maximum permissible plastic strain at the crack tip is reached (which translates into a critical COD). This criterion was found to be equivalent to both the stress and energy

criteria in case when LEFM applies. Another very popular criterion for crack growth in EPFM is the J-integral approach {53}.

2.3.1 Stress Criterion (K_C)

This criterion deals mainly with the elastic stress distribution field determined in the vicinity of the crack tip. The stress criterion aims to calculate the critical stress intensity factor K_{IC} for mode I fracture which is a material parameter.

2.3.1.1 Stresses in Crack Vicinity

Consider an infinite plate subjected to a tensile stress with a crack of length $2a$ in an opening mode (Fig. 2.4). In the vicinity of the crack tip there exists an elastic stress field (Fig. 2.5). Stresses in the rectangular coordinate system in the vicinity of the crack tip are given by the following equations (1-4).

$$\sigma_x = \sigma\sqrt{\frac{a}{2r}}\cos\frac{\theta}{2}\{1-\sin\frac{\theta}{2}\sin\frac{3\theta}{2}\} \quad (1)$$

$$\sigma_y = \sigma\sqrt{\frac{a}{2r}}\cos\frac{\theta}{2}\{1+\sin\frac{\theta}{2}\sin\frac{3\theta}{2}\} \quad (2)$$

$$\tau_{xy} = \sigma\sqrt{\frac{a}{2r}}\sin\frac{\theta}{2}\cos\frac{\theta}{2}\cos\frac{3\theta}{2} \quad (3)$$

$$\sigma_z = 0 \quad \textit{(Condition of Plane Stress)}$$
$$\sigma_z = \nu(\sigma_x+\sigma_y) \quad \textit{(Condition of Plane Strain)} \quad (4)$$

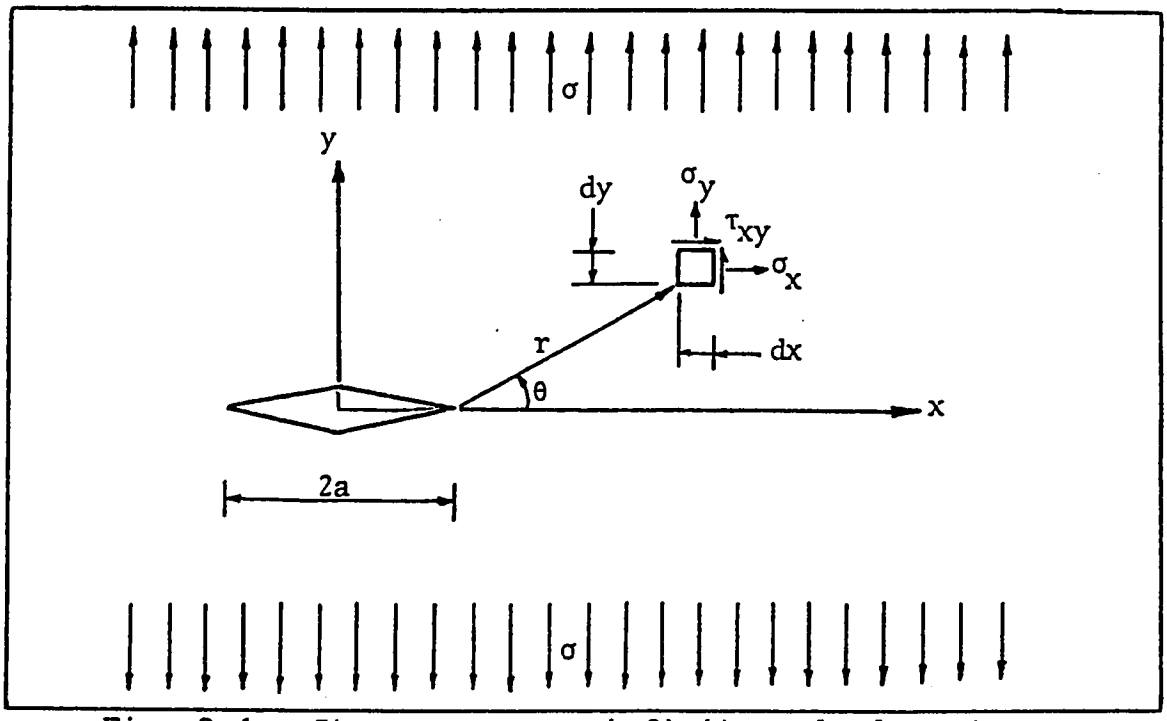

Fig. 2.4 : Stresses on an infinitesmal element (Rectangular Coordinates)

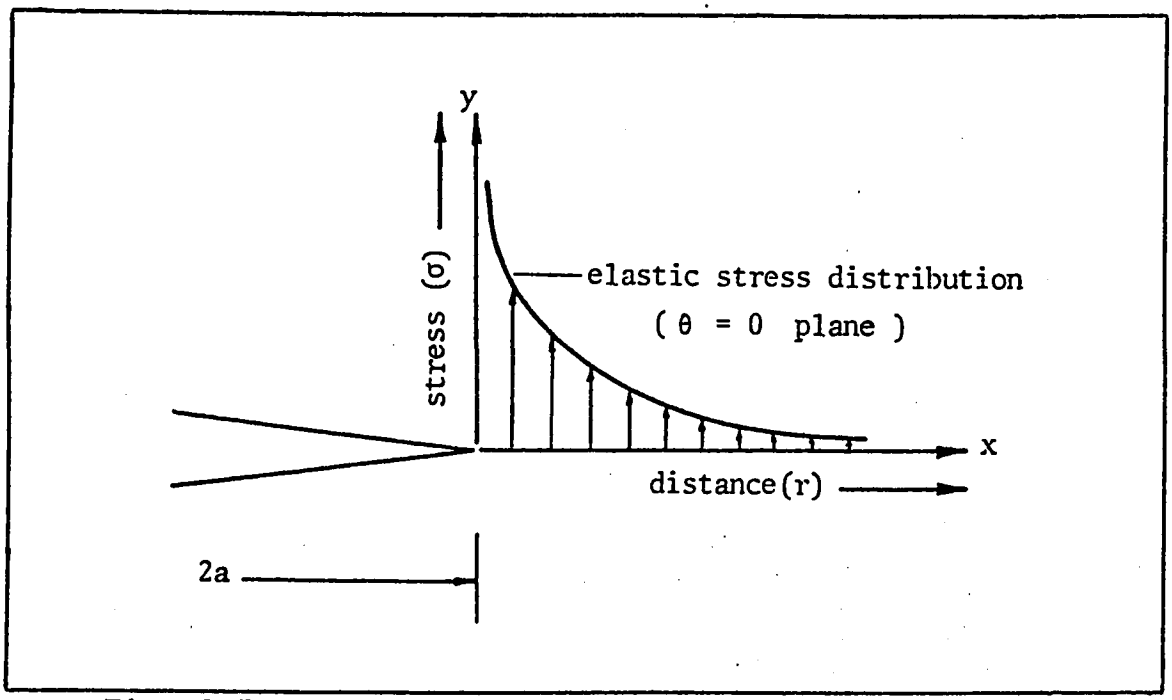

Fig. 2.5 : Elastic stress distribution in the crack tip vicinity

From these equations stresses may be easily computed at any position located a distance r from the crack tip with an angle 0 measured counterclockwise from the x-axis. Note that the above stress equations possess the variable r in their denominator, hence a singularity exists as r approaches zero (at the crack tip, theoretical stresses tend to infinity). Also as r tends to infinity, the theoretical stresses approach to zero instead of σ (the stress at the boundary). These elastic stress equations are therefore valid only for a limited area around the crack tip (Fig. 2.6 & 2.7).

2.3.1.2 Critical Stress Intensity Factor K_{IC}

The stress formulas presented previously may be written in a more generalized form as shown below.

$$\sigma_{ij} = \frac{K_I}{\sqrt{2\pi r}} f_{ij}(\theta) \qquad (5)$$

where $K_I = \sigma\sqrt{\pi a}$

The factor K_I is called the stress intensity factor where I indicates the mode I type of cracking. The entire stress field around the crack tip is defined by just knowing the stress intensity factor K_I. Cases having equal stress intensity factors possess similar stress fields.

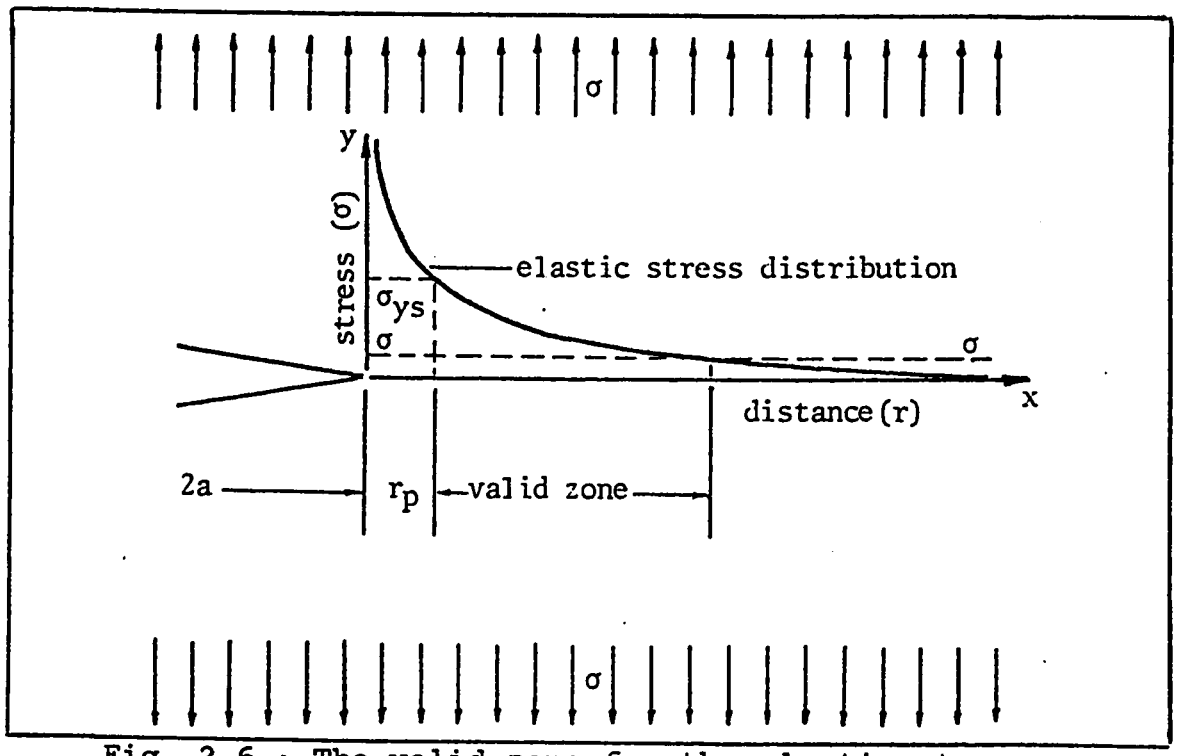

Fig. 2.6 : The valid zone for the elastic stress distribution

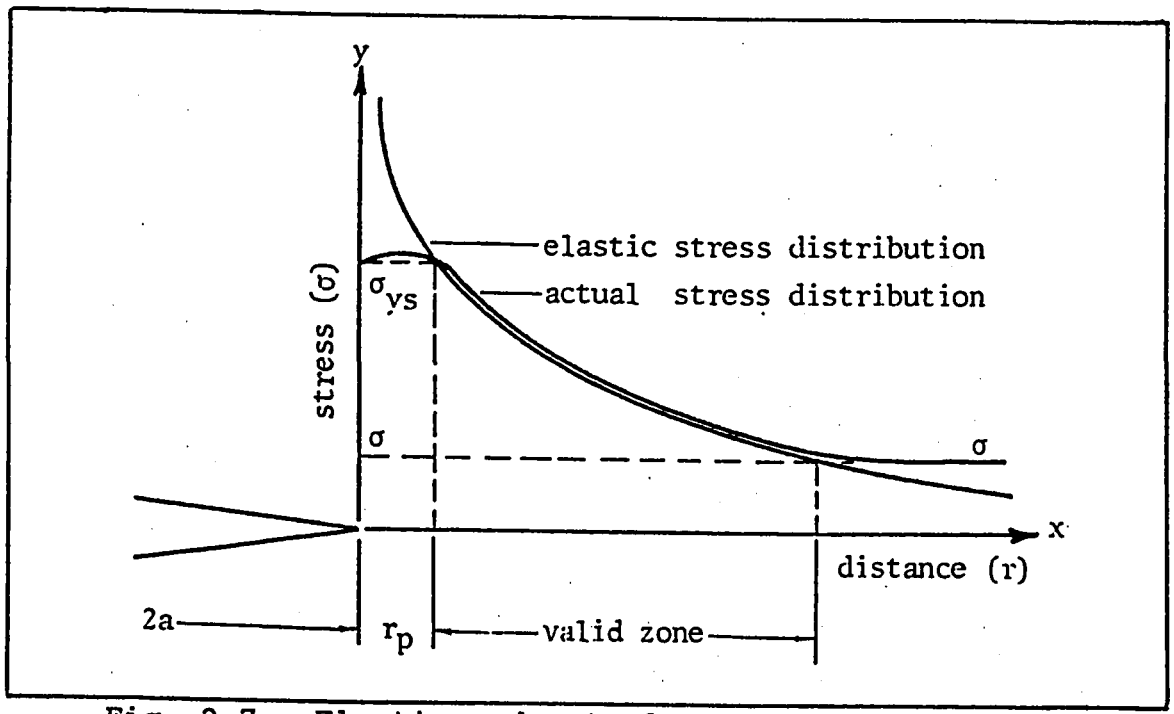

Fig. 2.7 : Elastic and actual stress distributions showing deviation at invalid zones

Crack extension and propagation occur only when the stresses and strains reach their critical value.

Consider a failure stress σ_c calculated from a fracture load. The critical stress intensity factor denoted by K_{IC} may be expressed as shown below.

$$K_{IC} = \sigma_c\sqrt{\pi a} \tag{6}$$

The critical stress intensity factor is a material parameter and through testing other specimens of the same material with variable crack lengths, the same value should be obtained i.e. K_{IC} should be invariant.

2.3.1.3 Plastic Zone Effect

From the elastic solution, stresses become infinite at the crack tip which can not possibly occur, therefore plastic deformation takes place keeping the stress value finite and not exceeding the yield stress σ_{ys} (plane stress). The stress state through out the plastic zone is assumed to be yielding, hence the plastic zone range may be determined considering the plane $\theta=0$ (Fig. 2.7).

$$\sigma_y = \frac{K_I}{\sqrt{2\pi r_p}} = \sigma_{ys} \tag{7}$$

$$r_p = \frac{K_I^2}{2\pi\sigma_{ys}^2} = \frac{\sigma^2}{2\sigma_{ys}^2} \tag{8}$$

Beyond this pastic zone of range r_p the stress field is elastic and given by LEFM expressions described by the presented equations (8).

A concept of notional crack may be introduced in order to simulate small scale yielding {54}, where the notional crack length is assumed greater than actual crack length to account for limited plasticity in vicinity of crack tip.

2.3.2 Energy Criterion (G_I)

The energy criterion developed by Griffith 1921 {55} states that any structural element possessing a crack when subjected to loads sufficient to initiate crack propagation, release energy along with crack extension. Therefore, its elastic energy content consequently decreases, provided no work is done by external forces at the boundary.

Crack propagation occurs if the energy released upon crack growth is enough to provide all the energy that is required for crack growth. Therefore the condition for crack growth is as follows :

$$\frac{dU}{da} = \frac{dW}{da} \qquad (9)$$

where U *is the elastic energy,*

and W *is the energy comsumed by crack growth*

Usually elastic energy dU/da is replaced by G_I which is called the rate of elastic energy release and the energy consumed in crack propagation dW/da is replaced by R and is called the crack resistance. The energy condition states that G_I must be equal to R in order to allow crack propagation.

Inglis and Griffith calculated the G_I value for the stress field of an elliptical flaw {56-57}

$$G_I = \frac{\pi\sigma^2 a}{E} \qquad \textit{(Plane Stress)} \qquad (10)$$

where E *is Elastic Modulus*

and σ *is the stress subjected the plate*

and a *is the crack length*

If R is constant, then G_I must exceed a certain critical value G_{IC} at which crack extension occurs.

$$G_{IC} = \frac{\pi\sigma_c^2 a}{E} \qquad (11)$$

where G_{IC} *is the critical elastic energy release rate*

The equivalence between both the stress and energy criteria is obvious, after further equation manipulations.

$$\frac{K_I^2}{E} = G_I \qquad \frac{K_{IC}^2}{E} = G_{IC} \qquad \textit{(Plane Stress)} \qquad (12)$$

$$\frac{K_I^2}{(1-\nu^2)E} = G_I \qquad \frac{K_{IC}^2}{(1-\nu^2)E} = G_{IC} \qquad \textit{(Plane Strain)} \qquad (13)$$

2.3.2.1 Gurneys' Approach

This energy approach will entirely be used through out this study, hence special case illustrations are discussed, regarding compliance and fracture toughness measurements using the Gurney approach {58-59}.

It is considered mathematically direct and the physical explanation involved is much simpler than the stress intensity factor concept. It is a one-sided crack area approach where only one side of the crack surface is considered.

Consider a plate of constant thickness t possessing a crack of length a. On subjecting the plate to a load P it exhibits a displacement u. The P-u plot of the loaded body shows a straight line (for a linear elastic body). The compliance ($C=u/P$) of the body is simply the inverse of the stiffness ($K=P/u$). At any instant, the strain energy stored in the body is directly equivalent to the area under the loading line. When a certain critical value of load is reached the crack length a extends an amount Δa.

On considering the behavior of P, u, and a after the critical loading is reached, the fracture toughness G_{IC} may be determined. The fracture toughness G_{IC} is defined to be the energy or work required to produce a unit change in crack area (also called the rate of energy release) so it has units of $\frac{F\text{-}L}{L^2}$ or $\frac{F}{L}$.

2.3.2.2 Energy Equilibrium Equation

The mathematical formulation of the equilibrium equation during crack extension under quasistatic loading is presented by :

$$dF = d\Lambda + dW \qquad (14)$$

or

$$\Delta F = \Delta\Lambda + \Delta W$$

dF is work done by external boundary forces

dΛ is the change in strain energy due fracture loading

dW is the energy or work done create the fracture surface

Consider the following special cases where both loading and unloading are totally linear.

Case I: Constant Displacement (Fixed Grip Test)

Linear Elastic Material (Fig. 2.8)

(No Plastic Deformation i.e. on unloading one arrives back at point O).

The Energy Balance Equation is given by :

$$dF = d\Lambda + dW \quad or \quad \Delta F = \Delta\Lambda + \Delta W \tag{15}$$

where

$$\Delta F = P\Delta u = 0 \quad (u_2 = u_1 \ , \ \Delta u = 0) \tag{16}$$

$$\Delta\Lambda = area\ OBC - area\ OAC$$

$$\Delta\Lambda = \tfrac{1}{2}P_2 u - \tfrac{1}{2}P_1 u = \tfrac{1}{2}(P_2 - P_1)u \tag{17}$$

$$\Delta W = G_{IC}\,\Delta A = G_{IC}\,t\Delta a \quad (where\ t\ is\ the\ thickness) \tag{18}$$

Substituting equations (16, 17 & 18) into equation (15)

$$0 = \tfrac{1}{2}(P_2 - P_1)u + G_{IC}\,t\Delta a \tag{19}$$

$$G_{IC} = \frac{(P_1 - P_2)u}{2t\ \Delta a} = \frac{P_1 u - P_2 u}{2t\ \Delta a} \tag{20}$$

Note that

$$u = P_1 C_1 = P_2 C_2 \quad and \quad \Delta C = C_2 - C_1 \tag{21}$$

Substituting into equations (21) into equation (20)

$$G_{IC} = \frac{P_1 P_2 C_2 - P_1 P_2 C_1}{2t\ \Delta a} = \frac{P_1 P_2\ (C_2 - C_1)}{2t\ \Delta a} \tag{22}$$

$$G_{IC} = \frac{P_1 P_2}{2t}\ \frac{\Delta C}{\Delta a} = \frac{P_1 P_2}{2t}\ \frac{dC}{da} \tag{23}$$

Equation (23) is valid for a linear elastic material.

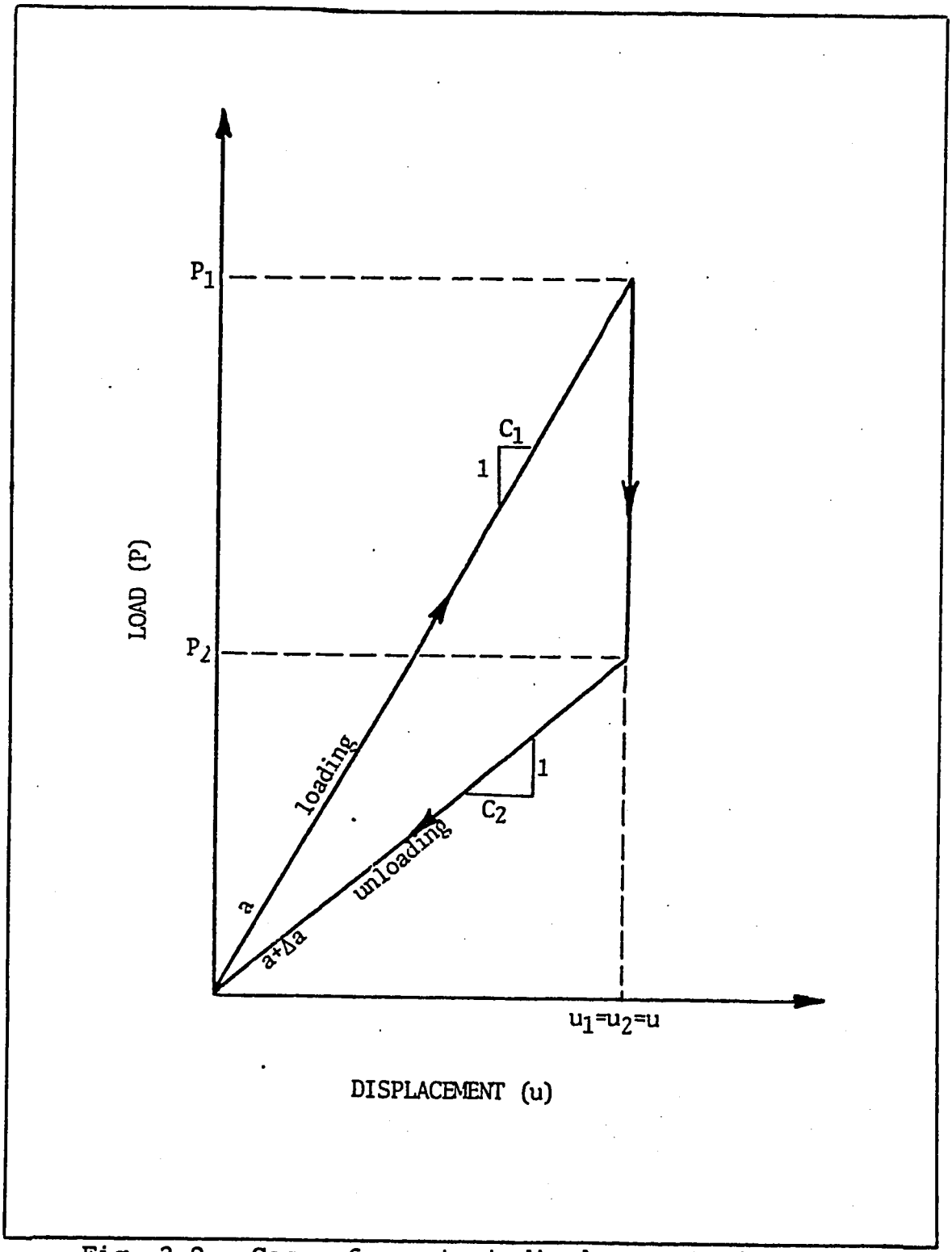

Fig. 2.8 : Case of constant displacement with no plastic deformation (Fixed Grip Test)

Case II: Constant Load

Linear Elastic Material (Fig. 2.9)

(No Plastic Deformation i.e. on unloading one arrives back at point O).

The Energy Balance Equation is given by :

$$dF = d\Lambda + dW \quad or \quad \Delta F = \Delta\Lambda + \Delta W \tag{24}$$

where

$$\Delta F = P\Delta u = P(u_2 - u_1) \tag{25}$$

$\Delta\Lambda$ = *area OBC – area OAD*

$$\Delta\Lambda = \tfrac{1}{2}Pu_2 - \tfrac{1}{2}Pu_1 = \tfrac{1}{2}P(u_2 - u_1) \tag{26}$$

$$\Delta W = G_{IC}\,\Delta A = G_{IC}\,t\Delta a \quad (\textit{where t is the thickness}) \tag{27}$$

Substituting equations (25,36 & 27) into equation (24)

$$P(u_2 - u_1) = \tfrac{1}{2}P(u_2 - u_1) + G_{IC}\,t\Delta a \tag{28}$$

$$G_{IC} = \frac{P(u_2 - u_1)}{2t\,\Delta a} = \frac{Pu_2 - Pu_1}{2t\,\Delta a} \tag{29}$$

Note that

$$u_1 = PC_1 \quad \text{and} \quad u_2 = PC_2 \tag{30}$$

Substituting equations (30) into equation (29)

$$G_{IC} = \frac{P^2C_2 - P^2C_1}{2t\,\Delta a} = \frac{P^2(C_2 - C_1)}{2t\,\Delta a} \tag{31}$$

$$G_{IC} = \frac{P^2}{2t}\,\frac{\Delta C}{\Delta a} = \frac{P^2}{2t}\,\frac{dC}{da} \tag{32}$$

Equation (32) is valid for a linear elastic material.

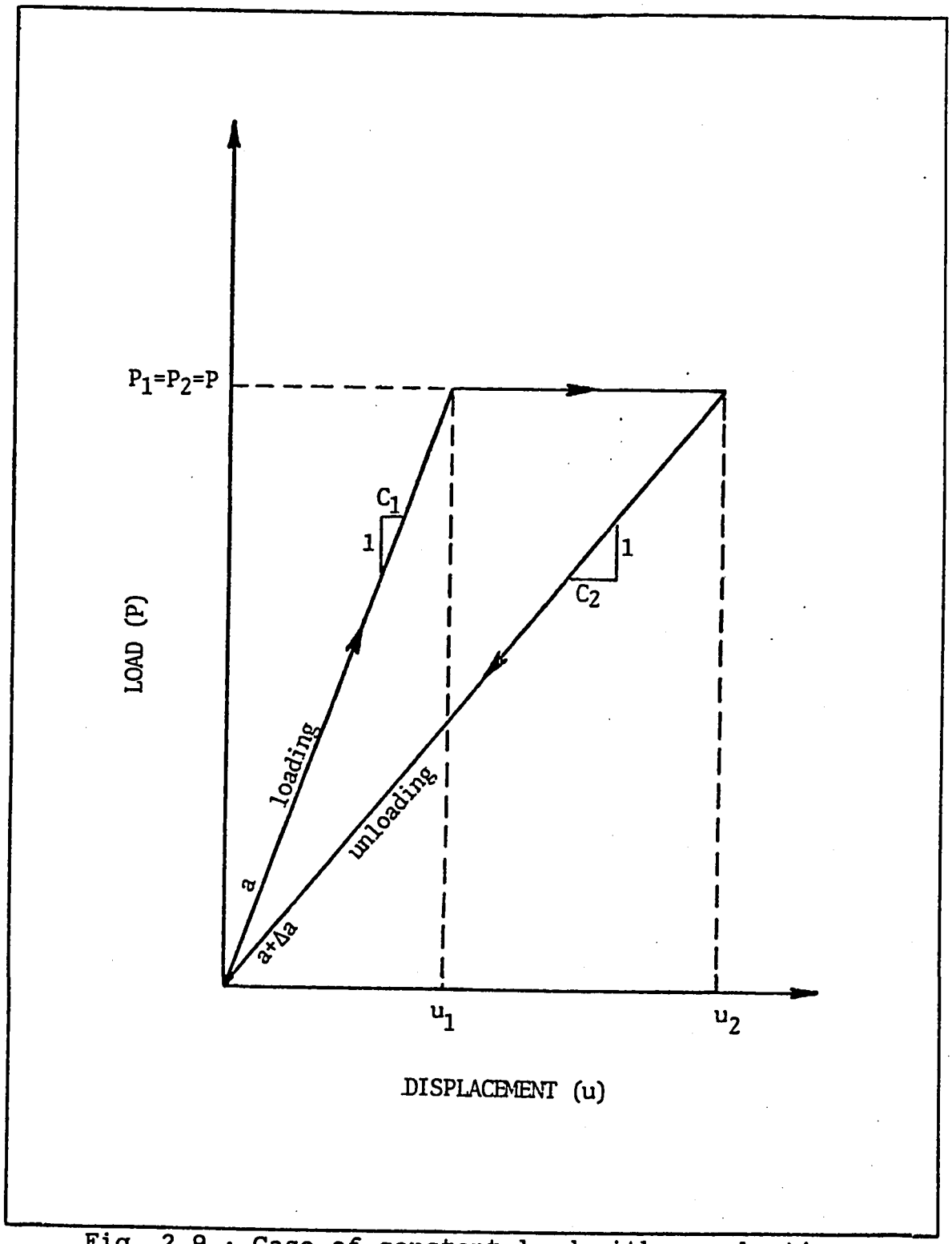

Fig. 2.9 : Case of constant load with no plastic deformation

Case III: Variable Displacement and Load

A More General Case

Linear Elastic Material (Fig. 2.10)

(No Plastic Deformation i.e. on unloading one arrives back at point O).

The Energy Balance Equation is once again given by :

$$dF = d\Lambda + dW \quad or \quad \Delta F = \Delta\Lambda + \Delta W \tag{33}$$

where

$$\Delta F = P\Delta u = \tfrac{1}{2}(P_1 + P_2)(u_2 - u_1)$$

$$\Delta F = \tfrac{1}{2}(P_1u_2 + P_2u_2 - P_1u_1 - P_2u_1) \tag{34}$$

$\Delta\Lambda$ = *area OBC − area OAD*

$$\Delta\Lambda = \tfrac{1}{2}P_2u_2 - \tfrac{1}{2}P_1u_1 = \tfrac{1}{2}(P_2u_2 - P_1u_1) \tag{35}$$

$$\Delta W = G_{IC}\,\Delta A = G_{IC}\,t\Delta a \quad (\textit{where t is the thickness}) \tag{36}$$

Substituting equations (34,35 & 36) into equation (33)

$$\tfrac{1}{2}(P_1u_2 + P_2u_2 - P_1u_1 - P_2u_1) = \tfrac{1}{2}(P_2u_2 - P_1u_1) + G_{IC}\,t\Delta a \tag{37}$$

$$G_{IC} = \frac{(P_1u_2 - P_2u_1)}{2t\ \Delta a} \tag{38}$$

Note that

$$u_1 = P_1C_1 \quad \text{and} \quad u_2 = P_2C_2 \quad \text{and} \quad \Delta C = C_2 - C_1 \tag{39}$$

Substituting equations (39) into equation (38)

$$G_{IC} = \frac{P_1P_2C_2 - P_1P_2C_1}{2t\ \Delta a} = \frac{P_1P_2(C_2 - C_1)}{2t\ \Delta a} \tag{40}$$

$$G_{IC} = \frac{P_1P_2}{2t}\,\frac{\Delta C}{\Delta a} = \frac{P_1P_2}{2t}\,\frac{dC}{da} \tag{41}$$

Again, this equation (41) is for a linear elastic material.

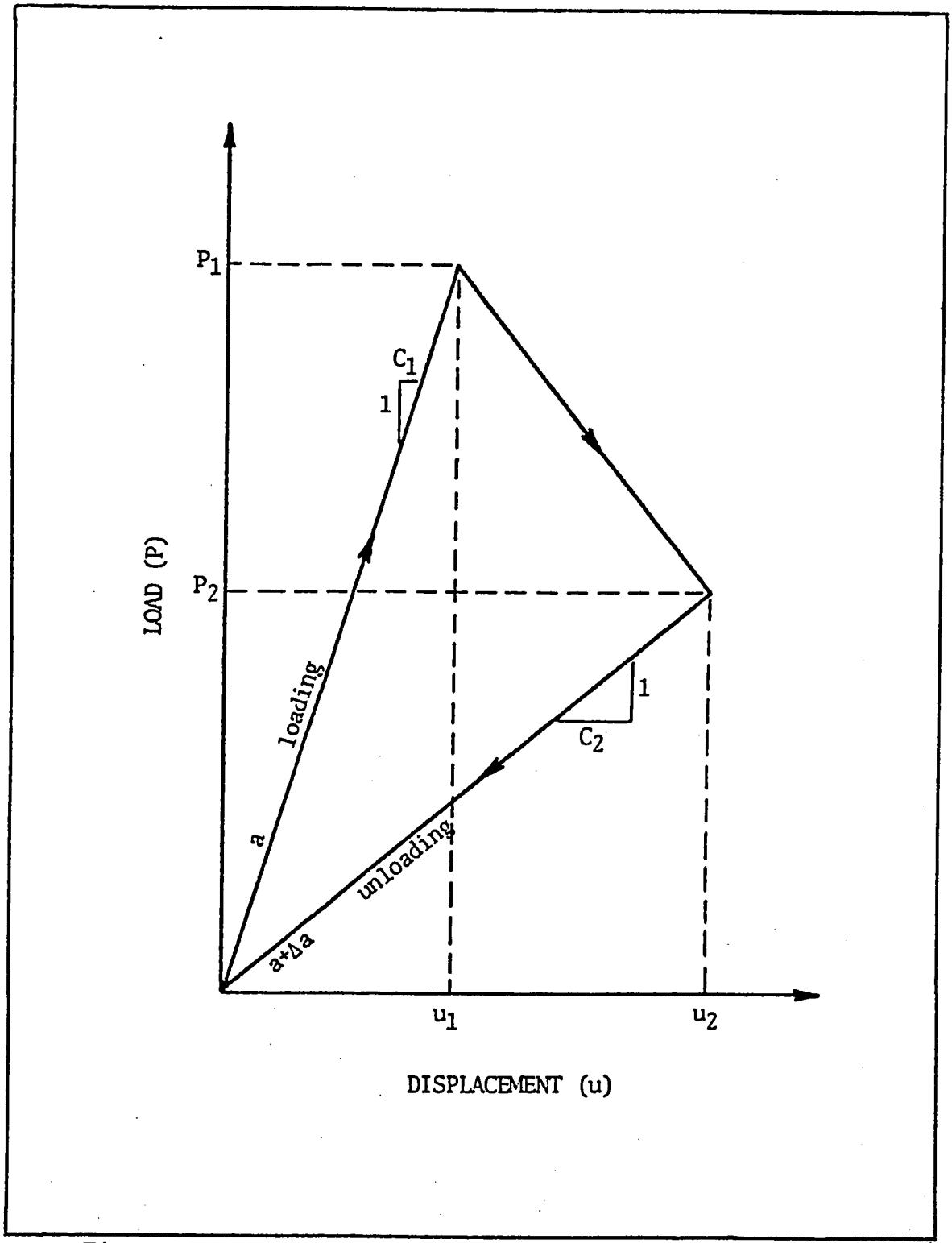

Fig. 2.10 : Case of variable load and displacement with no plastic deformation

Case IV: Variable Displacement and Load

The Most General Case

Partially Plastic Material (Fig. 2.11)

(Plastic Deformation is allowed i.e on unloading one does not arrive at point O).

The Energy Balance Equation is also given by :

$$dF = d\Lambda + dW \quad or \quad \Delta F = \Delta\Lambda + \Delta W \tag{42}$$

where

$$\Delta F = P\Delta u = \tfrac{1}{2}(P_1 + P_2)(u_2 - u_1)$$

$$\Delta F = \tfrac{1}{2}(P_1 u_2 + P_2 u_2 - P_1 u_1 - P_2 u_1) \tag{43}$$

$\Delta\Lambda$ = *area EBC − area OAD*

$$\Delta\Lambda = \tfrac{1}{2}P_2(u_2 - \Delta\delta_p) - \tfrac{1}{2}P_1 u_1 = \tfrac{1}{2}(P_2 u_2 - P_1 u_1). \tag{44}$$

$$\Delta W = G_{IC}\,\Delta A = G_{IC}\,t\Delta a \quad (\textit{where t is the thickness}) \tag{45}$$

Substituting equations (43,44 & 45) into equation (42)

$$\tfrac{1}{2}(P_1 u_2 + P_2 u_2 - P_1 u_1 - P_2 u_1) = \tfrac{1}{2}(P_2 u_2 - P_1 u_1 - P_2\Delta\delta_p) + G_{IC}\,t\Delta a \tag{46}$$

$$G_{IC} = \frac{(P_1 u_2 - P_2 u_1 - P_2\Delta\delta_p)}{2t\,\Delta a} \tag{47}$$

Note that

$$u_1 = P_1 C_1 \quad \text{and} \quad u_2 = P_2 C_2 + \Delta\delta_p \quad \text{and} \quad \Delta C = C_2 - C_1 \tag{48}$$

Substituting equations (48) into equation (47)

$$G_{IC} = \frac{P_1 P_2 C_2 + P_1\Delta\delta_p - P_1 P_2 C_1 + P_2\Delta\delta_p}{2t\,\Delta a} = \frac{P_1 P_2 (C_2 - C_1) + (P_1 + P_2)\Delta\delta_p}{2t\,\Delta a} \tag{49}$$

$$G_{IC} = \frac{P_1 P_2}{2t}\,\frac{\Delta C}{\Delta a} + \frac{(P_1 + P_2)}{2t}\,\frac{\Delta\delta_p}{\Delta a} = \frac{P_1 P_2}{2t}\,\frac{dC}{da} + \frac{(P_1 + P_2)}{2t}\,\frac{d\delta_p}{da} \tag{50}$$

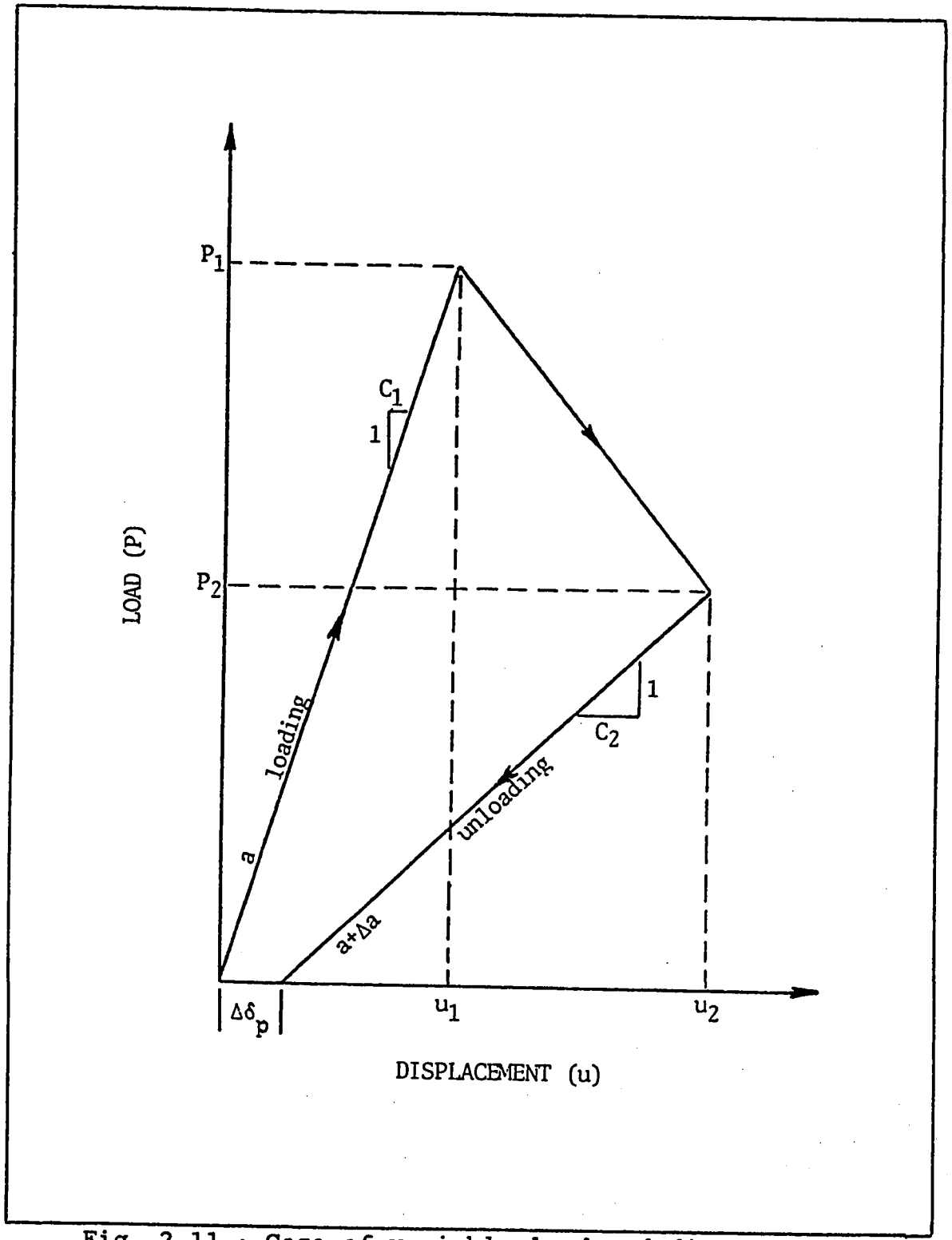

Fig. 2.11 : Case of variable load and displacement with plastic deformation

Equation (50) shows the critical rate of elastic energy release possessing both elastic and plastic contributions and as given by Wecharatana and Shah {60-61}.

2.3.2.3 Suitability For Concrete

The application of Linear Elastic Fracture Mechanics LEFM criteria and in particular the Gurney energy approach to concrete was found to be satisfactory considering the following assumptions.

1. Concrete is considered to be an inelastic material and therfore equation (50) as given by Wacharatana and Shah {60-61}, was thought to be appropriate for measurements of critical energy release rate.
2. Concrete is assumed to behave linearly during an incremental loading and unloading cycle.

PERMEABILITY AS A DURABILITY MEASURE

3.1 General

Durable concrete is that which withstands conditions designed for, with a tolerable level of deterioration, throughout its service life. Deterioration of concrete is due to both external and internal causes. External causes may be due to physical, chemical, and mechanical aggencies. Internal causes may be due to aggregate-alkali reaction, volume changes due to thermal incompatability of concrete components, and the permeability of concrete {36}.

3.2 Definition of Permeability

Permeability of concrete is defined to be the acceptance of concrete to fluid penetration. Impermeable concretes have a tendency to resist fluid ingress while permeable concretes have less resistance {36}.

3.3 Importance of Permeability to Durability

Permeability of concrete is of great importance since it determines the vulnerability of concrete to external agencies. Therefore durable concretes must be relatively impervious in character, especially in areas of severe and aggressive environmental and climatic conditions, namely the Arabian peninsula.

As previously mentioned, the environment of the soil surrounding substructures possesses high sulphate and chloride salt concentrations, that are highly soluble in the presence of water. These soluble salts can form a component of an aggressive external attack.

Immediately after the salt penetration of concrete, reinforcement corrosion starts and subsequently volumetric changes occur due to both steel rusting and successive salt crystallization. The concrete hardened paste within the matrix becomes over stressed, hence producing more micro cracks.

Accordingly, the permeability increases, causing the concrete to become more vulnerable to external damaging agencies. Climatic conditions are also such that high daily and seasonal temperature variations are often exhibited. The concept of TICC comes into view where it also affects the durability. Relatively impermeable concretes may become highly permeable due to thermal incompatability of concrete constituents TICC over a period of time.

Due to high temperature variations, any concrete that possesses thermally incompatible components becomes over stressed and micro cracking increases throughout the material, causing the permeability to increase to higher levels.

Consequently previously impermeable concretes become permeable and their vulnerability to attack by external agencies increases profoundly. Therefore their durability is considerably lowered.

Measuring the permeability of thermally cycled concrete in this study would present a fair idea about the amount of damage caused due to increased cracking within the concrete.

3.4 Pores in the Hydrated Cement

The pores in the micro structure of the hydrated cement paste determine its permeability. Fresh cement paste consists of a plastic network of cement particles in water that solidify, preventing any further volume changes.

The hardened cement paste consists of hydrates of various compounds that are refered to collectively as gel of calcium hydroxide crystals, some minor components, unhydrated cement, and the residue of water filled spaces in the fresh paste that form voids when dried out. The voids are called capillary pores, but within the gel itself there exists interstitial voids called gel pores. The permeability of concrete depends on the intensity, size, distribution, and continuity of such pores which express the porosity of the material {36}.

Mainly, capillary pores are of greater influence to permeability than gel pores. Capillary pores are much larger in size than gel pores, having an estimated size in the order of 1.3 μ ($1.3x10^{-6}$ *m*) , while the size of gel pores is estimated to be in the order of 20 *A* ($20x10^{-10}$ *m*) which is only one order greater than a single water molecule {36}.

3.4.1 Capillary Pores

At any stage of hydration, the capillary pores represent the portion of the gross volume that has not been filled by the products of hydration. With the progress of hydration, the capillary pores are reduced by getting filled in by the gel matter. Hydration increases the solid content of the paste and in mature and dense pastes, capillaries may become blocked by gel and segmented so that they turn into discontinuous capillary pores interconnected only by gel pores {62}.

The volume of gel is not sufficient to fill all the capillary voids even after complete hydration has occured. Therefore capillaries must be present in any concrete, but it varies in intensity, size, distribution, and continuity, depending on the methods of concrete production followed. The capillary porosity depends generally on the w/c ratio and the degree of hydration {36}.

3.4.2 Gel Pores

Gel pores are interconnected interstitial spaces between gel particles. The gel is considered porous due to the capacity of the gel pores in retaining large amounts of evaporable water. These gel pores are much smaller than capillary pores and their size is only one order greater than the size of a single water molecule. Therefore the movement of water through the gel material is very difficult to an extent that the gel pores barely contribute to the permeability of the concrete.

Capillary pores present the major contribution to permeability due to their special capillarity characteristic. Gel pores occupy 28 per cent of the total volume of gel material after solidifying {63}. As hydration proceeds the volume of gel material increases and the associated gel pores consequently increase. Consequently, the capillary pores get partially filled with the surplus gel material, decreasing the number, size, and continuity, of the capillary pores therefore enhancing the permeability to a lower value {36}.

3.5 Fabricating Impermeable Concretes

From the discussion of both types of pores along with the filling gel material, there is one approach to take in order to produce relatively impermeable concrete. This may be

acheived by using a low w/c ratio in the mix, that produces the largest amount of gel material to fill the vast majority of capillary pores, hence arresting the permeability to very low levels. Also assuring complete hydration is of equal importance, which is achieved by using improved curing methods such as steam curing. This is due to the fact that the gel matter increases in volume with the progress of hydration {36}.

3.6 Factors Affecting Permeability

Permeability of concrete is affected by various factors. Since permeability depends mostly on the intensity, size, distribution, and continuity of capillary pores rather than gel pores, it is highly affected by the degree of hydration or age of concrete. This is due to the formation of more gel material that clogs the capillary pores and hence decreases their intensity, size, distribution, and continuity, resulting in a consequent rapid decrease in permeability. Using steam curing lowers the permeability of the produced concrete, where a higher degree of hydration is achieved at earlier ages {36}.

Permeability is also greatly affected by the cement content where the lower the w/c ratio, the lower the permeability coefficient. The cement property is another important factor, so fine cements used in the mix produce

less porous cement pastes while coarse cements produce highly porous pastes, but in general high strength concretes possess lower permeability coefficients.

Aggregates too, have a role in concrete permeability where highly permeable aggregates used within the mix may increase the overall permeability coefficient. On the other hand, aggregates of very low porosity may arrest the overall permeability to lower levels.

3.7 Permeability as Compared to Absorption

It was decided to measure the permeability of concrete using the German Standard Code Specification (DIN) {64} since the American Standards for Testing Materials (ASTM) lacks such a test for concrete. Measuring the absorption by ASTM was not used due to the reason that widely different results are obtained when measuring the absorption of concrete and hence the test results are considered inconsistent.

The method of measuring absorption according to the American Standards of Testing Materials (ASTM) {65} is dictated by drying the specimen to a dry constant weight, then immersing it in water till complete saturation is achieved after which its increase in weight is calculated. The absorption is the increase in weight as a percentage of the specimen's dry weight.

The reason the absorption is not consistent when successively measured is that drying of the specimens at ordinary temperatures does not remove all the contained water, whilst on the other hand drying the specimens at high temperatures may remove some of the combined water. Absorption therefore is not used as a measure of concrete quality.

The measure of permeability is considered indeed more consistent where specimens are dried at ordinary temperatures, then placed in the permeability test machine where water is forced under pressure to penetrate the specimen from bottom to top (Fig. 3.1).

The pressure is applied for a duration of four days where the water pressure is held at 1 bar for the first two days, then it is increased to 3 bars on the third day and finally to 7 bars on the fourth day. After the four days, the test specimen is directly split by applying compression to the specimen while placed between two steel bars e.g. as in a split tension test. The maximum depth of penetration of water is taken to be the permeability value of that specimen.

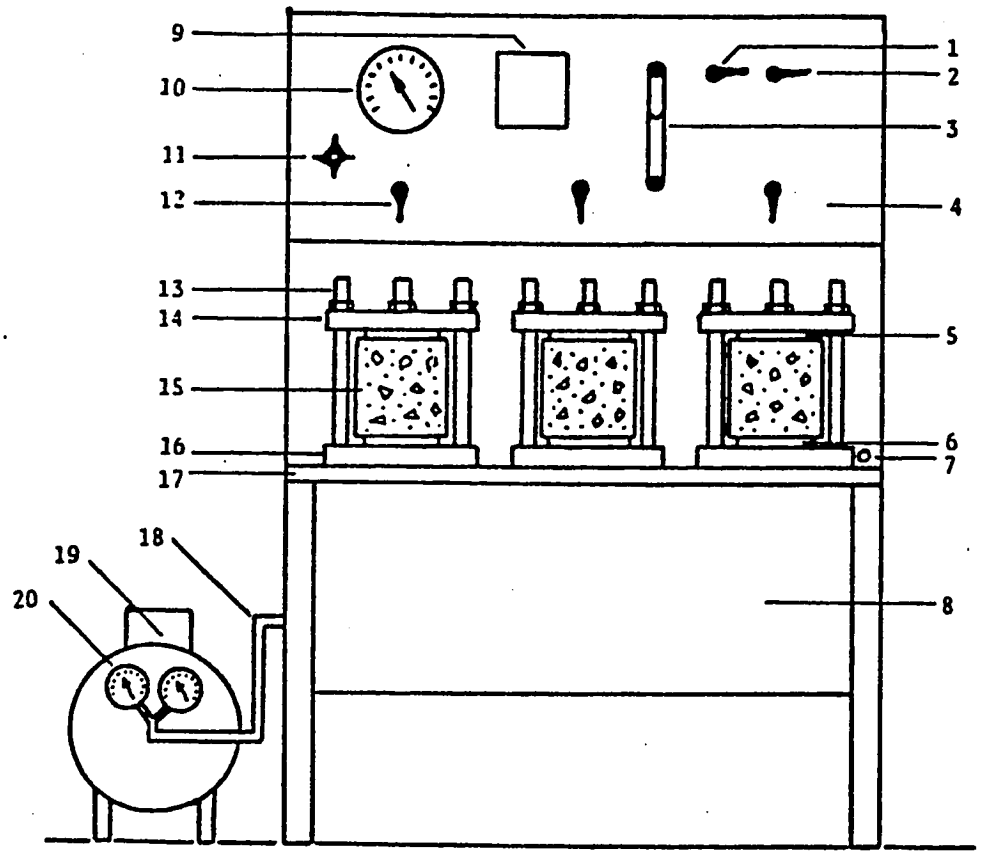

(1) Water Supply Valve
(2) Water Overflow Valve
(3) Water Level Column
(4) Control Panel
(5) Top Rubber Gasket
(6) Bottom Rubber Gasket
(7) Overflow Outlet
(8) Pipe and Hose Cabinet
(9) Valve Instruction Panel
(10) Pressure Dial Gage
(11) Pressure Adjustment Tap
(12) Compartment Water Valve
(13) Anchoring Nut and Thread
(14) Top Triangular Steel Plate
(15) Concrete Cube Specimen
(16) Bottom Triangular Steel Plate
(17) Permeability Machine Table
(18) High Air Pressure Hose
(19) Air Compressor Unit
(20) Compressor Pressure Dial Gages

Fig. 3.1 : Permeability machine diagram

EXPERIMENTAL METHODOLOGY

4.1 General

The work presented tends to detect the deterioration of various concretes, that possess a thermal incompatibility of concrete constituents (TICC) problem. Local types of aggregates used in the mixes such as Abu-Hadriyah, Jabal Dhahran, and Riyadh aggregate have low coefficients of thermal expansion as compared to that of the hardened cement paste. All various concrete groups cast GREFC ,GRYDC ,GJDHC ,GSMXC ,GSWDC ,GSRTC ,GSPLC ,and GLTXC (Table 4.1) were subjected to thermal cycling prior to being tested. Thermal cycling was meant to simulate diurnal and seasonal temperature changes and accelerate the concrete deterioration process.

Some different concrete groups cast considered variables other than the aggregate type, such as the coarse/fine aggregate ratio of the mix, and the addition of admixtures to the mix. Others considered identical concrete groups subjected to different conditioning such as alternate wetting and drying, and support restraint.

The entire study consisted mainly of two major phases. The first phase dealt with the determination of the fracture characteristics of the various thermally cycled concretes cast.

Table 4.1 : Details of cast concrete specimens

Variables Considered	Group ID	Aggregate Type	C/F Agg.	W/C Ratio	Admixture added	Conditioning
Aggregate Type	GREFC	Abu-Hadriyah	1.5	0.54	----	----
	GRYDC	Riyadh	1.5	0.57	----	----
	GJDHC	Jabal Dhahran	1.5	0.71	----	----
Mix Design	GSMXC	Abu-Hadriyah	0.5	0.64	----	----
Admixture	GSPLC	Abu-Hadriyah	1.5	0.46	Super Plasticizer (1.15% cement)	----
	GLTXC	Abu-Hadriyah	1.5	0.31	Latex (10.0% cement)	----
Restraint	GSRTC	Abu-Hadriyah	1.5	0.54	----	Beams are support restrained
Soaked Wet/Dry cycle	GSWDC	Abu-Hadriyah	1.5	0.54	----	Beams are soaked for 12 hours after each H/C cycle

The second phase involved study of permeability values of the same concrete groups referred to above in addition to permeability of cores drilled from reinforced concrete panels exposed to natural thermal cycling over two and a half years plus their control groups GC, GS50, GS45, and GS40 (Table 4.2). The coefficient of thermal expansion of Riyadh aggregate was also found while the coefficient of thermal expansions of other aggregates used were obtained from reference {45}.

Explanation of the process of fabrication and production, curing and cycling, and preparing and testing of both fracture and permeability specimens along with the coefficient of thermal expansion of Riyadh aggregate are presented later on in this chapter. Both fracture and permeability data would be utilised for the interpretation of the level of deterioration of the various thermally degraded concretes.

4.2 Standard Specifications Used

Standard specifications were followed throughout the thesis. The ASTM Standards were used in (i) selection, and preparation of concrete materials (cement, aggregates, admixtures, etc) and (ii) in the process of fabrication, production, conditioning, preparation and testing of concrete specimens.

Table 4.2 : Details of cored concrete specimens

Group ID	Curing Method	Cores ID	W/C Ratio	Super Plasticizer (L/50 Kg Cement)
GC	Good	GC1 G	0.57	None
		GC2 G		
	Bad	GC1 B		
		GC2 B		
GS50	Good	GS50 G	0.50	0.60
	Bad	GS50 B		
GS45	Good	GS45 G	0.45	0.75
	Bad	GS45 B		
GS40	Good	GS40 G	0.40	1.00
	Bad	GS40 B		

Curing Method :

1. Good : Covered with burlap and watered twice daily for 7 days then left uncovered for the remaining 21 days.
2. Bad : Covered with burlap and watered only once on the first day then uncovered and left for the remaining 27 days.

Super Plasticizer COMPLAST M1 was used.

The German Standards (DIN) were used in conducting the permeability test on the concrete specimens due to the lack of such a test suitable for concrete in ASTM Standards. A summary of the standard specifications along with a brief one-line description is presented (Table 4.3).

4.3 Variables Considered

The variables considered in this study may either be classified as being either favourable or unfavourable with reference to durability of concrete. Favourable variables are those that retard the rate of TICC deterioration to low levels such as, the use of a superior type of aggregate within the mix, the addition of admixtures to the mix, or a well graded aggregate mix design. Unfavourable variables are those which accelerate the rate of TICC deterioration to high levels such as, the use of an inferior type of aggregate within the mix, or a unifomly graded aggregate mix design. The following section and its subsections discuss each variable separately.

4.4 Details of the Different Groups Cast

The mix proportions of the two mixes used in the design of groups GREFC, GRYDC, GJDHC, GSMXC, GSWDC, GSRTC, GSPLC, and GLTXC are presented (Tables 4.4 & 4.5). A summary of all the above mentioned groups with specific features (rather than the mix proportions) is also given (Table 4.6).

Table 4.3 : Standard specification summary

Code	Description
ASTM	
Cement :	
C 150-85	Specification for Portland Cement
C 183-83	Methods of Sampling Hydraulic Cement
C 219-84	Terminology Relating to Hydraulic Cement
Rel. Mat.	Manual of Cement Testing
Aggregate :	
C 33-85	Specification for Concrete Aggregates
C 75-82	Practice for Sampling Aggregates
C 125-82	Definition of Terms (Concrete & Aggregates)
C 136-84	Sieve Analysis of Fine & Coarse Aggregates
C 702-80	Reducing Field Samples of Agg. to Test Size
Rel. Mat.	Manual of Aggregate and Concrete Testing
Concrete :	
C 39-84	Compressive Strength of Cylindrical Specimens
C 42-84	Obtaining and Testing Drilled & Sawed Specime
C 78-84	Flex. Strength of Concrete (3-Point Loading)
C 143-78	Slump of Portland Cement Concrete
C 171-69	Specification of Sheet Materials for Curing
C 172-82	Sampling Freshly Mixed Concrete
C 192-81	Making & Curing Concrete Specimens in the Lab
C 293-79	Flex. Strength of Concrete (Mid-Point Loading)
C 341-84	Length Change of Drilled or Sawed Specimens
C 470-81	Specifications for Forming Concrete Cylinders
C 494-82	Specifications for Chemical Admixtures
C 617-85	Capping Cylindrical Concrete Specimens
C 873-85	Compressive Strength of Concrete Cylinders
Rel. Mat.	Metric Practice Guide
DIN (FRG ST)	
DIN 1048	Permebility of Concrete Cube Specimens

Table 4.4 : Proportions of Mix No.1 (C/F Agg.=1.5)

Components	Percentage of Total Dry Weight
Cement	17.0
Aggregates	
Coarse 3/4" - 1/2"	15.0
1/2" - 3/8"	15.0
3/8" - No.4	20.0
Fine Dune Sand	33.0
Water/Cement	Variable
Admixture	Variable

Remarks :

Cement Type (Portland Cement Type I)

Coarse Agg. (Abu-Hadriyah, Riyadh, and Jabal Dhahran)

Fine Agg. (Dune Sand from Dhahran)

Admixtures (Super Plasticizer, and Latex)

Coarse/Fine Agg. ratio was 1.5

Table 4.5 : Proportions of Mix No.2 (C/F Agg.=0.5)

Components	Percentage of Total Dry Weight
Cement	17.0
Aggregates	
Coarse 3/4" - 1/2"	8.3
1/2" - 3/8"	8.3
3/8" - No.4	11.1
Fine Dune Sand	55.3
Water/Cement	0.64
Admixture	None

Remarks :

Cement Type (Portland Cement Type I)

Coarse Agg. (Abu-Hadriyah)

Fine Agg. (Dune Sand from Dhahran)

Coarse/Fine Agg. ratio was 0.5

Table 4.6 : Special features for the cast groups

Group ID	Mix No.	C/F Agg.	Aggregate	W/C Ratio	Admixtrue added
GREFC	1	1.5	Abu-Hadriyah	0.54	----
GRYDC	1	1.5	Riyadh	0.57	----
GJDHC	1	1.5	Jabal Dhahran	0.71	----
GSMXC	2	0.5	Abu-Hadriyah	0.64	----
GSPLC	1	1.5	Abu-Hadriyah	0.46	Super Plasticizer (1.15% cement)
GLTXC	1	1.5	Abu-Hadriyah	0.31	Latex (10.0% cement)
GSRTC	1	1.5	Abu-Hadriyah	0.54	----
GSWDC	1	1.5	Abu-Hadriyah	0.54	----

The mix design of the cored specimens and the referenced concrete groups GC, GS50, GS45, and GS40 is presented (Table 4.7). This mix design was used after being obtained from reference {66}. A summary of the four concrete groups mentioned above is presented along with the associated w/c ratio and amount of added super plasticizer (Table 4.8).

4.4.1 Aggregate Type

Three types of local aggregates available in the eastern province of Saudi Arabia were used in groups GREFC, GRYDC, and GJDHC, namely (i) Abu-Hadriyah (ii) Jabal Dhahran and (iii) Riyadh aggregate. These groups of identical mix designs were cast each, containing one of the above mentioned aggregate types (Tables 4.1). Due to the difference in water absorption of the three aggregates, variations in the water/cement ratios of the mixes were required in order to maintain a three inch slump value. Abu-Hadriyah aggregate was the reference type of aggregate used when considering variables other than aggregate type. The three concrete groups were subjected to thermal cycling in order to accelerate the damage caused by TICC. Subsequently the specimens of the groups would be tested both for fracture and permeability characteristics. Comparison of the resulting data would allow the determination of the superior performing aggregate type.

Table 4.7 : Proportions of Mix No.3
(Mix Design of Cores)

Components	Percentage of Total Dry Weight
Cement	21.0
Aggregates	
Coarse 3/4" - 1/2"	41.0
1/2" - 3/8"	8.0
3/8" - No.4	6.0
Fine Dune Sand	24.0
Water/Cement	Variable
Admixture	Variable

Remarks :

Cement Type (Portland Cement Type I)

Coarse Agg. (Abu-Hadriyah)

Fine Agg. (Dune Sand from Dhahran)

Admixture (Super Plasticizer COMPLAST M1)

Table 4.8 : Special features for the cored groups

Group ID	W/C Ratio	Super Plasticizer (1/50Kg Cement)
GC	0.57	----
GS50	0.50	0.60
GS45	0.45	0.75
GS40	0.40	1.00

4.4.2 Mix Design

Two mix designs were used for groups GREFC, and GSMXC, where the type of aggregate used was Abu-Hadriyah aggregate (Table 4.1). The reference Abu-Hadriyah aggregate mix (GREFC) possessed a coarse/fine aggregate ratio of 1.5 while the second mix (GSMXC) was more or less sandy in nature possessing a coarse/fine aggregate ratio of 0.5. Accordingly, the water/cement ratio of the second mix was greatly increased to obtain an initial slump of three inches. This increase in the water/cement ratio was due to the vast increase in the specific surface area of the mix due to the presence of more fine particles. The reference mix of a coarse/fine aggregate ratio of 1.5 was used when considering other variables.

4.4.3 Admixtures

Two chemical admixtures locally available in the market, latex and super plasticizer, were used in making sample groups GLTXC, and GSPLC respectively (Table 4.1). Addition of admixtures to the mix enhanced the concrete strength property. By increasing the workability of the mix, the water/cement ratio required to achieve a three inch initial slump was subsequently decreased. Also latex and super plasticizer concretes had the tendency to pick up strength at early ages faster than ordinary concrete.

4.4.4 Wetting and Drying

Another group (GSWDC) identical to the reference Abu-Hadriyah aggregate group (GREFC) having a coarse/fine aggregate ratio of 1.5 was cast (Table 4.1). During the regular thermal cycling of the fracture beam specimens, a single wet/dry cycle per each heat/cool cycle was carried out. Specimens were to be heated for six hours then cooled for another six hours, after which they would be immersed in water for the remaining twelve hours of the day. From comparison of the data of both unsoaked and soaked groups, the influence of presence of moisture during thermal cycling on the durability of concrete may be obtained.

4.4.5 Support Restraint

A third group (GSRTC) identical to the reference concrete group (GREFC) of Abu-Hadriyah aggregate with a coarse/fine aggregate ratio of 1.5 was cast (Table 4.1). In this group the fracture beam specimens were subjected to thermal cycling while gripped at the supports by being placed in a bolted steel frame (Fig. 4.1). Strains at the notch tip were monitored by means of a portable data logger and an initial strain of 40 μ *mm/mm* was to be maintained on both sides of the beam (Plate 4.1). The influence of restraint in the form of a "prestress" on the durability of concrete specimens was detected by comparing both groups.

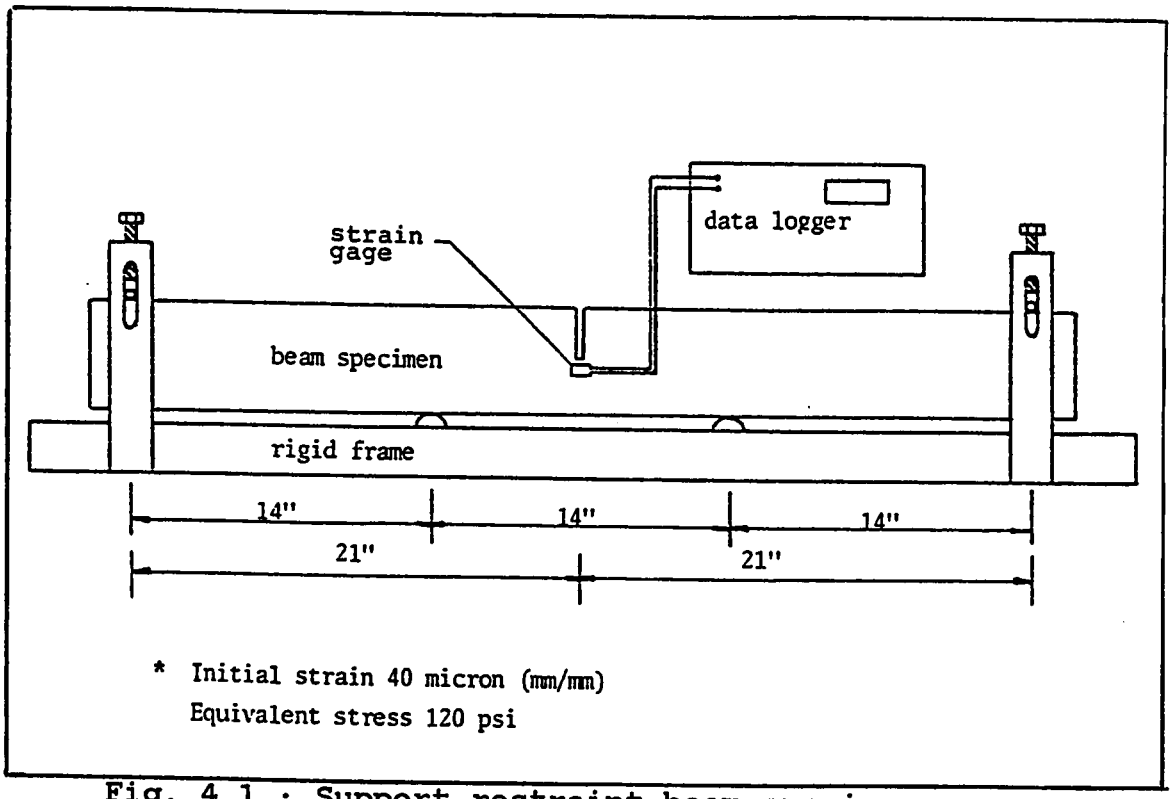

Fig. 4.1 : Support restraint beam specimen

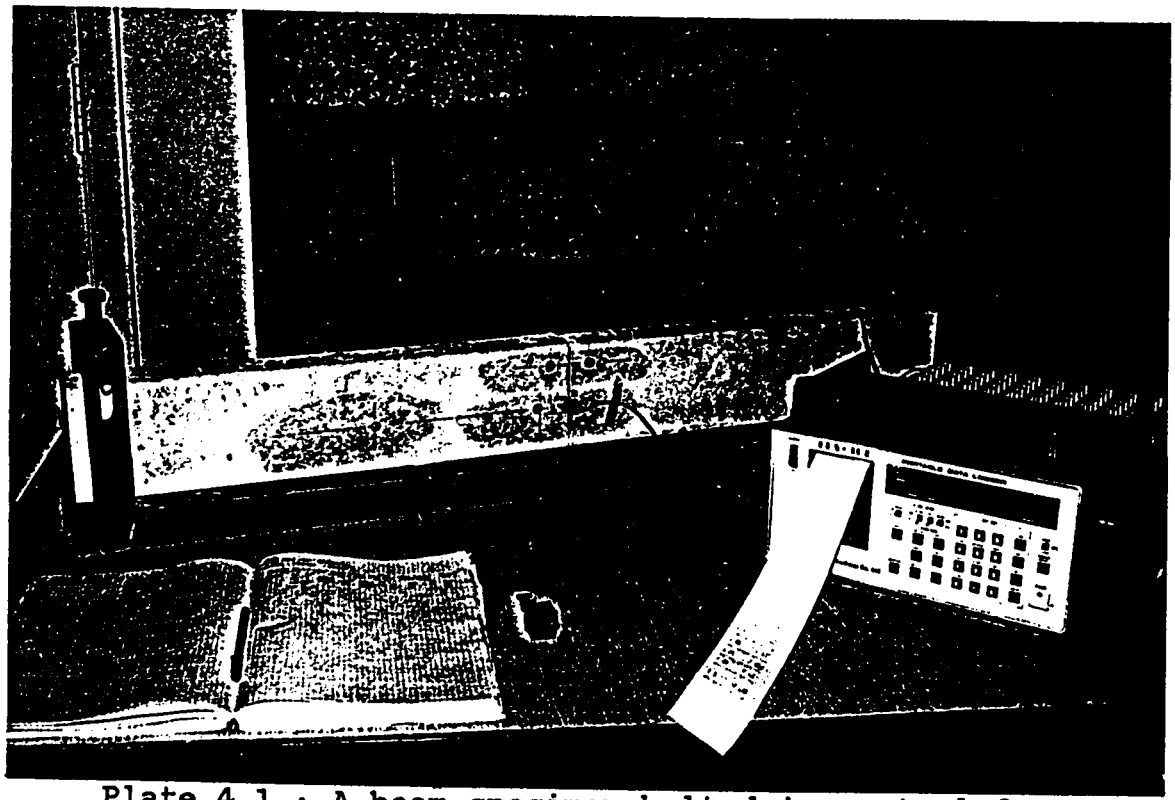

Plate 4.1 : A beam specimen bolted in a steel frame and strains monitored by a Portable Data Logger

4.5 Fracture Phase

This phase deals with the determination of the fracture characteristics of the various concretes discussed earlier in this chapter. Fracture toughness parameter in the form of critical elastic energy relaese rate G_{IC} of the cast concrete specimens is obtained. The next subsections explain and illustrate the processes of fabrication, casting, curing, cycling, preparation, and testing of the concrete specimens. The modulus of rupture M_R of each specimen is also determined.

4.5.1 Fabrication

Two types of specimens were made, beams and cylinders. The beam specimens were 2"x5"x45" especially dimensioned to be slender to assure sufficient flexibility of specimen in order to facilitate in measurement of compliance and ensure stable fracture. It would have been preferable to have used larger sized beams in order to render fracture parameters size independent, but the constraint of oven dimensions limited the beam size.

The specimens were configured so as to have a notch located at the mid span (Plate 4.2). The notch was immersed half way through the beam depth a distance of 2.5 inches at a ninety degree angle, from the top surface of the beam (Fig. 4.2).

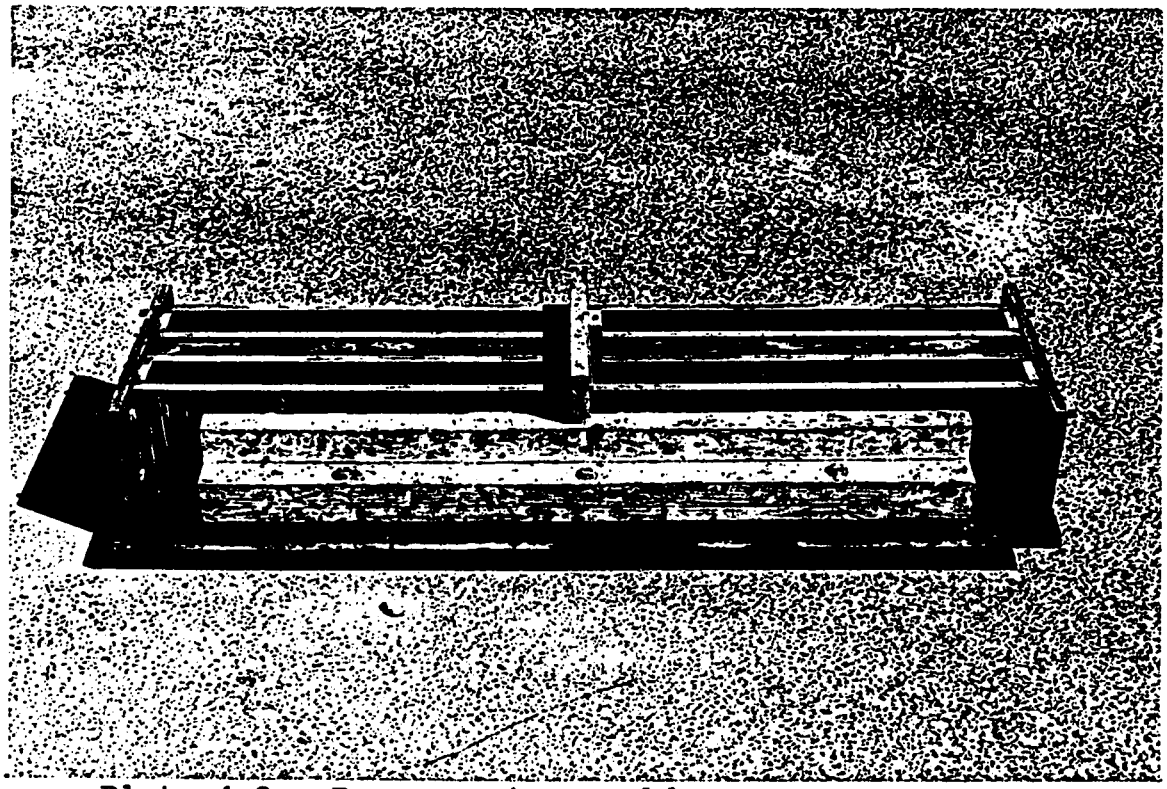

Plate 4.2 : Beam specimen molds

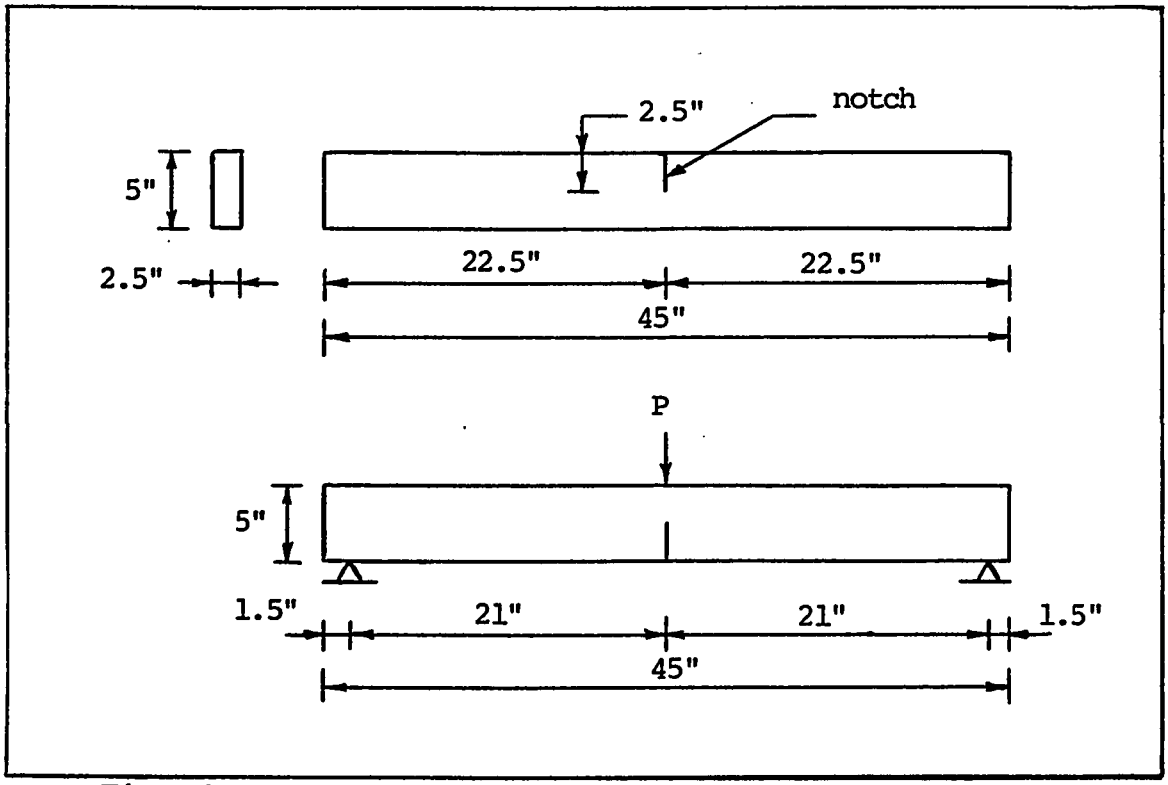

Fig. 4.2 : Dimensions and details of beam specimens

The purpose of the notch was to simulate an initial pre-existing crack and to force the beam to fail at that location during the three point loading test. Cylinder specimens were dimensioned 3"x6" for compressive strength determination.

4.5.2 Casting

Plywood beam molds were fabricated by the mechanical workshop and steel cylinder molds were used. Both beam and cylinder molds were well oiled and notches were greased prior to casting in order to ease demolding. All beam and cylinder specimens of each concrete group were cast in duplicate. Beams and cylinders were cast in two layers each approximately 2.5 inches thick. Each layer received sufficient vibration using the laboratory vibration table, assuring the extraction of most air bubbles, in order to produce a good quality, dense concrete. Finally beams and cylinders were troweled off to obtain a reasonably good surface finish, after which they were then covered by plastic sheets to prevent escape of water by evaporation. All specimens were directly demolded two days after casting.

4.5.3 Curing

Concrete beam and cylinder specimens were cured, after being cast and surface finished, for two days covered by plastic sheets. Specimens were then demolded and curing was

further carried out for 28 days more, being immersed in potable water laboratory tanks. At the end of the curing period, specimens were removed from water tanks and left out to dry within the lab at ambient room temperature, before being subjected to thermal cycling.

4.5.4 Thermal Cycling

Only beam specimens were subjected to thermal cycling. Cylinders were left uncycled and tested in compression later on. Four beams in each group were left uncycled and to be tested used as control groups while six beams were cycled up to 45, 90, and 120 cycles before being tested. Groups GJDHC, GSWDC, and GLTXC each had two extra specimens that were cycled up to 180 cycles, while for group GSWDC thermal cycling was extended to 210 cycles for two more specimens. The thermal cycling decided upon was of a more or less realistic nature as compared to the daily and seasonal natural climatic conditions prevailing through out the year in the Eastern Province region. All specimens to be cycled were stacked in the laboratory oven, where the temperature was raised to 80 degree Celsius for a duration of six hours to heat up the specimens. Subsequently, the oven was shut off and then the doors opened and specimens allowed to cool down to room temperature (approximately 27 degree Celsius) by means of directed moderate speed fans (Plate 4.3).

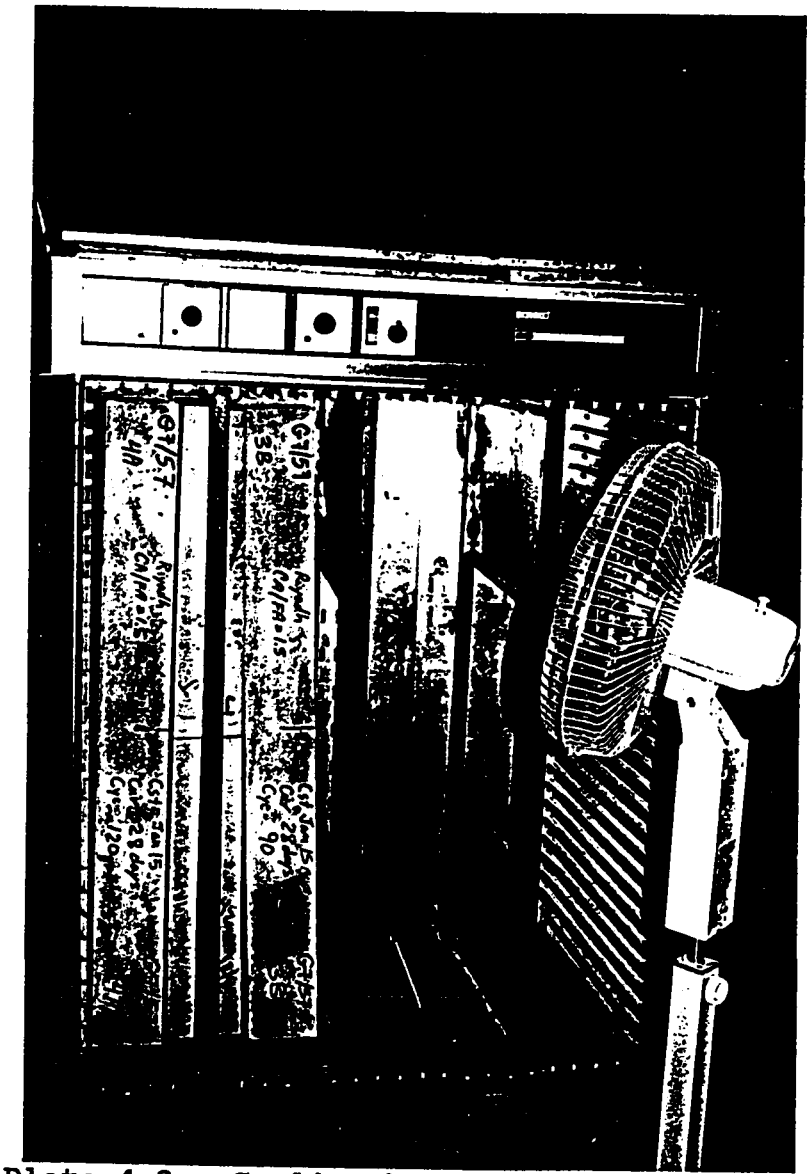

Plate 4.3 : Cycling beam specimens in oven

This cycle was repeated twice daily for all groups except group GSWDC, where the thermal cycle mentioned above was followed by 12 hours of specimen soaking in water, and hence one cycle was achieved per day.

4.5.5 Preparation for Testing

Fracture beam specimens were to be tested for fracture toughness by being loaded under three point bending. Positions of the end supports were filled off smoothly to aid the beam leveling during the test. The notch was neatly finished horizontal to the beam base by a thin steel saw blade. Crack detection at the notch location was performed by using a fluorescent dye that glowed when exposed to ultra violet (UV) light. Using the fluorescent dye on the beam surface showed the beam crazing at the sides and therefore the detection of the leading crack was indeed difficult. Therefore, there was a need to prepare an absorbent media ahead of the notch through out the beam depth on both sides of the beam, to cover up the crazing on the beam sides and ease the visibility of the leading crack during crack propagation. The absorbent media was prepared by dissolving a small amount of gypsum in water till a thin milky color was achieved. The solution was then spread and left to dry on the intended concrete surface, leaving a thin transluscent gypsum layer that easily broke along the crack during its propagation.

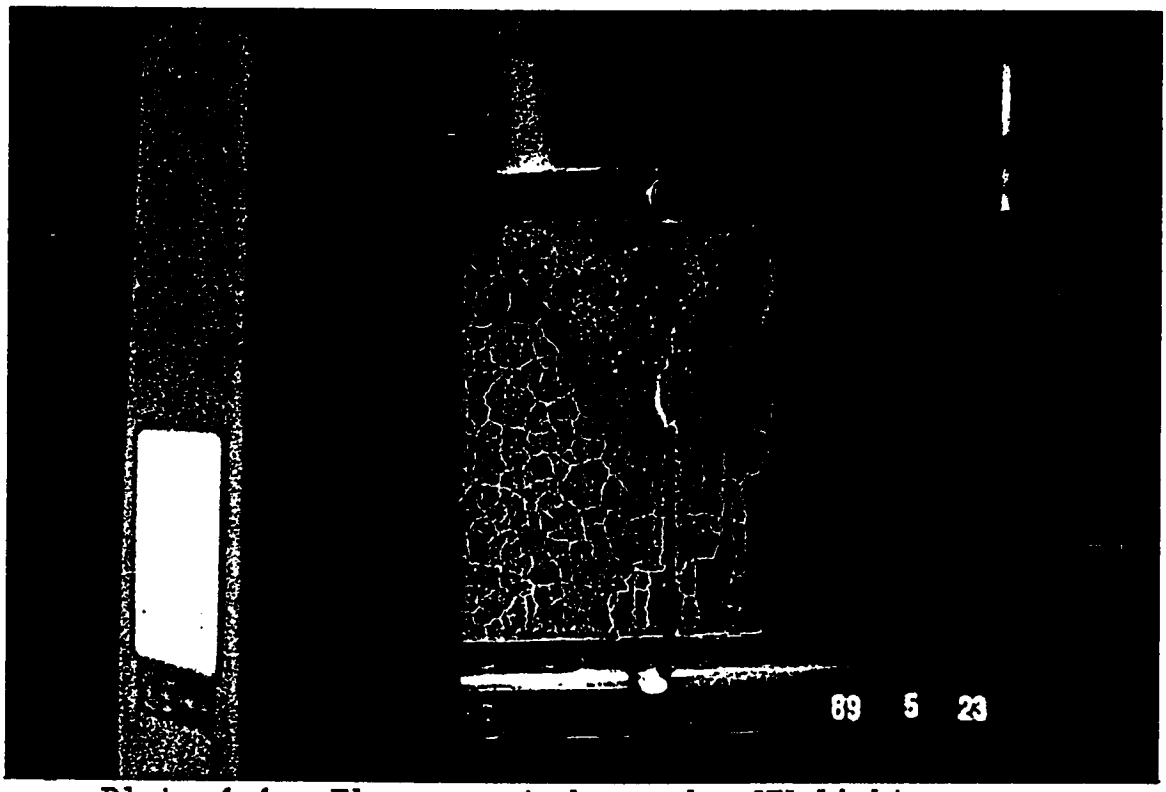

Plate 4.4 : Fluorescent dye under UV light

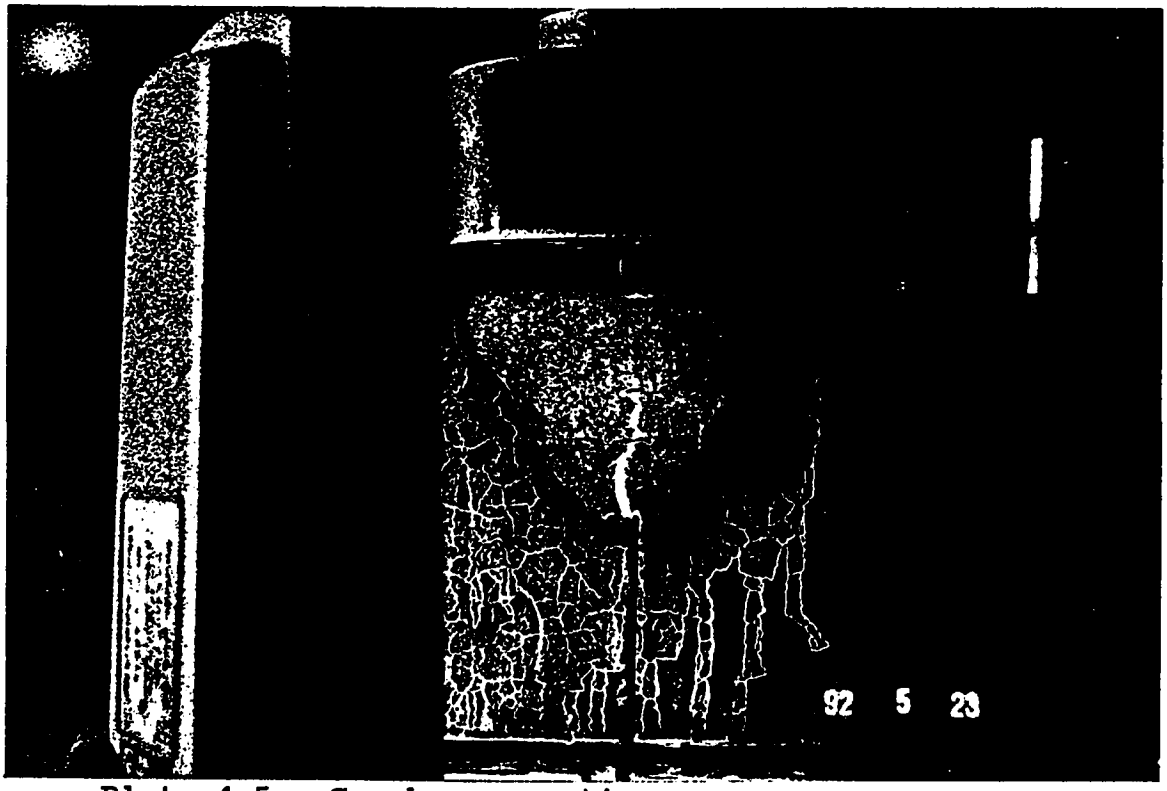

Plate 4.5 : Crack propagation

After the gypsum layer had completely dried it was slightly filled off by ones finger tips to achieve a smooth surface texture. On exposing the gypsum treated beam notch, sprayed by fluorescent dye, to ultra violet light, locations where the crack had propagated showed a higher intensity of glow and hence the crack detection was simple and easily carried out (Plates 4.4 & 4.5). Cylinder specimens were capped at the rough troweled surface with bituminous material to allow uniform stress distribution during compression testing.

4.5.6 Testing

Each beam specimen was subjected to two types of tests. After breaking the beams while determining the fracture toughness by the three point bending test, the two halves were each subjected to flexure under four point bending to determine the modulus of rupture of the specimen. Following are the details of the fracture toughness test and the modulus of rupture test.

4.5.6.1 Fracture Toughness Test

After preparing all beam specimens for testing as mentioned previously, each beam to be tested was mounted on a steel rigid frame placed on the Instron machine 1196. The beam was well levelled, plumb, and centered under the loading drum of the Inston machine (Plate 4.6).

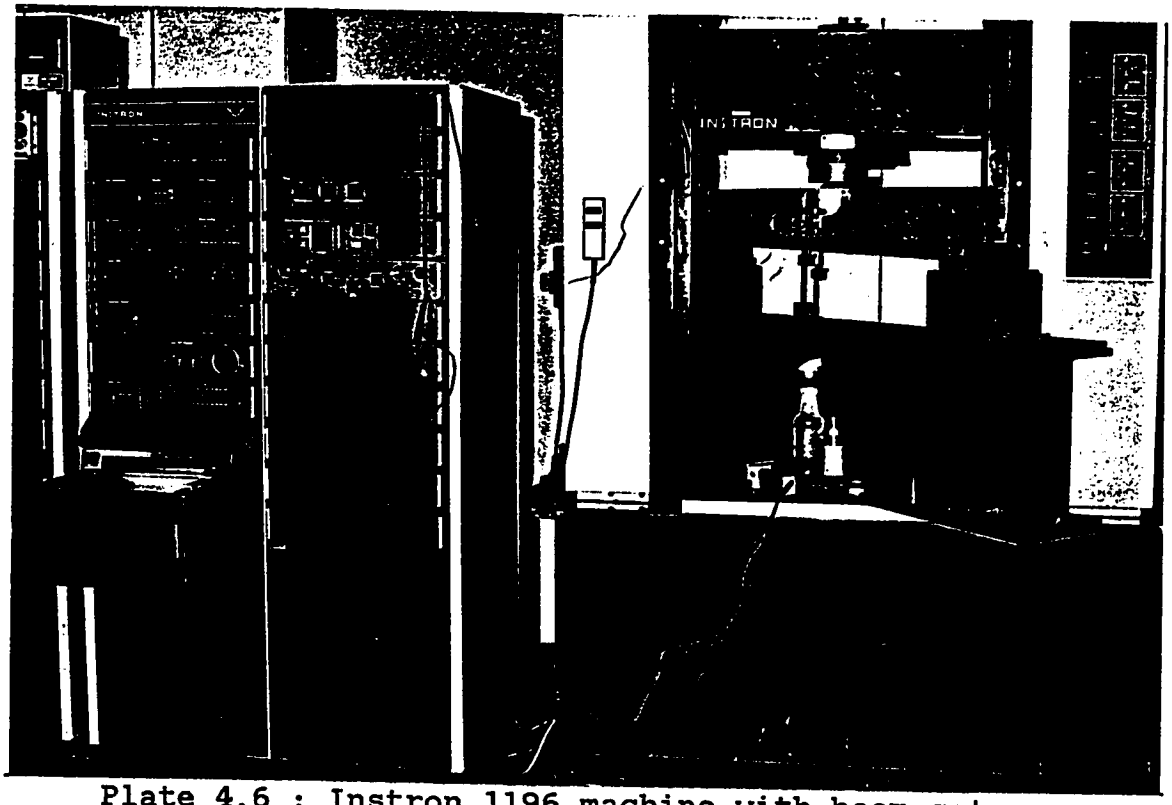

Plate 4.6 : Instron 1196 machine with beam set up

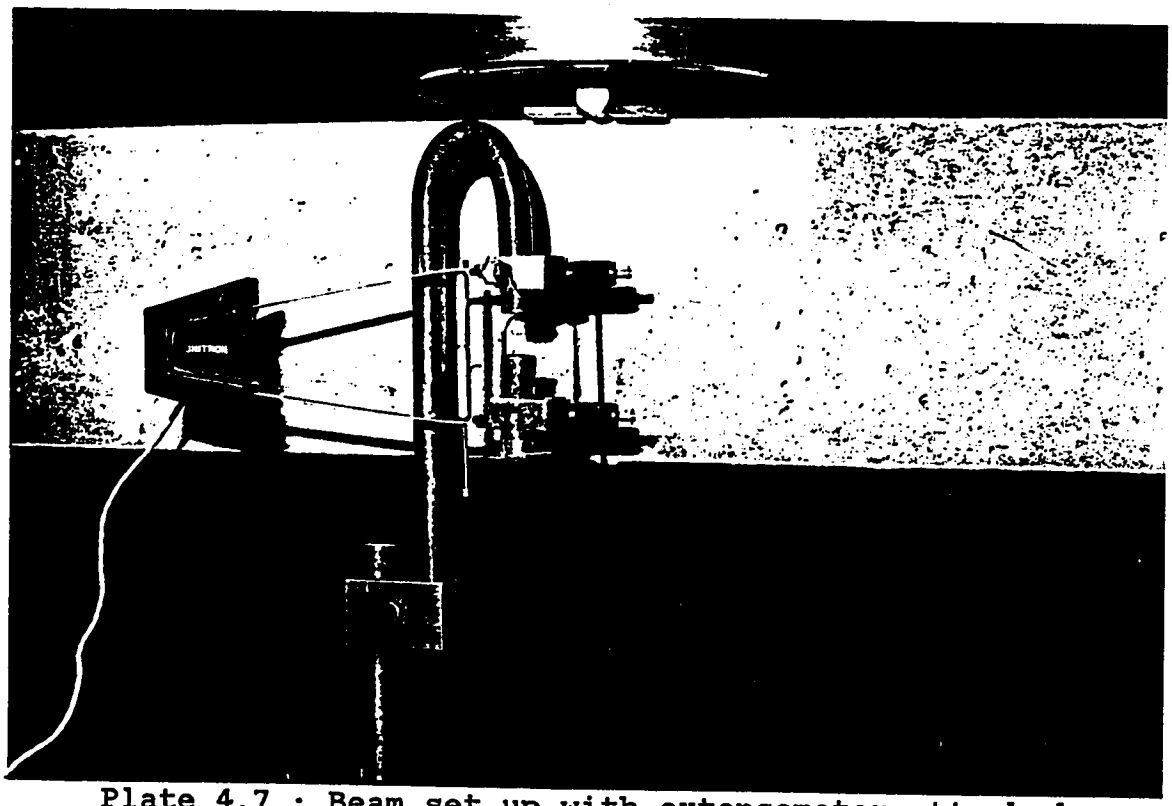

Plate 4.7 : Beam set up with extensometer attached

An LVDT (Linear Variable Differential Transducer) or an extensometer was attached to a small rigid right angle plate connected to the beam side for measuring the deflection during both the loading and unloading processes (Plate 4.7). Both the load cell and the extensometer were calibrated to the required scale for plotting the load-deflection history (P-u plot) of the specimen (Fig. 4.3). The maximum load and deflection were set to be 1.0 KN and 1.5 mm respectively, while the loading rate was kept constant throughout the test at 0.5 mm/sec.

The fluoresent dye spray bottle, ultra violet lamp, lenses, and other accessories were close at hand, then lights were dimmed and the specimen was ready for testing. The loading was started and the P-u plot showed an increase in load (P) with a consequent increase in deflection (u). At the point on the P-u plot, where the load leveled off and started to decrease, the crack started to propagate from its previous initial value. At that instant, the loading process was paused till the crack extension was marked. At the same time, the fluorescent dye was sprayed on both sides of the beam on the white gypsum layer prepared ahead of the notch. By exposing the region sprayed by fluorescent dye to ultra violet light using the UV lamp, the crack was easily visible and the crack extension on both sides of the beam was marked.

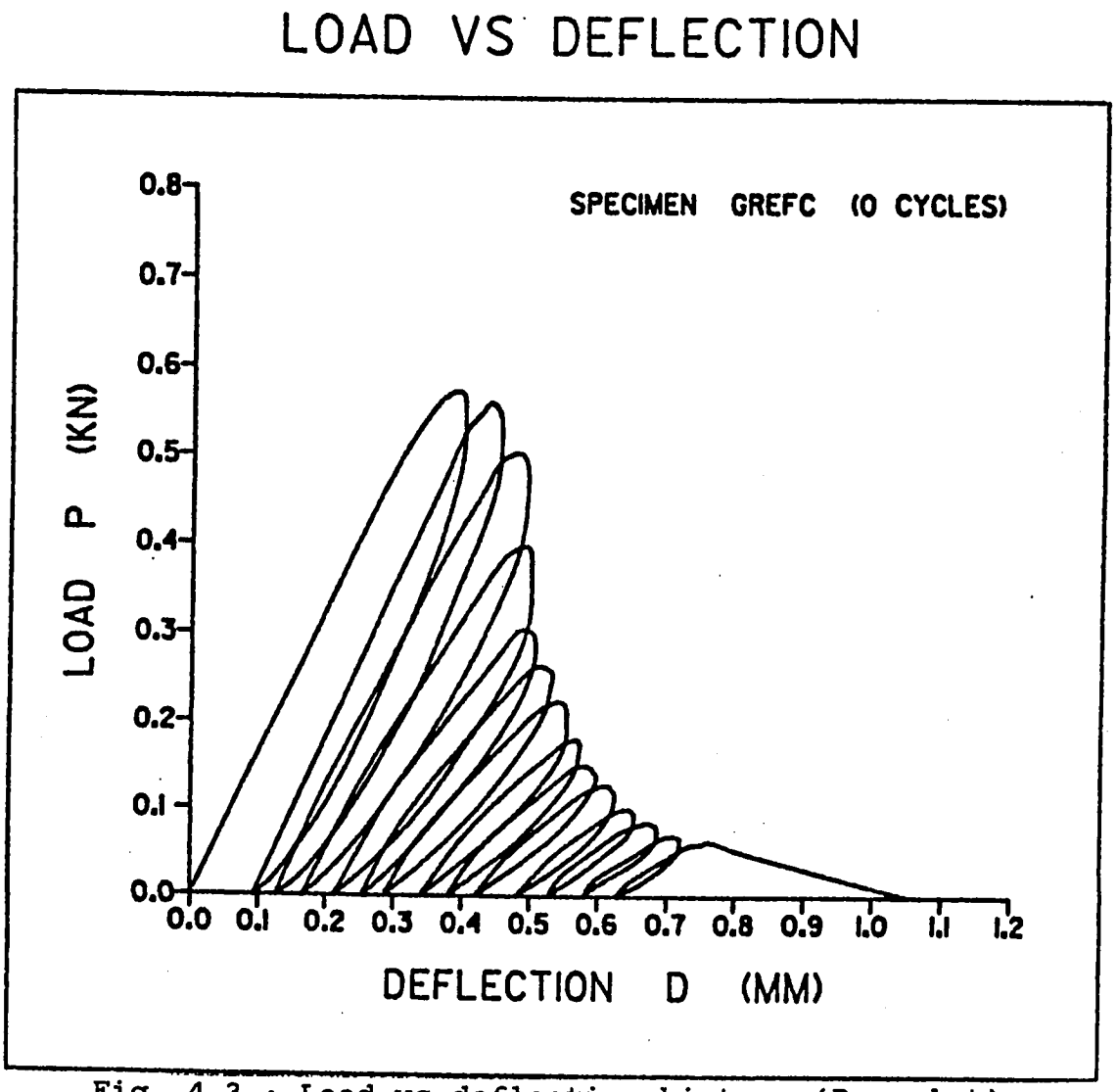

Fig. 4.3 : Load vs deflection history (P-u plot)

After marking the crack on both sides of the beam the specimen was unloaded and the beam exhibited a permanent deflection that was clearly shown on the P-u plot. Both the crack extension and permanent deflection was caused during the first loading/unloading cycle. Other cycles were run using the same procedure mentioned above. When the peak load of any cycle decreased to about 15 per cent of the peak load of the first load cycle, the specimen was loaded till it broke into two halves. The successive extended crack lengths of all cycles were recorded from both sides of the beam. Then each half was tested under four point bending for modulus of rupture values.

4.5.6.2 Modulus of Rupture Test

Each half was marked and prepared for the flexure test under four point bending. The specimen was leveled and centered on the Toni Pact 3000 machine (Plate 4.8 & 4.9). The specimen was loaded at a rate of 2.7 KN/sec till it broke, and the maximum failure load was recorded, then the modulus of rupture M_R determined. Specimens that broke at locations outside the middle third were discarded.

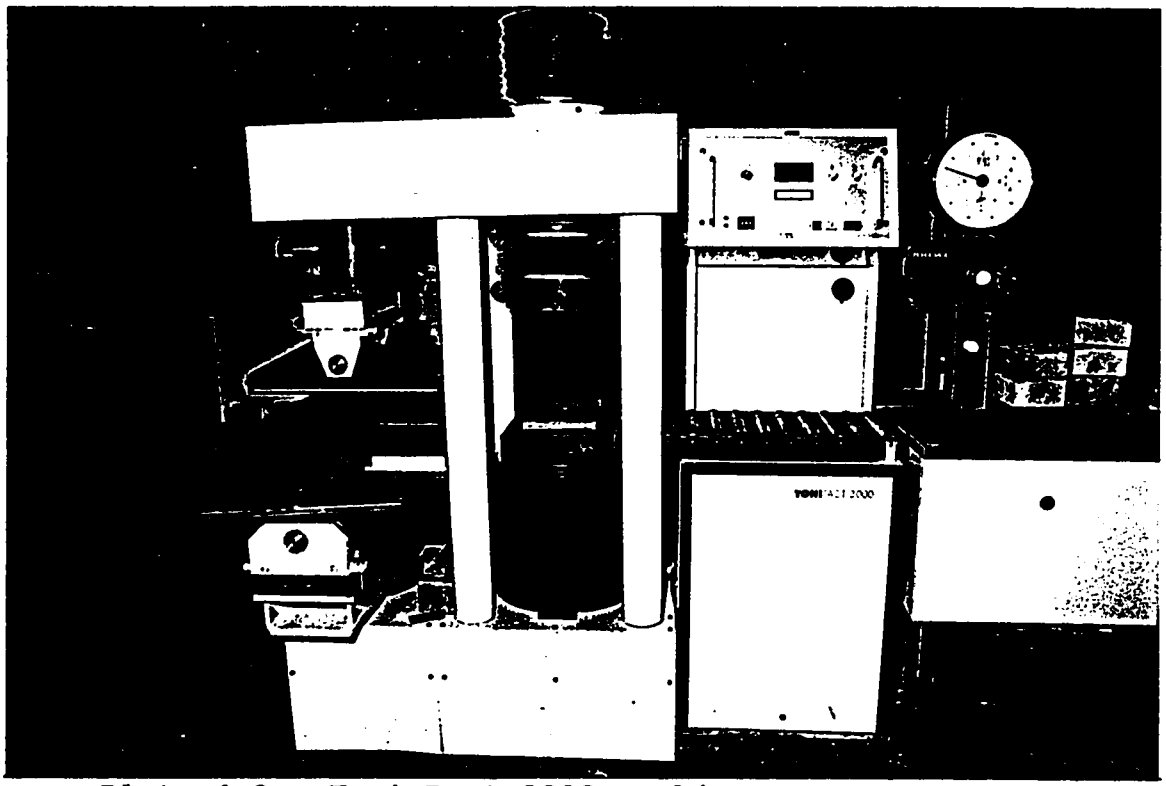

Plate 4.8 : Toni Pact 3000 machine

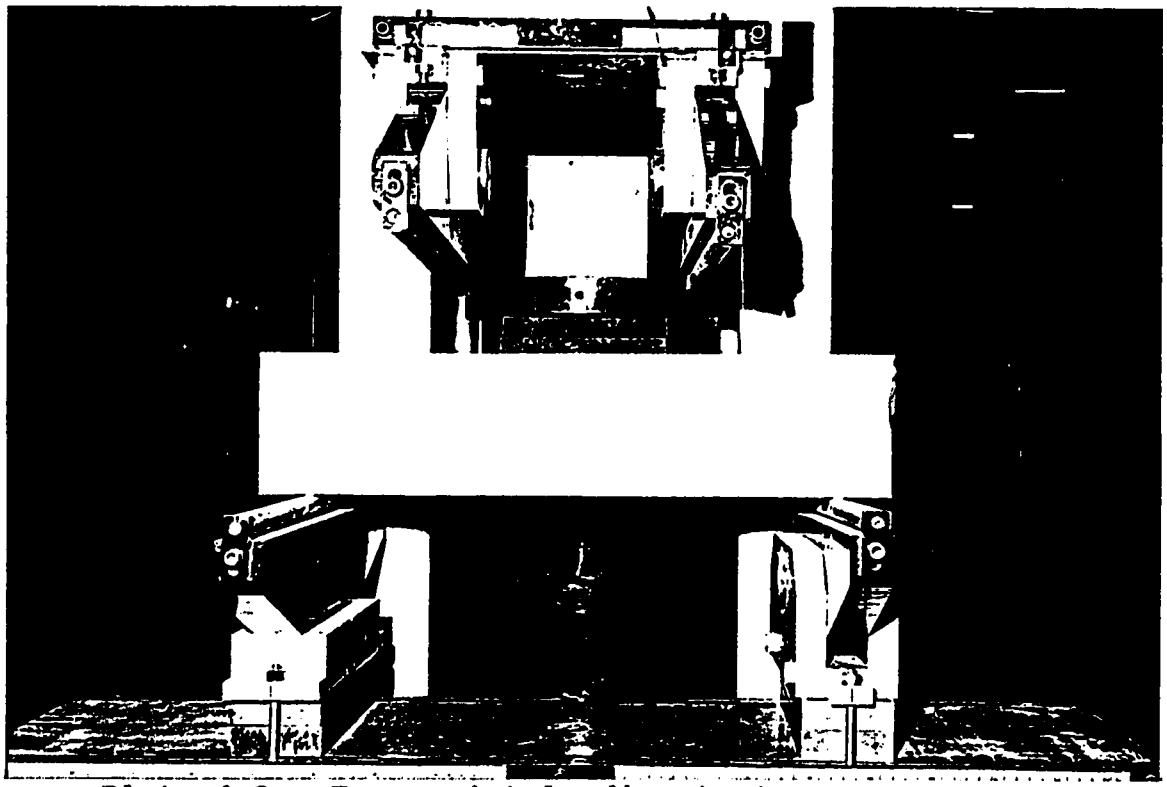

Plate 4.9 : Four point loading test

4.6 Permeability Phase

This phase considered the evaluation of the permeability values of the various concretes, including those that were cast and those that were cored. The permeability expressed by the maximum depth of water penetration through the specimen according to the German Standard test (DIN 1048) was evaluated for both uncycled and cycled concrete specimens. The following subsections explain the processes of fabrication, casting, curing, cycling, preparation and testing of specimens.

4.6.1 Fabrication

Three types of specimens were used: cubes, cylindrical cores, and cast cylinders. Cubes were 6"x6"x6", cores 6"x6", and cylinders 3"x6" in dimension. Eight 6" cubes were cast for every group of GREFC, GRYDC, GJDHC, GSMXC, GSPLC, and GLTXC. Ten 6" diameter cores were drilled by means of an electric driven Hilti core driller from reinforced concrete slab panels located at the laboratory exposure site (Plate 4.10). Four groups GC, GS50, GS45, and GS40 of reference uncycled concrete cube specimens were made of the same mix design as the drilled cores. All cubes and cores were tested for permeability while cylinders were tested for compressive strengh.

Plate 4.10 : Coring procedure

4.6.2 Casting

Both cube and cylinder specimens were cast in steel molds. Molds were well oiled to ease the demolding process. Materials of the various mixes were weighed, first thoroughly mixed dry, then the required amount of water was added in small quantities at three to four intervals. The contents were left to agitate in the mixer till a homogeneous cement paste covered all coarse aggregate particles. A slump test was taken directly after mixing. The cubes and cylinders were cast in the molds in two equal layers of approximately 3 inches thick. Each layer was sufficiently vibrated till most of the air bubbles escaped from the surface of the fresh concrete. The last layer was then trowelled off smoothly and plastic sheets were used to cover up the trowelled surface preventing water evaporation from the concrete surface. Both cube and cylinder specimens were demolded two days later.

4.6.3 Curing

All cube and cylinder specimens of groups GREFC, GRYDC, GJDHC, GSMXC, GSPLC, and GLTXC were left in their molds covered by plastic sheets for two days, after which they were demolded. Curing was commenced immediately after demolding, and specimens were immersed in laboratory water tanks for another 28 days. Then they were removed from the

water tanks and left to dry for another two days in ambient room temperature in the laboratory. Cube specimens were then ready for cycling while cylinders were ready for compression testing. For groups GC, GS50, GS45, and GS40, cube and cylinder specimens were demolded after two days. Two cubes and two cylinders of each of the above four groups received good curing by being covered with hessian burlap that was watered twice daily for a duration of seven days, then they were uncovered and left exposed for the remaining 21 days of curing. The other two cubes and two cylinders received bad curing where they were covered with burlap and watered only once on the first day immediately after being demolded, then they were uncovered and left exposed for the remaining 27 days of curing. The curing regimes were selected in order to match the curing of the reinforced concrete slabs at the exposure site, according to casting details as reported in the Progress Report of the National Bridge Deck Cracking {66}.

4.6.4 Thermal Cycling

Only six of eight cubes from every group of GREFC, GRYDC, GJDHC, GSWDC, GSRTC, GSPLC, and GLTXC were cycled in the laboratory oven, while all four cubes of each group of GC, GS50, GS45, and GS40 were uncycled and tested for permeability directly after curing. The six cubes were cycled so that each two received 45,90, and 120 thermal

cycles, before permeability testing. Cube specimens were placed in the oven and heated up to 80 degrees Celsius for a duration of six hours. The oven then was shut off and the doors opened, then moderate speed fans were directed to cool the specimens down to room temperature (approximately 27 degrees Celsius) for another six hours. The heat/cool cycle mentioned was repeated twice daily for all cube specimens till the specified number of cycles was achieved, afterwhich they were removed from the oven and tested for permeability.

The naturally cycled core samples were taken from reinforced concrete slab panels left outside in the laboratory exposure site (Plate 4.11). These slab panels were cast two and half years ago {66}. Since then, natural thermal cycling of the core specimens has taken place.

4.6.5 Preparation for Testing

Only core specimens had to be treated before being subjected to permeability testing. The sides of the core specimens were very porous therefore leakage occured and the water pressure of the permeability test machine could not be constantly maintained throughout the test. Hence there was a need to confine the sides with a material that sustained the pressure allowing the water to penetrate through the specimen and not leak from its sides. A pressure resistant epoxy resin putty was used and all core specimens were

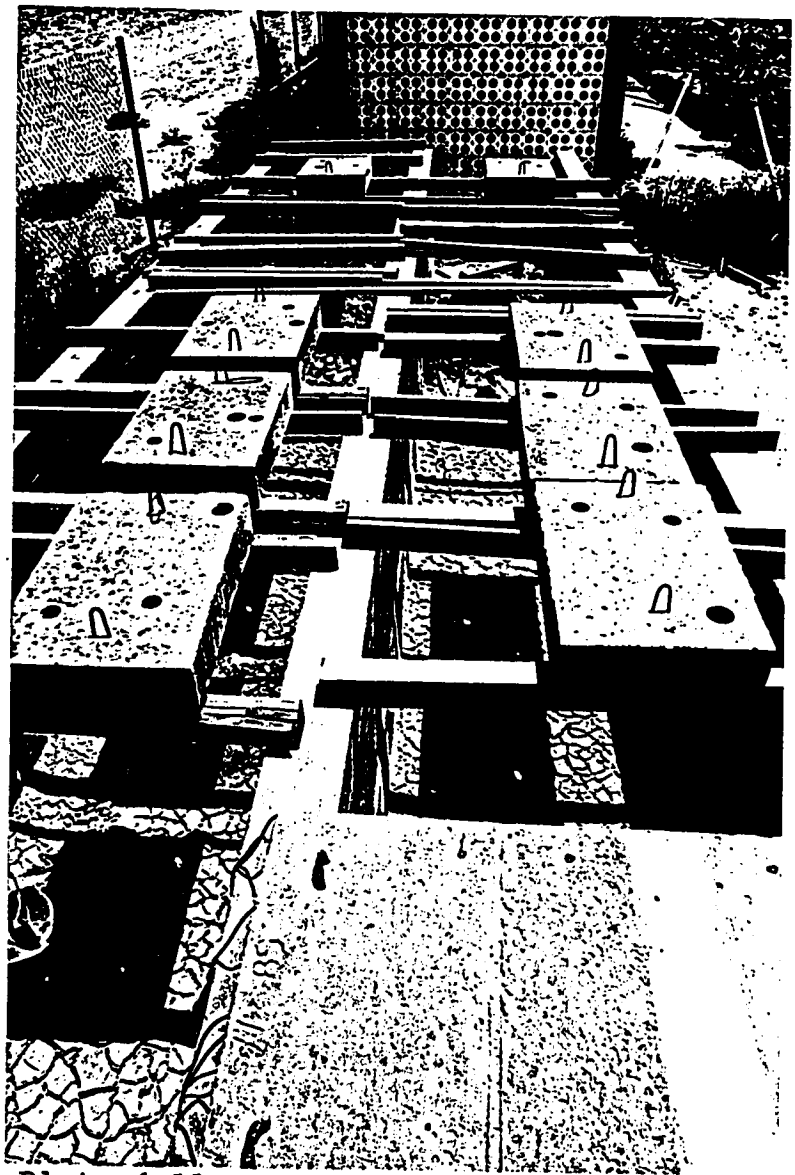

Plate 4.11 : Slabs at the exposure site

covered on the sides by a homogeneous thin layer that clogged up all leaking areas. The cores were then subjected to permeability testing after the epoxy resin had finally set and achieved full strength.

Cube specimens that were cast in steel molds were impervious due to the formation of a smooth dense cement paste layer at the sides caused during the vibration process. Cylinders were capped by a bituminous material to allow uniform stress distribution during compression testing.

4.6.6 Testing

All cubes and cores were subjected to permeability testing, while cylinders were crushed for compressive strength determination by use of the Toni Pact 3000 machine in the lab.

4.6.6.1 Permeability Test

Cubes and core specimens were placed in the permeability test machine compartments between the rubber gaskets connected to the upper and lower steel plates (Plate 4.12). The purpose of the rubber gaskets is to prevent any water leakage from the bottom side of the specimen. The compartment valves were turned to the open position and the water level rose till it came in contact with the specimen.

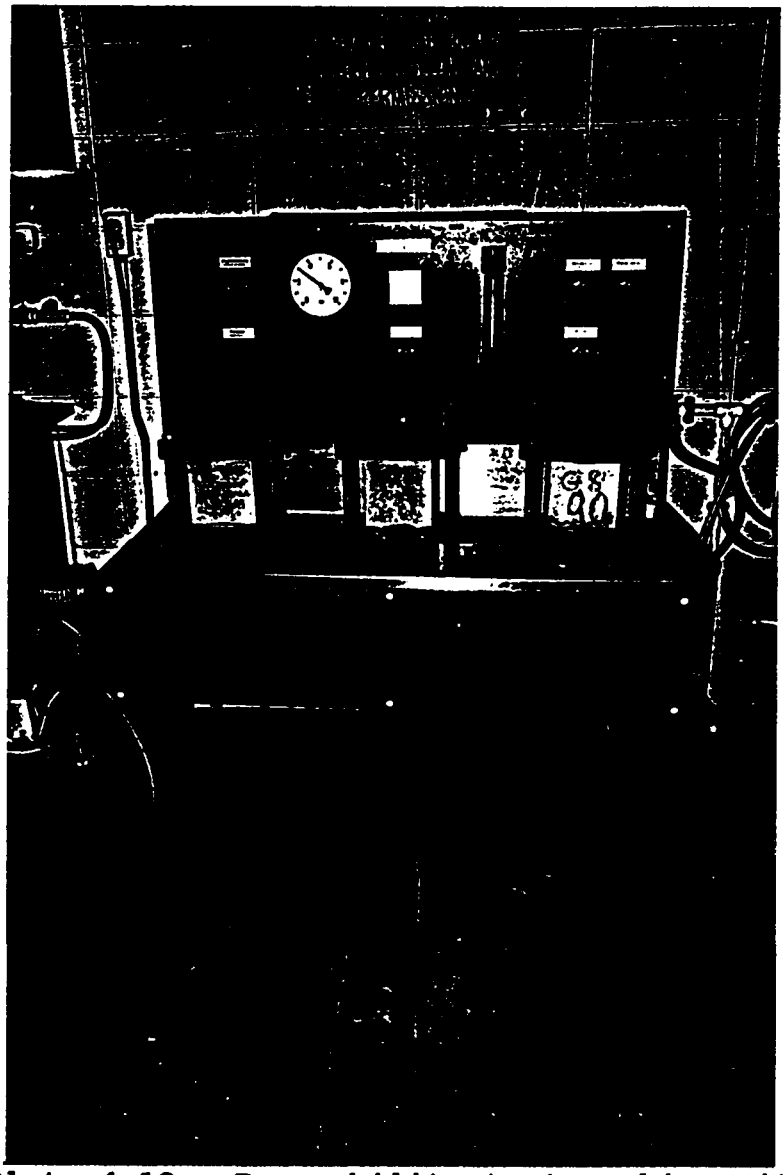

Plate 4.12 : Permeability test machine with cube specimens

All nuts were tightened well and approximately an equal amount of torque was applied to each nut, maintaining a uniform grip at all sides of the specimen. When the water level in the water column was assured to be full, the water supply valve was closed, then the pressure adjustment tap was turned till the pressure dial gage showed a one bar value. The specimens were left under one bar pressure for two days while frequently checking the pressure dial gage for adjustment of any pressure variation, whether rise or fall. Then the pressure was increased to three bars for a third day, and finally 7 bars for the fourth day. Immediately after removing the specimens from the test machine, the specimens were split into two halves by placing each between two steel rods and then applying compression i.e. as in a split tension test. The maximum depth of water penetration was recorded to be the permeability value of that specimen.

4.7 Coefficient of Thermal Expansion Test

The coefficient of thermal expansion of Riyadh aggregate was determined while Jabal Dhahran and Abu-Hadriyah aggregates were as previously determined by Muse {45}.

4.7.1 Specimen Preparation

Boulders were selected from three locations along Riyadh Al-Kharj highway at distances of 10,17, and 40 Km from the center of Riyadh, and then transported to the King Fahd University of Petroleum and Minerals in Dhahran. These boulders were specially chosen by visual inspection, to be sound, and in good condition possessing little or no cavities. They were selected so that 10 cm cube specimens were sawed from them. Using an electrical circular saw, six 10 cm cube specimens were sawed from the boulders, two specimens for each location mentioned (Plate 4.13). These cube specimens were washed, cleaned and dried, then marked according to their origin. Twelve Demec gages (locating discs) were adhered by a heat resistant epoxy resin, on three mutually perpendicular sides. Four gages were stuck on each side on the ends of a virtual right angled cross (Fig. 4.4). The distance between the two opposing discs was fixed by using the fixing bar of the Demec gage reader (Plate 4.14). Then the epoxy resin was left to set and achieve full strength before testing.

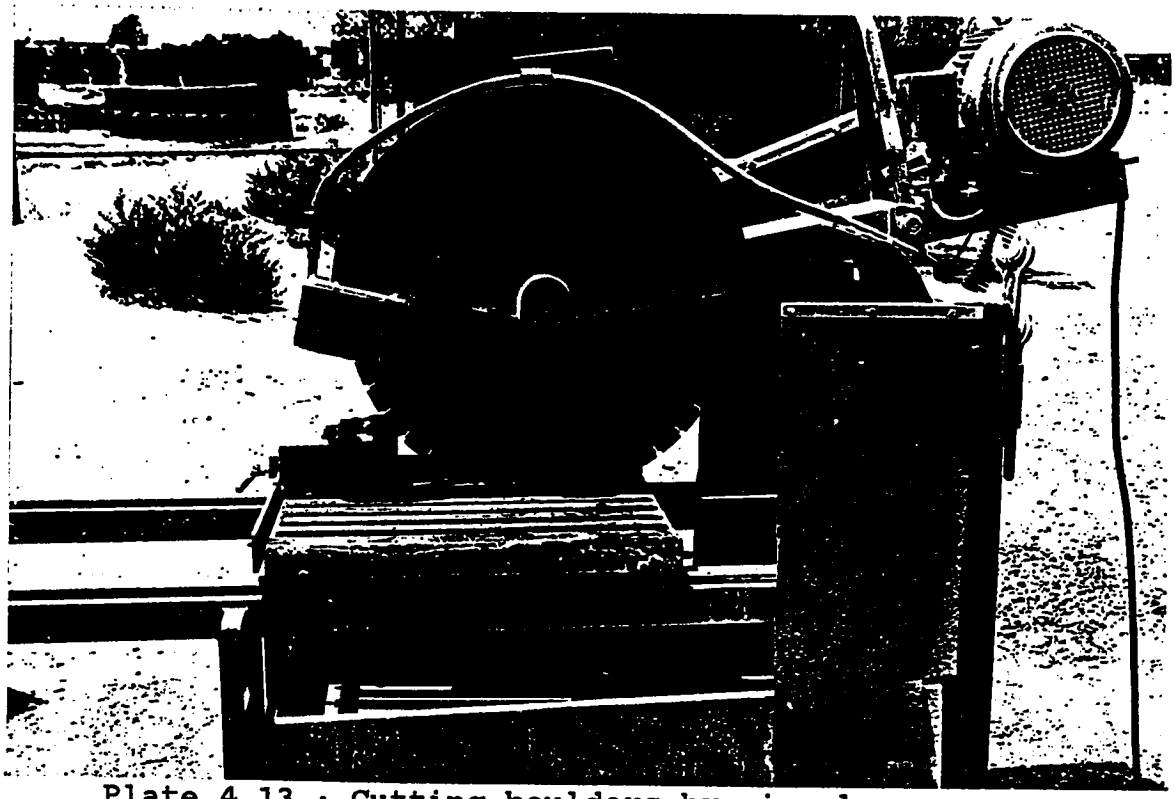

Plate 4.13 : Cutting boulders by circular saw

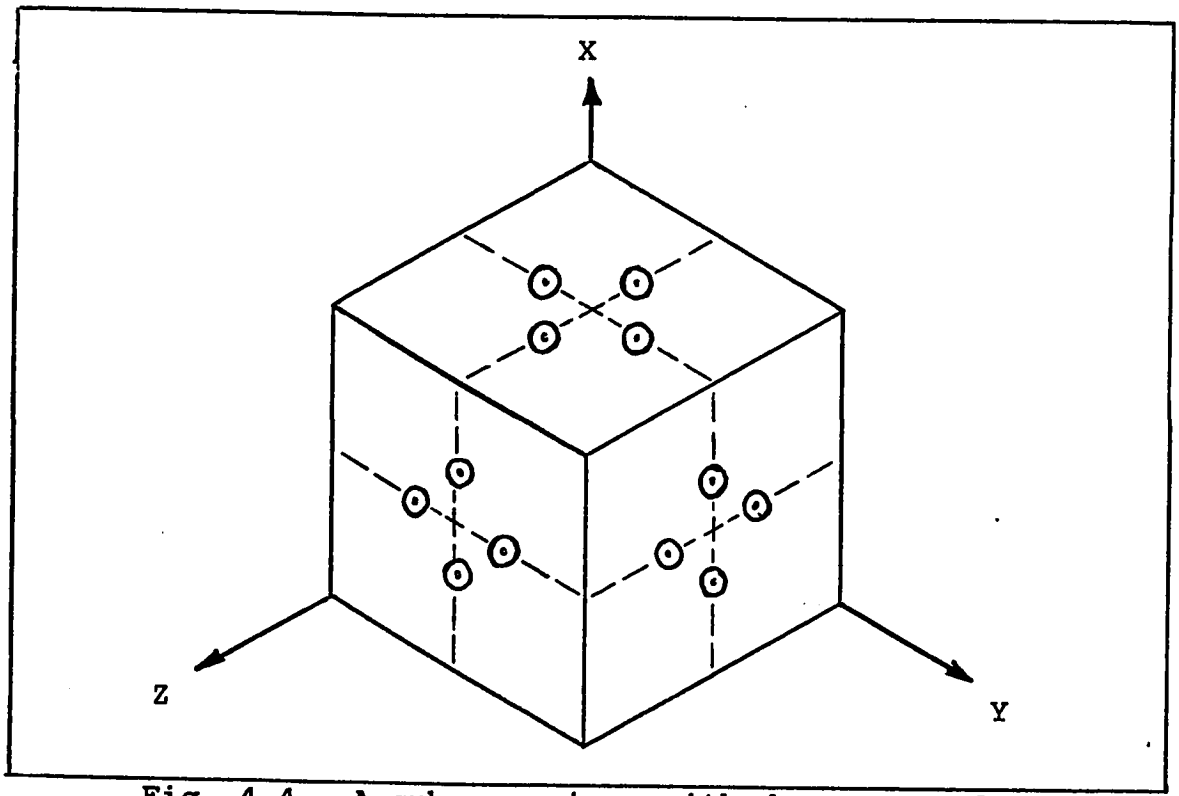

Fig. 4.4 : A cube specimen with demec gage locations

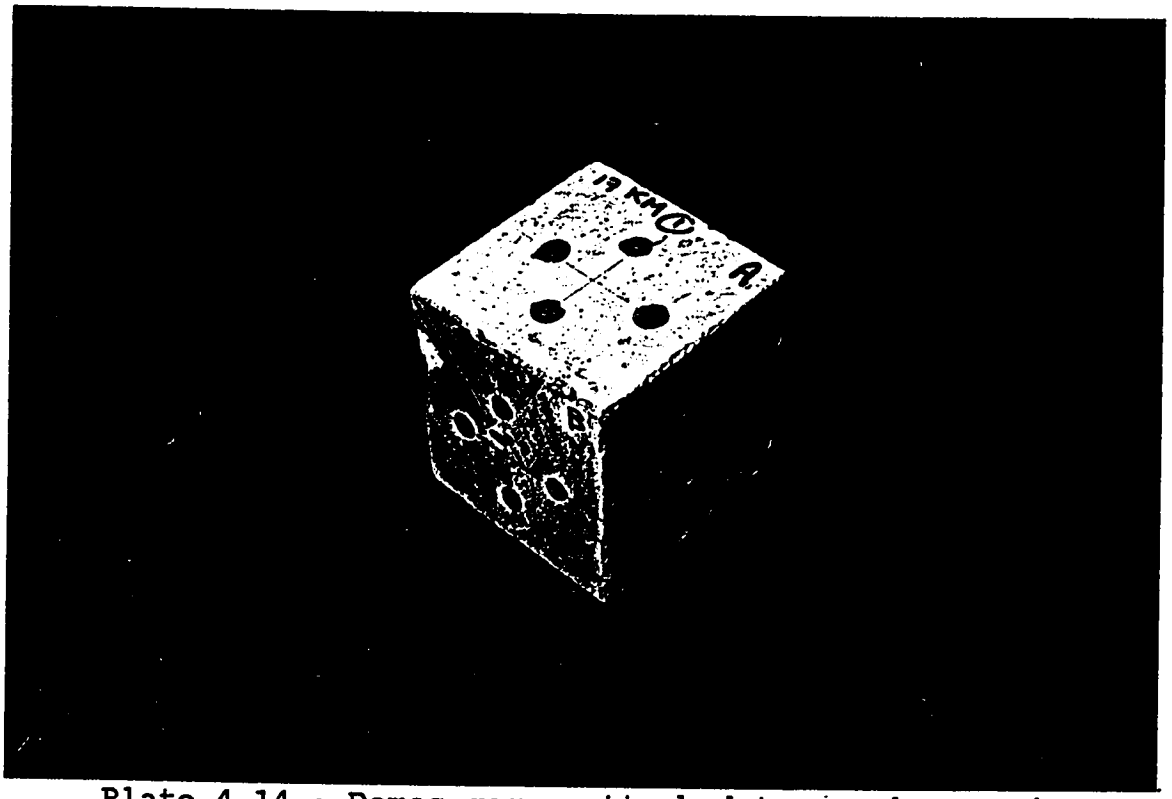

Plate 4.14 : Demec gages attached to a cube specimen

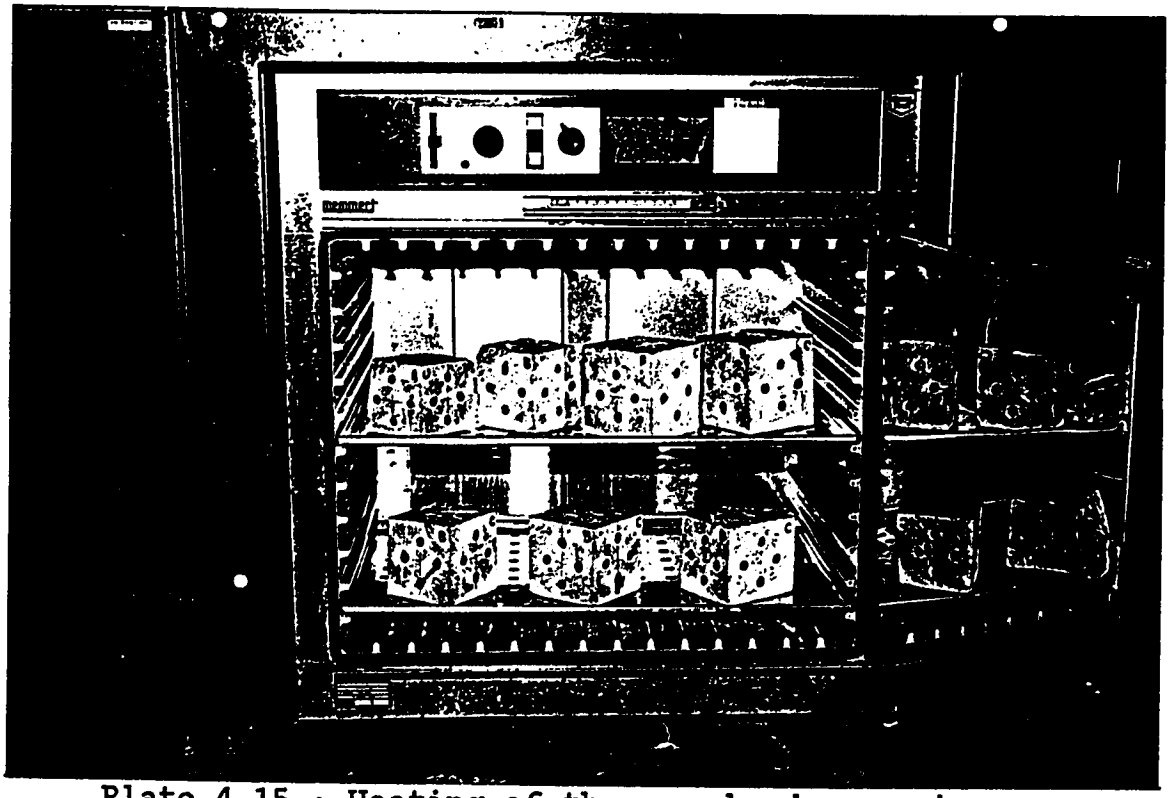

Plate 4.15 : Heating of the sawed cube specimens

4.7.2 Testing

At the beginning of the test, the distance between every two opposite discs of all six cubes specimens was measured at room temperature (27 degrees Celsius) using the Demec gage micrometer reader. The specimens were then heated in an oven for more than eight hours up to 40 degrees Celsius (Plate 4.15) and the distance between each opposite locating discs was remeasured by the Demec gage micrometer reader. These measurement were repeated for temperatures 60,80, and 100 degrees Celsius, then the temperature was decreased in a reverse manner and measurements were again taken at 80,60,40 and room temperature (27 degrees Celsius). The whole process of heating up the specimens to 100 degrees Celcius then cooling them down to room temperature in a stepwise fashion was repeated for a second cycle and measurements were once again recorded. Following the thermal coefficient of Riyadh aggregate was determined.

RESULTS AND DISCUSSION

5.1 Analysis and Results

This portion considers the analysis of the data produced by testing, and results. The following subsections consider each testing seperately namely the fracture toughness, modulus of rupture, permeability, coefficient of thermal expansion, and finally compressive strength. Test results would be illustrated seperately regarding the variables, aggregate type, mix design proportions, successive wetting and drying, support restraint, and admixtures.

5.1.1. Fracture Toughness

This section deals with the details of development of the fracture toughness results, for the cast groups GREFC, GRYDC, GJDHC, GSMXC, GSWDC, GSRTC, GSPLC, and GLTXC. From beam preparation and fracture toughness testing discussed in the previous chapter, a P-u history plot was produced for each specimen (Fig. 5.1). During fracture toughness testing the crack length a corressponding to every load/unload cycle was recorded. The compliance C of each load cycle was calculated to be the inverse slope of the loading portion of that cycle. Tabulated data showed the peak load P, compliance C, permanent deflection δ_p and crack length a (Table 5.1).

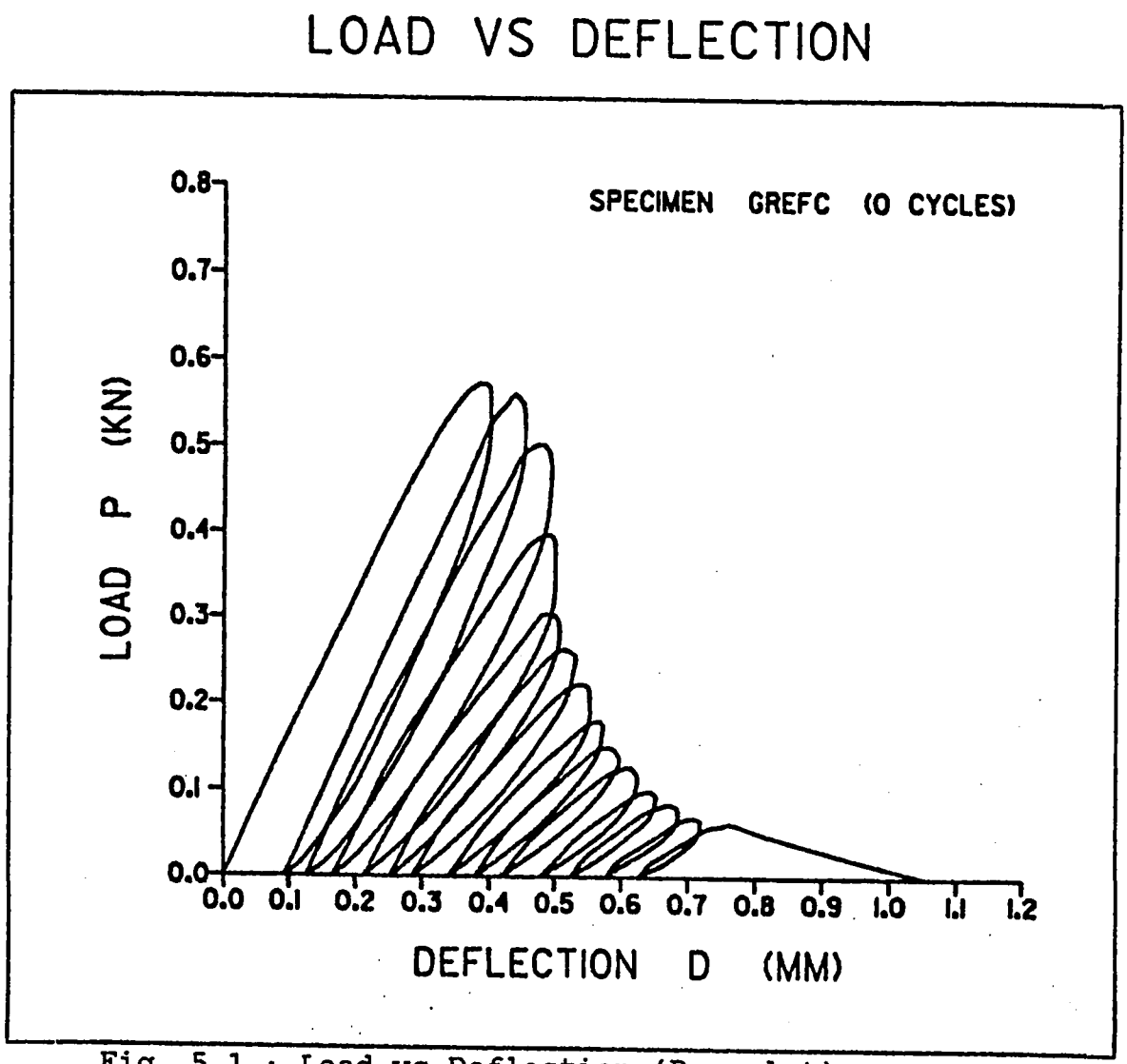

Fig. 5.1 : Load vs Deflection (P-u plot)

Table 5.1 : P-u history plot data

Cycle No.	Peak Load P (KN)	Compliance C (mm/KN)	Permanent Deflection dp (mm)	Crack Length a (mm)
0	0.575	0.618	0.000	61
1	0.560	0.571	0.097	71
2	0.505	0.667	0.127	82
3	0.400	0.889	0.170	89
4	0.308	0.952	0.213	91
5	0.265	1.046	0.253	94
6	0.223	1.180	0.290	99
7	0.180	1.311	0.347	103
8	0.153	1.477	0.380	106
9	0.128	1.604	0.420	107
10	0.100	1.711	0.480	109
11	0.085	1.750	0.530	111
12	0.073	1.833	0.580	113
13	0.065	1.933	0.633	115

The fracture toughness G_{IC} of each beam was calculated according to the Gurney approach using equation (50). The equation consists of an elastic and plastic contribution to the fracture toughness. The elastic portion of the equation possesses the first derivative of compliance C with respect to crack length a. Similarly, the plastic portion possesses the first derivative of permanent deflection δ_p with respect to crack length a. Therefore the relation between compliance C and crack length a was to be determined. Also, the relation between permanent deflection δ_p and crack length a was required.

Using a Fortran curve plotting program built in the PLOTSYS of the IBM 370 main frame, both compliance C vs crack length a, and permanent deflection δ_p vs crack length a, were plotted (Fig. 5.2 & 5.3). The data points were regressed and the best fit of a second degree polynomial was plotted and its equation formulated. These two equations were then differentiated once with respect to the crack length a. After which they were placed in a basic program that segmentally calculated the fracture toughness G_{IC} (for each load cycle) and presented (Table 5.2). The highest value of fracture toughness calculated in the table was to be taken as the critical fracture toughness of that beam specimen.

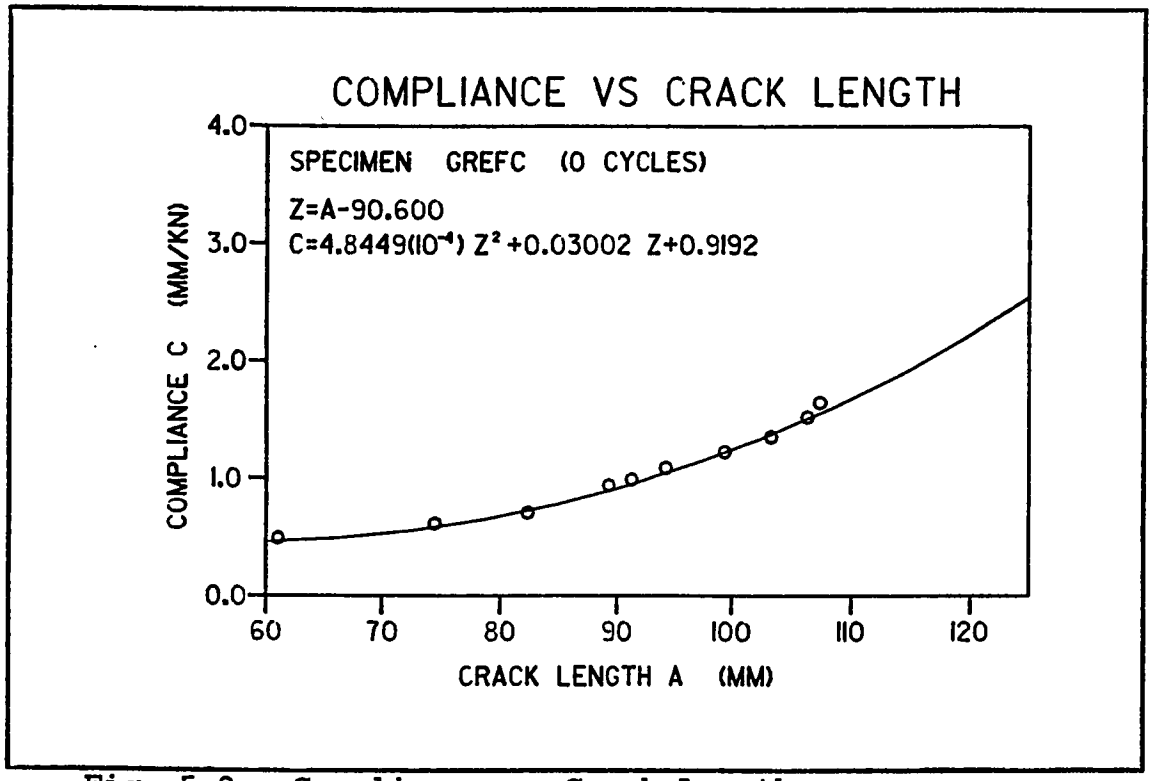

Fig. 5.2 : Compliance vs Crack Length

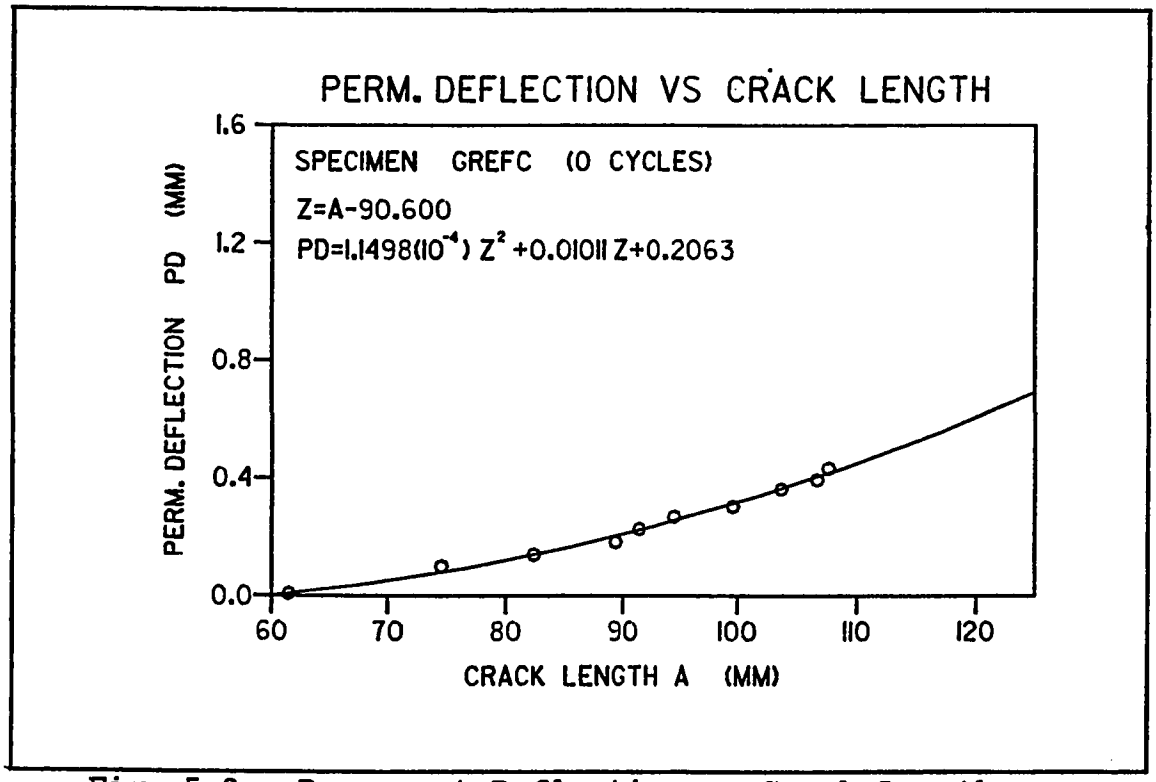

Fig. 5.3 : Permenant Deflection vs Crack Length

Table 5.2 : Calculation of fracture toughness

1 P (KN)	2 P1*P2 (KN^2)	3 P1+P2 (KN)	4 dC/da (1/KN)	5 ddp/da	6 C2xC4 (KN)	7 C3xC5 (KN)	8 C6+C7 (KN)	9 * Ge=C6xK (KN/mm)	10 * Gp=C8xK (KN/mm)
			(10^{-6})	(10^{-6})	(10^{-6})	(10^{-6})	(10^{-6})		
0.575	0.3220	1.135	1.338	3.303	0.431	3.749	4.180	4.241	41.142
0.560	0.2828	1.065	13.935	6.293	3.941	6.702	10.642	38.787	104.749
0.505	0.2020	0.905	21.687	8.132	4.381	7.360	11.740	43.117	115.556
0.400	0.1232	0.708	28.470	9.742	3.507	6.897	10.405	34.522	102.410
0.308	0.0816	0.573	30.408	10.202	2.482	5.846	8.328	24.428	81.965
0.265	0.0591	0.488	33.315	10.892	1.969	5.315	7.284	19.377	71.692
0.223	0.0401	0.403	38.159	12.042	1.532	4.853	6.385	15.076	62.840
0.180	0.0275	0.333	42.035	12.962	1.158	4.316	5.474	11.394	53.876
0.153	0.0196	0.281	44.942	13.651	0.880	3.836	4.716	8.663	46.419
0.128	0.0128	0.228	45.911	13.881	0.588	3.165	3.753	5.784	36.935
0.100	0.0085	0.185	47.849	14.341	0.407	2.653	3.060	4.003	30.117
0.085	0.0062	0.158	49.787	14.801	0.309	2.339	2.648	3.041	26.058
0.073	0.0047	0.138	51.725	15.261	0.245	2.106	2.351	2.416	23.144
0.065	* K = (1/2t) = 1/(2x2x25.4) = 1/101.6 (1/mm)								

For each group the fracture toughness was calculated for both cycled and uncycled specimens (Table 5.3). Then the percentage difference between cycled and uncycled beam specimens was calculated for the various cycles (Table 5.4). This percent difference was then plotted vs the number of thermal cycles N. The influence of the TICC phenomenon on the fracture toughness G_{IC} has been affected by the different variables considered.

Examining the three types of aggregates i.e. Riyadh, Abu-Hadriyah, and Jabal Dhahran it was found that considering the fracture toughness values, Riyadh aggregate (GRYDC) showed a more superior performance in a TICC environment than both Abu-Hadriyah (GREFC) and Jabal Dhahran (GJDHC) (Fig. 5.4). The fracture toughness of the Riyadh aggregate concrete increased on cycling up to approximately 120 thermal cycles, while that of both Abu-Hadriyah and Jabal Dhahran aggregate concretes decreased immediately on thermal cycling, with Jabal Dhahran showing greater reduction than Abu-Hadriyah aggregate.

Investigating the fracture toughness of both the reference Abu-Hadriyah concrete (GREFC) with a coarse/fine aggregate ratio of 1.5 and the sandy mix (GSMXC) with a coarse/fine aggregate ratio of 0.5, it is obvious that mixes possessing relatively high amounts of fines speed up the TICC deterioration process (Fig. 5.5).

Table 5.3 : Fracture toughness of cast concrete

Group ID	Cycling Condition	Fracture Toughness after cycling					
		0	45	90	120	180	210
GREFC	Cycled	130	127	128	130	---	---
	Uncycled	130	85	118	106	---	---
GRYDC	Cycled	85	83	83	85	---	---
	Uncycled	85	122	118	80	---	---
GJDHC	Cycled	107	102	102	107	---	---
	Uncycled	107	53	83	88	96	---
GSMXC	Cycled	162	162	162	162	131	---
	Uncycled	162	63	85	72	---	---
GSPLC	Cycled	110	108	109	110	---	---
	Uncycled	110	xxx	108	107	---	---
GLTXC	Cycled	113	81	96	113	147	---
	Uncycled	113	87	122	97	100	---
GSRTC	Cycled	109	109	109	118	---	---
	Uncycled	109	111	89	60	---	---
GSWDC	Cycled	114	110	110	114	110	112
	Uncycled	114	122	68	91	81	112

Table 5.4 : Percent difference in fracture toughness

Group ID	% Difference due to cycling					
	0	45	90	120	180	210
GREFC	0.0	-33.1	-7.8	-18.5	---	---
GRYDC	0.0	47.0	42.2	-5.9	---	---
GJDHC	0.0	-48.0	-18.6	-17.8	-26.7	---
GSMXC	0.0	-61.1	-47.5	-55.6	---	---
GSPLC	0.0	xxx	-0.1	-2.7	---	---
GLTXC	0.0	7.4	27.1	-14.2	-32.0	---
GSRTC	0.0	1.8	-18.3	-49.2	---	---
GSWDC	0.0	10.9	-38.2	-20.2	-26.4	0.0

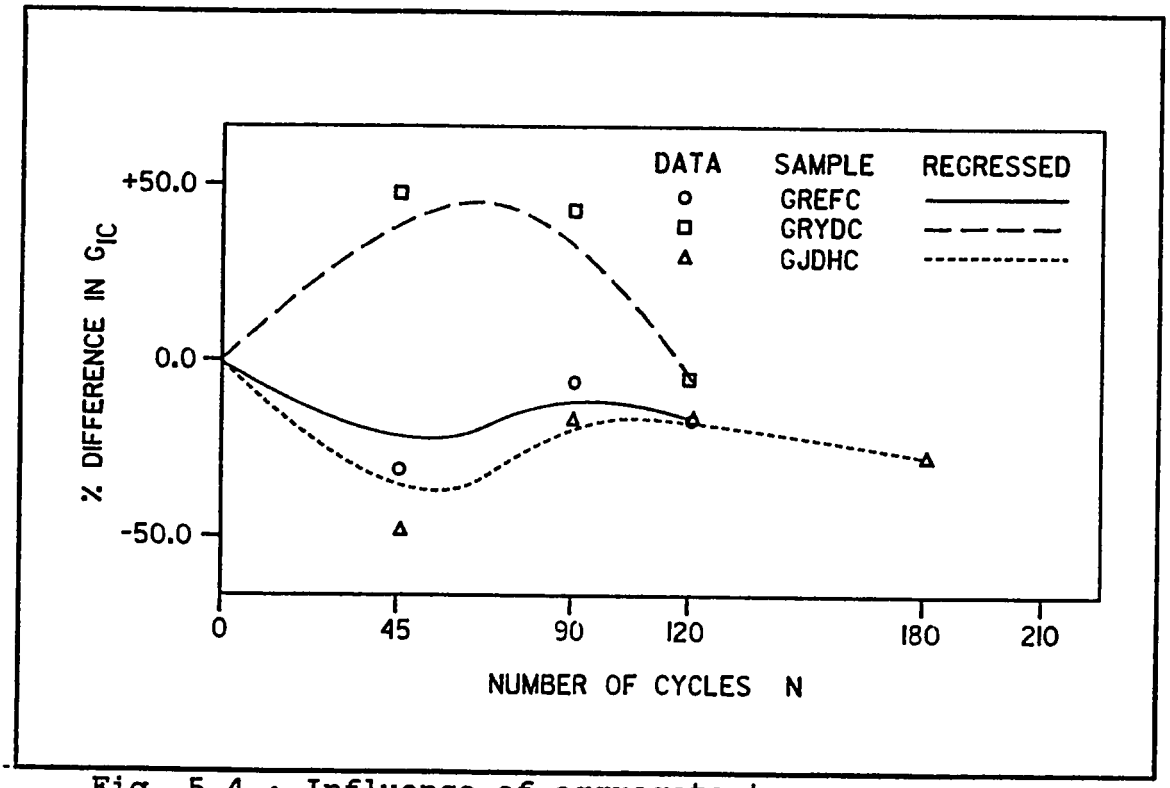

Fig. 5.4 : Influence of aggregate type on fracture toughness

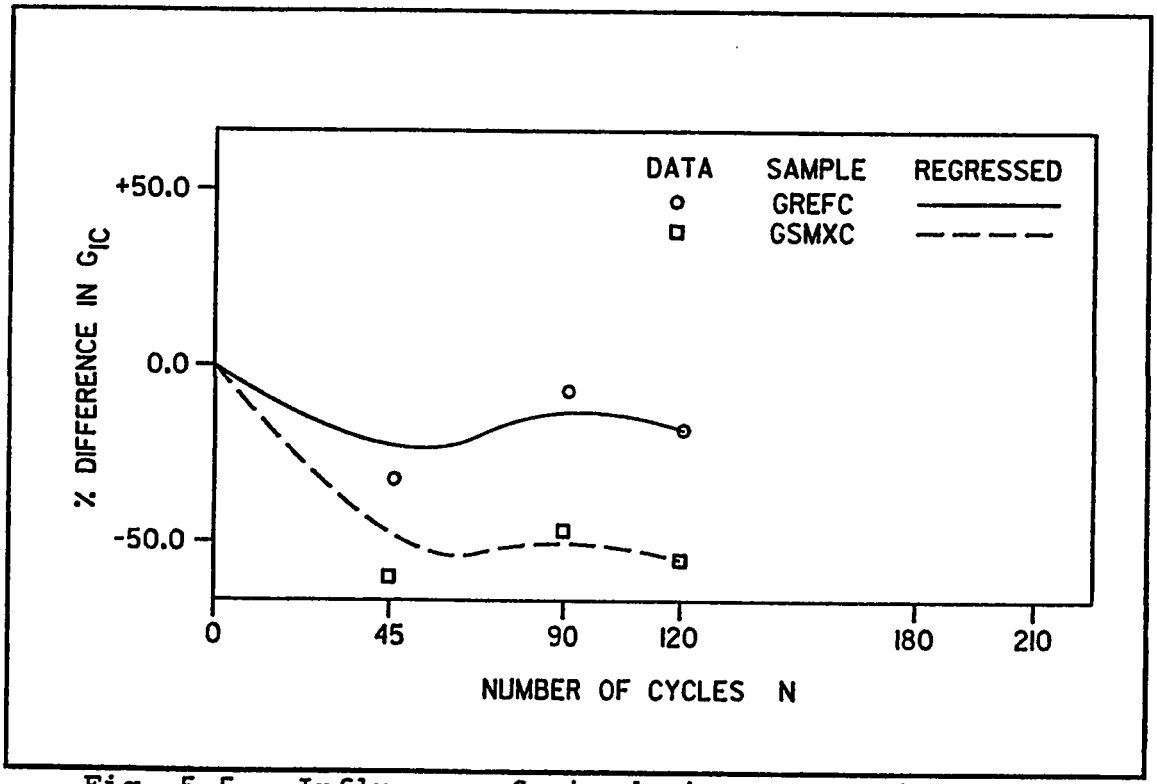

Fig. 5.5 : Influence of mix design proportions on fracture toughness

This is mainly due to the severe harmful effect caused by the thermal coefficient of expansion of the fines, where the coefficient of thermal expansion of sand plays a great role in the damaging process. Therefore sandy mixes in a TICC environment are more susceptible to thermal deterioration than well proportioned mixes, especially where the fines and coarse proportions are of different origin. In this work, the fine aggregate was quartzitic sand, with the coarse aggregate being limestone.

Looking into the influence of alternate wetting and drying on the fracture toughness by comparing both reference Abu-Hadriyah concrete (GREFC) and successive wet/dry concrete (GSWDC) (Fig. 5.6), one may state that presence of moisture in the early cycles may increase the fracture toughness of the concrete which is mainly due to further hydration of unhydrated cement at higher temperatures in addition to autogeneous healing that may possibly occur. On the other hand after complete hydration is nearly reached, presence of moisture affects the thermal properties of the concrete components and the difference in coefficient of thermal expansion of the concrete constituents may be reduced, leading to less incompatibility hence reducing the rate of TICC deterioration.

Presence of prestress on concrete (the field case) seems to aggravate the deterioration caused by TICC environment.

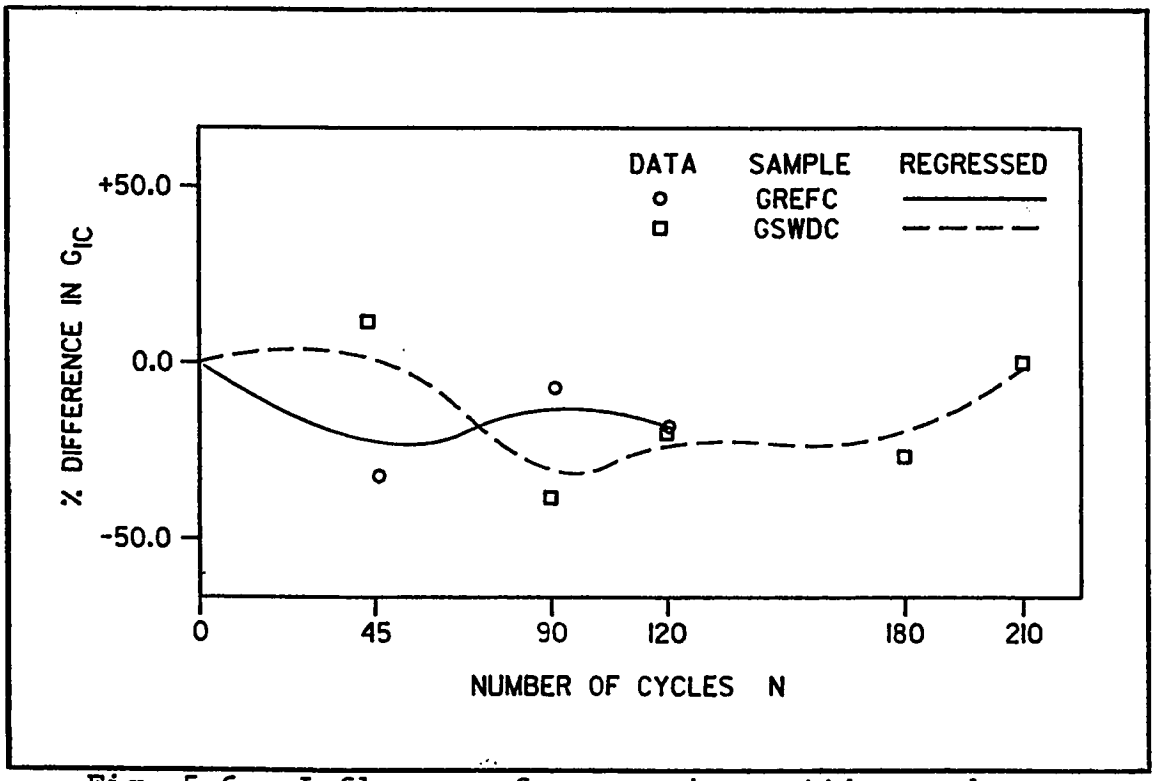

Fig. 5.6 : Influence of successive wetting and drying on fracture toughness

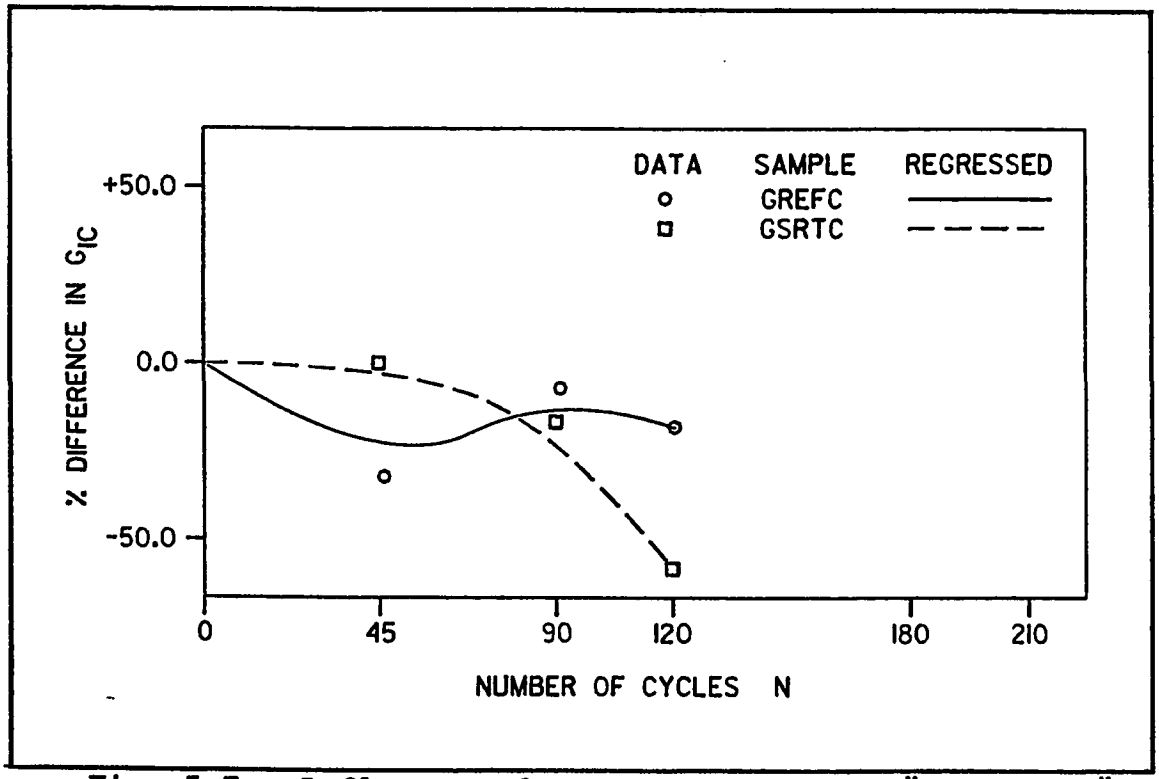

Fig. 5.7 : Influence of support restraint "prestress" on fracture toughness

This is well illustrated when viewing the fracture toughness curves (Fig. 5.7) of support restrained concrete (GSRTC) and reference Abu-Hadriyah concrete (GREFC), where the concrete under prestress exhibits rapid loss of fracture toughness while the reference concrete shows better resistance to loss of fracture toughness. The reasonable explanation of the rapid loss of fracture toughness is that certain zones of the concrete beam are originally under tensile stress, therefore when subjected to a TICC environment, tensile stresses due to the thermal incompatibility add up to those already existing from prestress. This superposition of tensile stresses highly accelerates the TICC damaging effect.

Examining the two types of admixtures super plasticizer (GSPLC) and latex (GLTXC), revealed that addition of admixtures to the mix enhances the resistivity of the concrete subjected to TICC environment to withstand loss of fracture toughness (Fig.5.8). The fracture toughness value of both super plasticizer and latex concretes showed improvement and stability up to about 120 thermal cycles, after which slight deterioration started. The latex concrete exhibited a higher rate of TICC deterioration than the super plasticizer concrete after 120 heat cycles. However, in general, addition of admixtures in the mix beneficially aids in retarding the TICC damage.

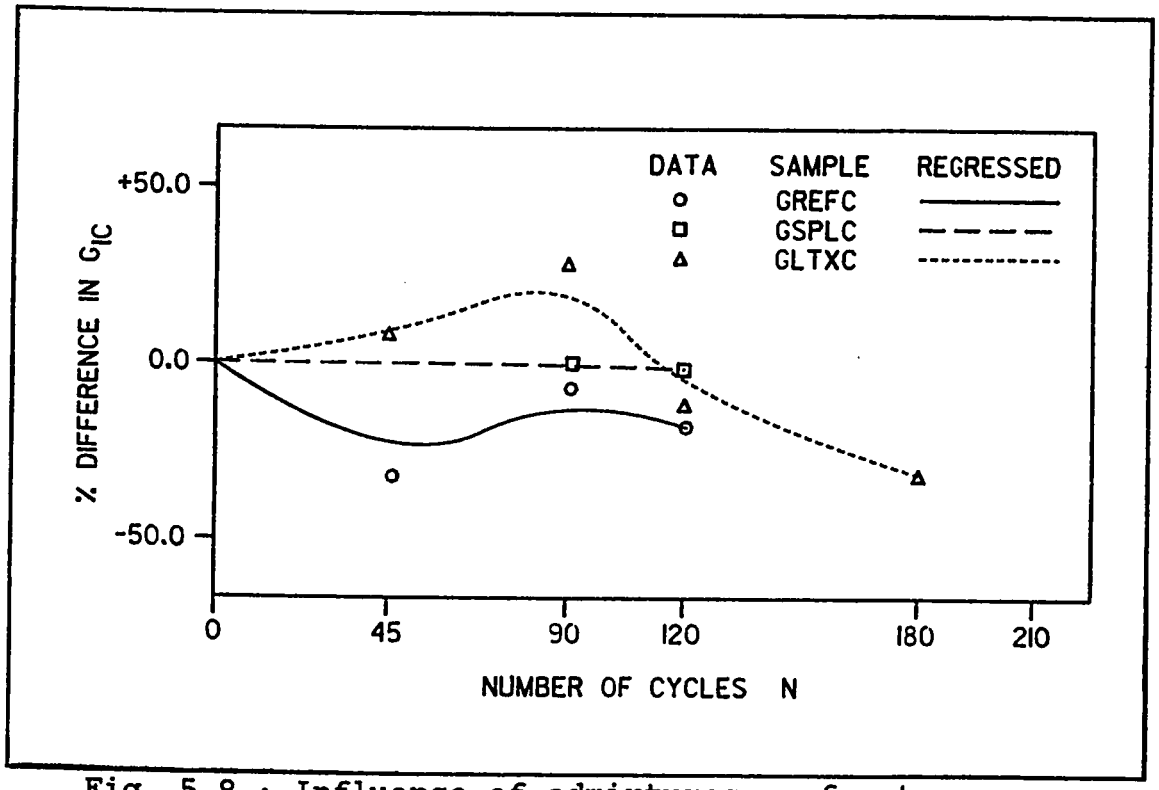

Fig. 5.8 : Influence of admixtures on fracture toughness

5.1.2 Modulus of Rupture

As previously mentioned, the failure load was used in calculating the modulus of rupture for each half beam specimen as obtained after the fracture toughness test. Modulus of rupture of the different cast concrete groups under various cycling are presented (Table 5.5). Also, the percentage difference between cycled and uncycled specimens are shown (Table 5.6). The percent difference in modulus of rupture was then plotted against the number of thermal cycles, where each variable was considered seperately.

The effect of aggregate type on the modulus of rupture indicates that both Abu-Hadriyah and Riyadh aggregate showed an increase in modulus of rupture while Jabal Dhahran aggregate showed a reduction in modulus of rupture due to thermal cycling (Fig. 5.9). Although Abu-Hadriyah showed a higher rate of modulus of rupture improvement, still Riyadh possessed the highest modulus of rupture values while Jabal Dhahran aggregate possessed the lowest values.

The influence of the mix design proportions on the modulus of rupture (Fig. 5.10) indicates that by comparing the sandy mix concrete (GSMXC) and the reference concrete (GREFC), concretes containing high amounts of fines exhibit immediate loss in modulus of rupture, which means that the performance of sandy mix concretes is unsatisfactory.

Table 5.5 : Modulus of rupture of cast concrete

Group ID	Number of Cycles					
	0	45	90	120	180	210
GREFC	3.008	4.613	4.960	4.510	---	---
	3.670	5.169	5.145	4.734	---	---
GRYDC	4.969	4.894	5.048	5.229	---	---
	4.779	5.123	4.815	5.610	---	---
GJDHC	4.443	3.872	4.776	4.688	3.083	---
	3.905	3.948	4.718	4.782	3.343	---
GSMXC	3.240	2.678	3.494	3.195	---	---
	4.135	3.249	3.422	3.264	---	---
GSPLC	4.570	5.589	5.565	5.244	---	---
	5.163	5.220	5.725	5.011	---	---
GLTXC	5.583	4.691	5.450	5.728	5.547	---
	5.438	5.734	5.099	5.522	5.111	---
GSRTC	5.287	4.900	4.159	3.162	---	---
	4.776	4.588	4.849	3.132	---	---
GSWDC	5.005	4.697	5.005	4.884	5.976	5.577
	5.145	4.894	5.232	4.446	5.531	6.360

Table 5.6 : Percent difference in modulus of rupture

Group ID	Number of cycles					
	0	45	90	120	180	210
GREFC	3.339	4.891	5.053	4.622	---	---
		46.5%	51.3%	38.4%	---	---
GRYDC	4.874	5.009	4.932	5.420	---	---
		2.8%	1.2%	11.2%	---	---
GJDHC	4.174	3.910	4.747	4.735	3.213	---
		-6.3%	13.7%	13.3%	-23.0%	---
GSMXC	3.688	2.964	3.458	3.230	---	---
		-19.6%	-6.2%	-12.4%	---	---
GSPLC	4.867	5.405	5.645	5.128	---	---
		11.1%	16.0%	5.4%	---	---
GLTXC	5.511	5.213	5.275	5.625	5.329	---
		-5.4%	-4.3%	2.1%	-3.3%	---
GSRTC	5.032	4.744	4.504	3.147	---	---
		-5.4%	-10.5%	-37.5%	---	---
GSWDC	5.075	4.800	5.119	4.665	5.754	5.969
		-5.4%	0.0%	-8.1%	13.4%	17.6%

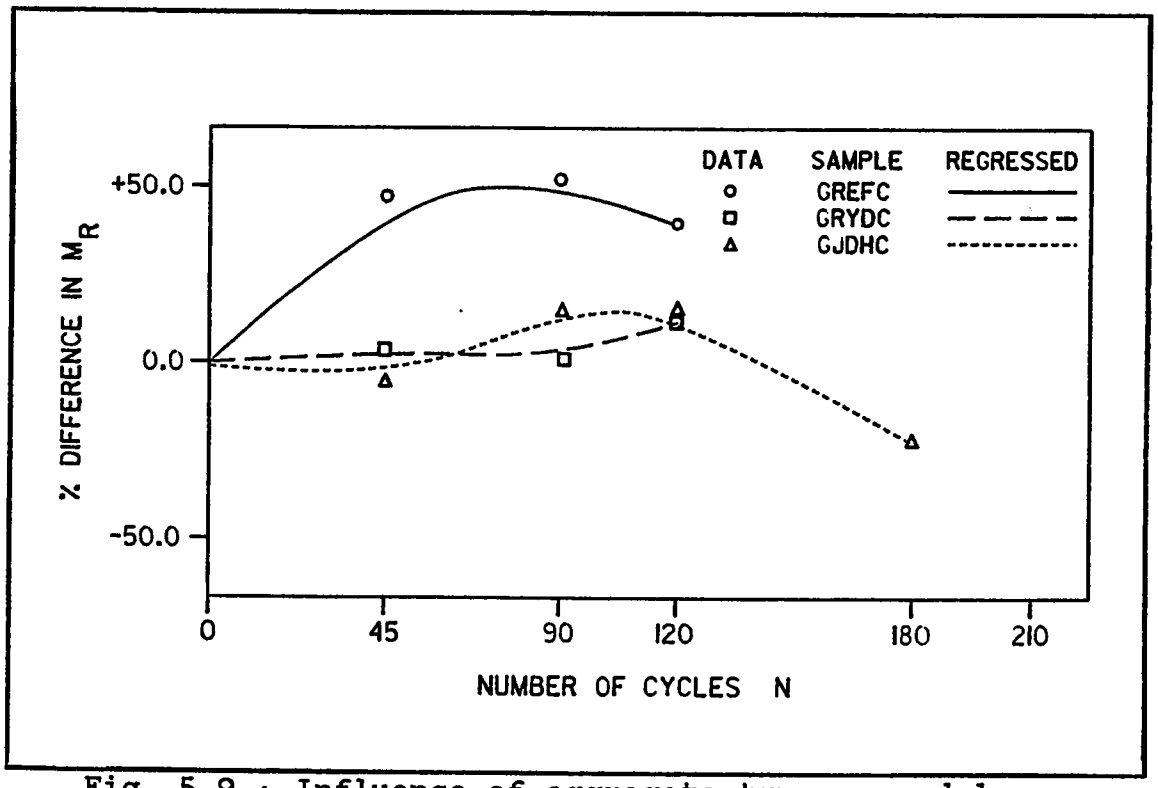

Fig. 5.9 : Influence of aggregate type on modulus of rupture

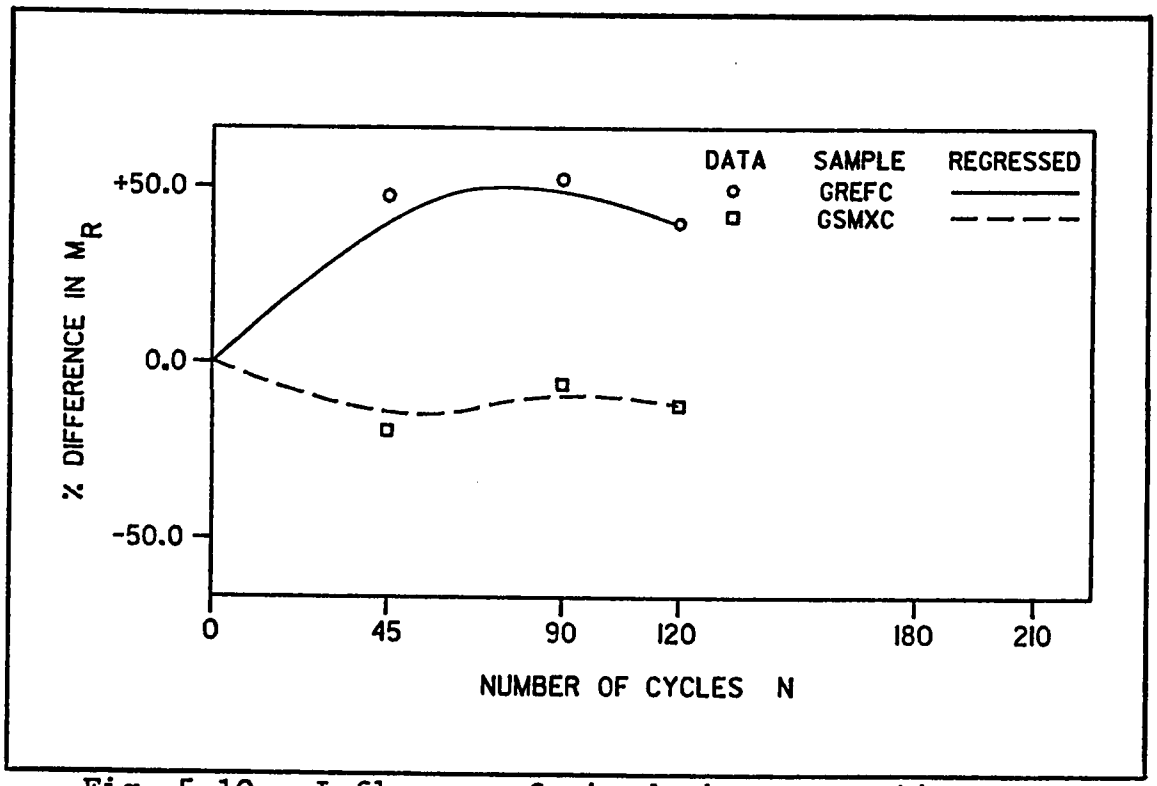

Fig. 5.10 : Influence of mix design proportions on modulus of rupture

This unsatisfactory performance is especially where conditions of a TICC environment prevails. Concretes of well proportioned mix designs gain some increase in modulus of rupture, and they are more suitable in a TICC environment.

The effect of the alternate wetting and drying on the modulus of rupture of concretes under TICC phenomenon of deterioration (Fig. 5.11), showed that soaked concrete (GSWDC) in thermal cycling possessed higher modulus of rupture values that continued to increase after 120 thermal cycles. The reference concrete (GREFC) showed an initial high rate of improvement in modulus of rupture up to 60 cycles followed by a high loss in modulus of rupture onwards. Presence of moisture appears to beneficially aid in arresting damage of concrete in TICC environment.

Initial prestress has a drastically detrimental effect on concrete in TICC environment. Comparing support restrained concrete (GSRTC) and reference concrete (GREFC), it is noticed that the modulus of rupture values of the support restrained specimens are much lower than those of the unstressed referenced specimens (Table 5.5). In addition, the rate of decrease in modulus of rupture for stressed concrete was recorded to be the highest of all other groups (Fig. 5.12). This again proves that presence of stress aggravates the TICC damage where tensile stresses from both prestress and TICC add up.

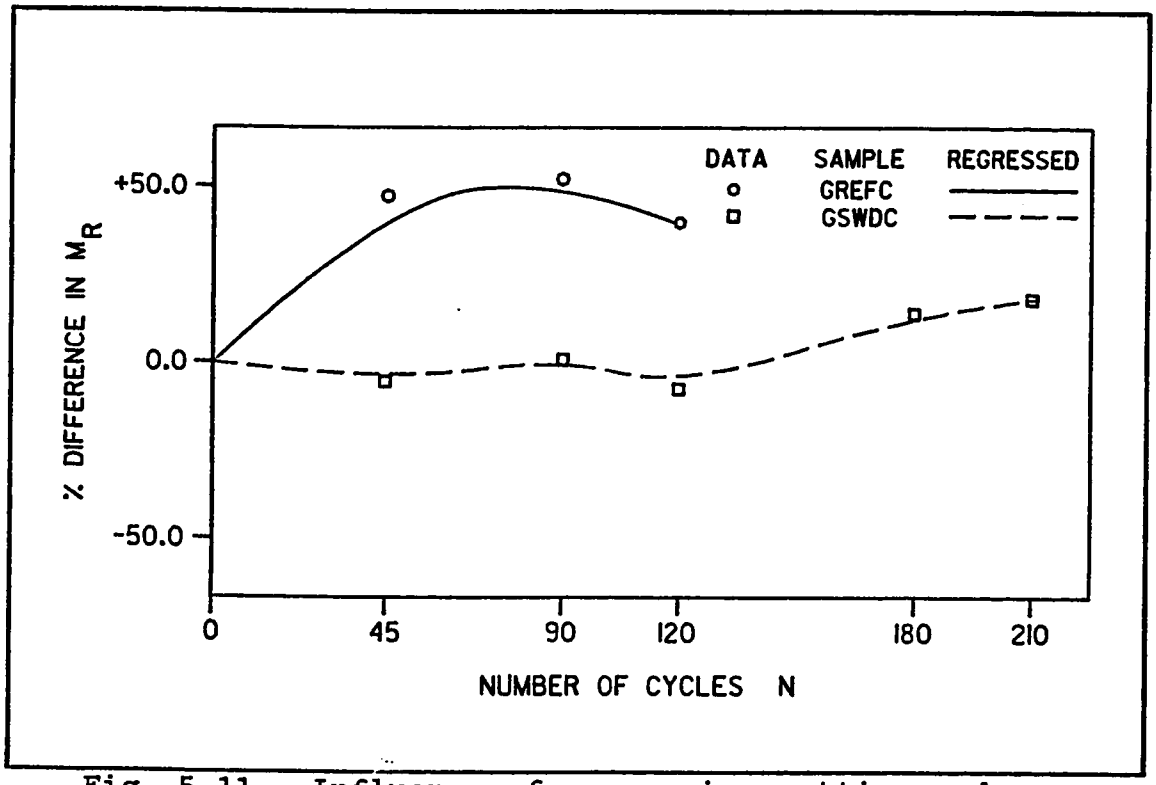

Fig. 5.11 : Influence of successive wetting and drying on modulus of rupture

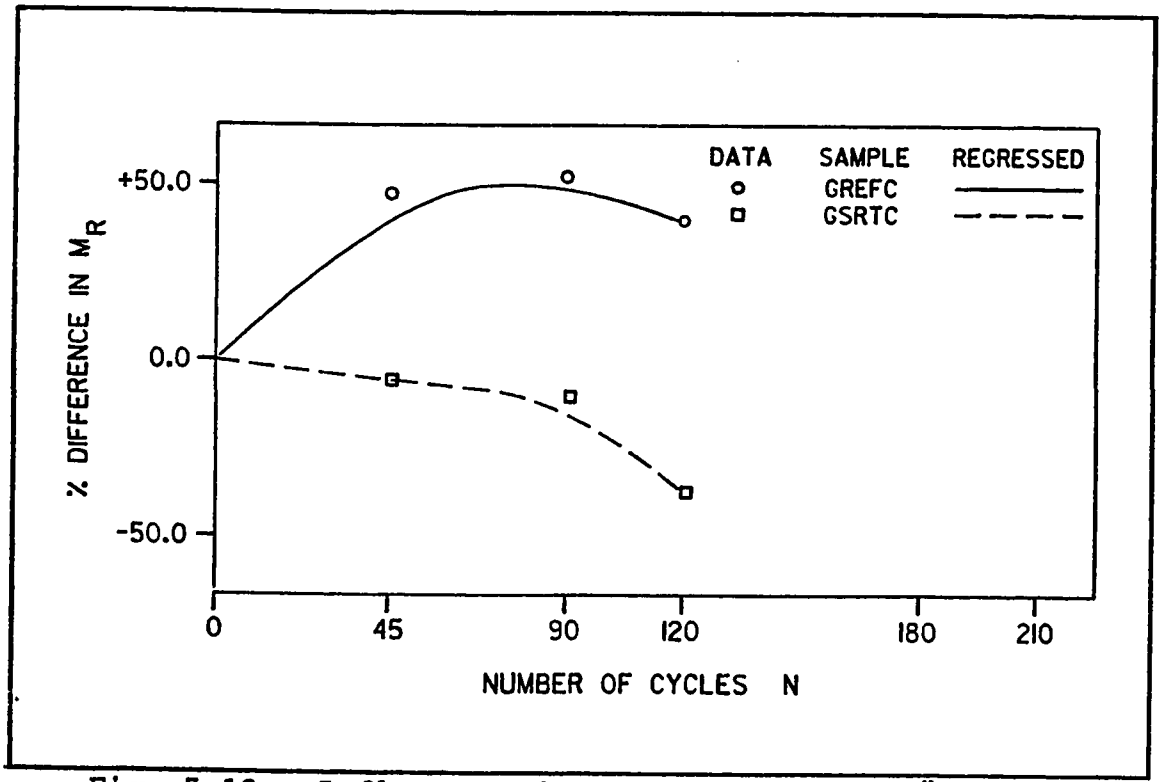

Fig. 5.12 : Influence of support restraint "prestress" on modulus of rupture

Admixtures showed beneficial effects in resisting the deterioration caused by TICC. Looking at both the admixture concretes, latex concrete (GLTXC) and super plasticizer concrete (GSPLC), in correlation with the reference concrete (GREFC), it is revealed that both the admixture concretes show very slow rates of TICC damage up to 180 thermal cycles. The reference concrete showed improvement in modulus of rupture up to 60 thermal cycles but it was followed by a high rate of deterioration afterwards (Fig. 5.13). Notice that the values of modulus of rupture for both the admixture concretes were much higher than those of the reference concrete (Table 5.5). Presence of admixtures in concrete under TICC environment proved to be very helpful in resisting and arresting the thermal damage.

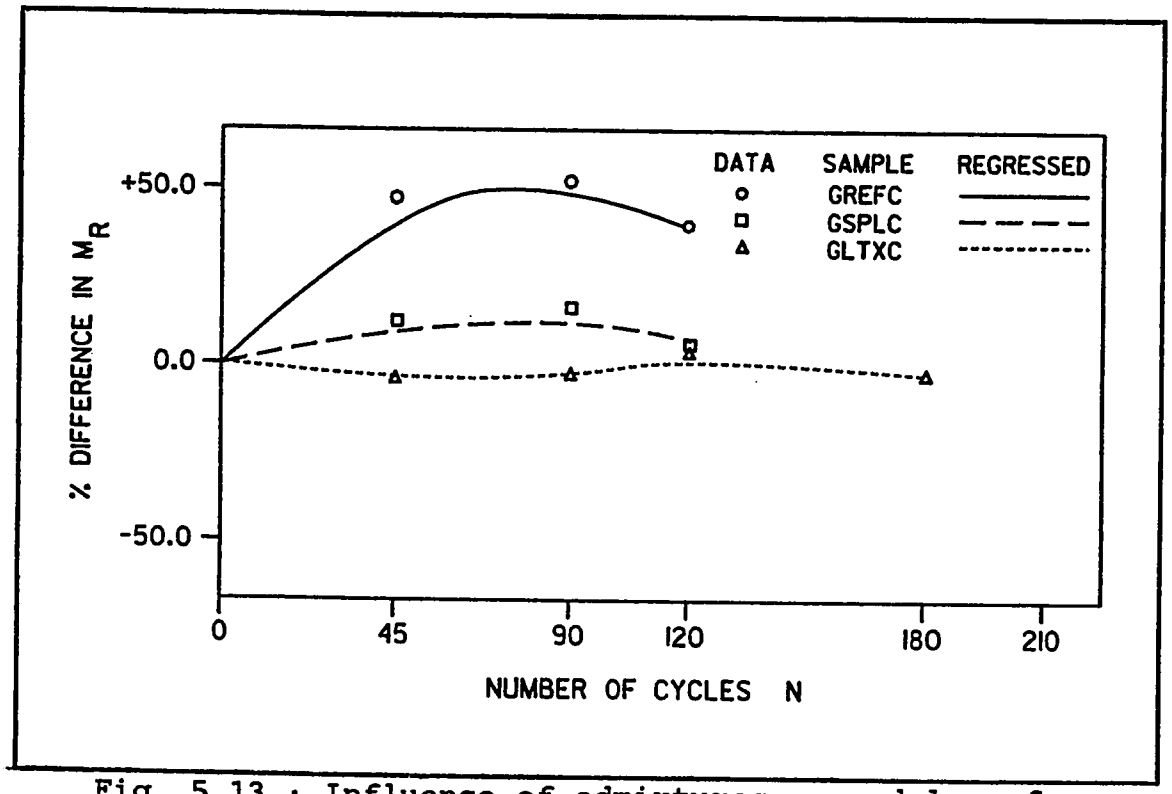

Fig. 5.13 : Influence of admixtures on modulus of rupture

5.1.3 Permeability

Permeability was found to be the most sensitive parameter that illustrated the intensity of damage caused by TICC, due to its direct dependence on the intensity, size, and continuity of cracks in the concrete. This was well illustrated by examining the permeability curves of all the groups (Fig. 5.14). Also after one and five cycles the permeability increased significantly (Fig. 5.15). This phase of the work consisted of determining the permeability of the cast concrete subjected to simulated TICC environment (lab cycling) (Table 5.7) in addition to the permeability of cored concrete under natural TICC environment over a period of two and a half years (natural cycling).

5.1.3.1 Cast concrete groups

The aggregate type affects the concrete permeability (Fig. 5.16) after being subjected to TICC environment, where both Riyadh and Jabal Dhahran aggregate showed low rates of permeability increase as compared to that of Abu-Hadriyah aggregate. Therefore both Riyadh and Jabal Dhahran aggregate proved to be suitable for a TICC environment. However, Jabal Dhahran aggregate possessed the highest initial permeability values that exceeded the DIN limits for waterproof concrete, therefore it is not recommended and is considered unsuitable due to its inferior soundness quality.

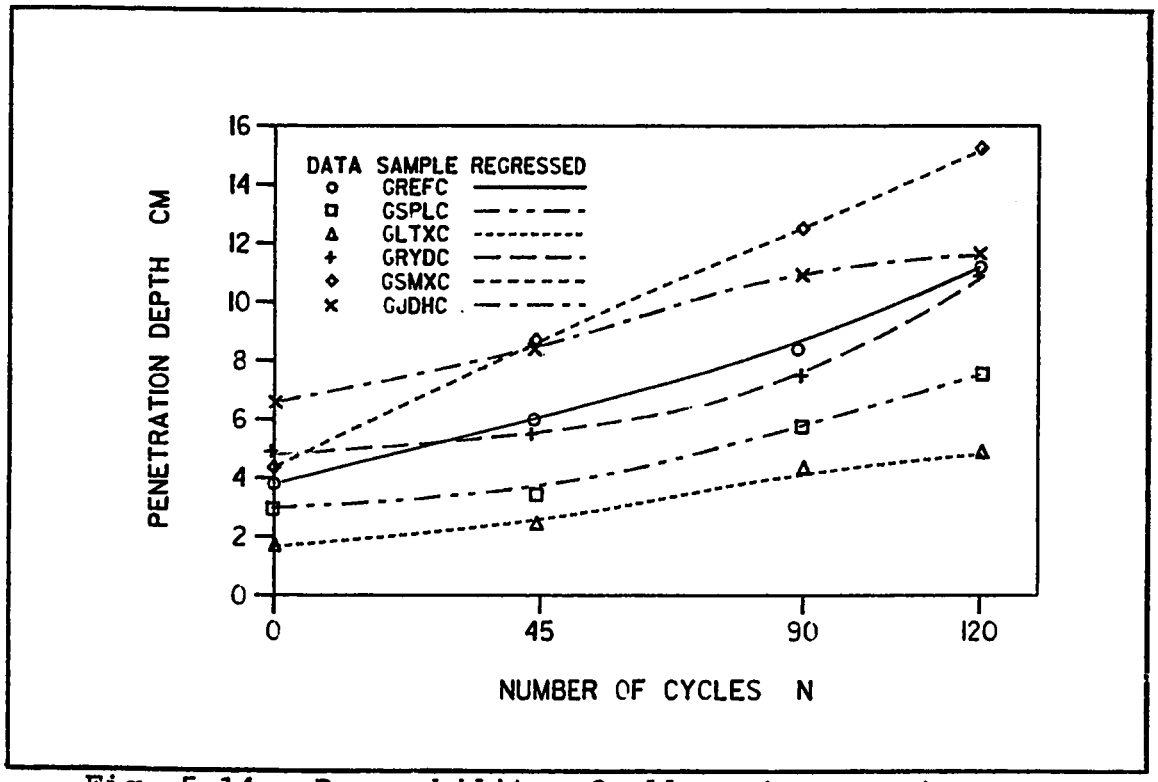

Fig. 5.14 : Permeability of all cast concrete groups

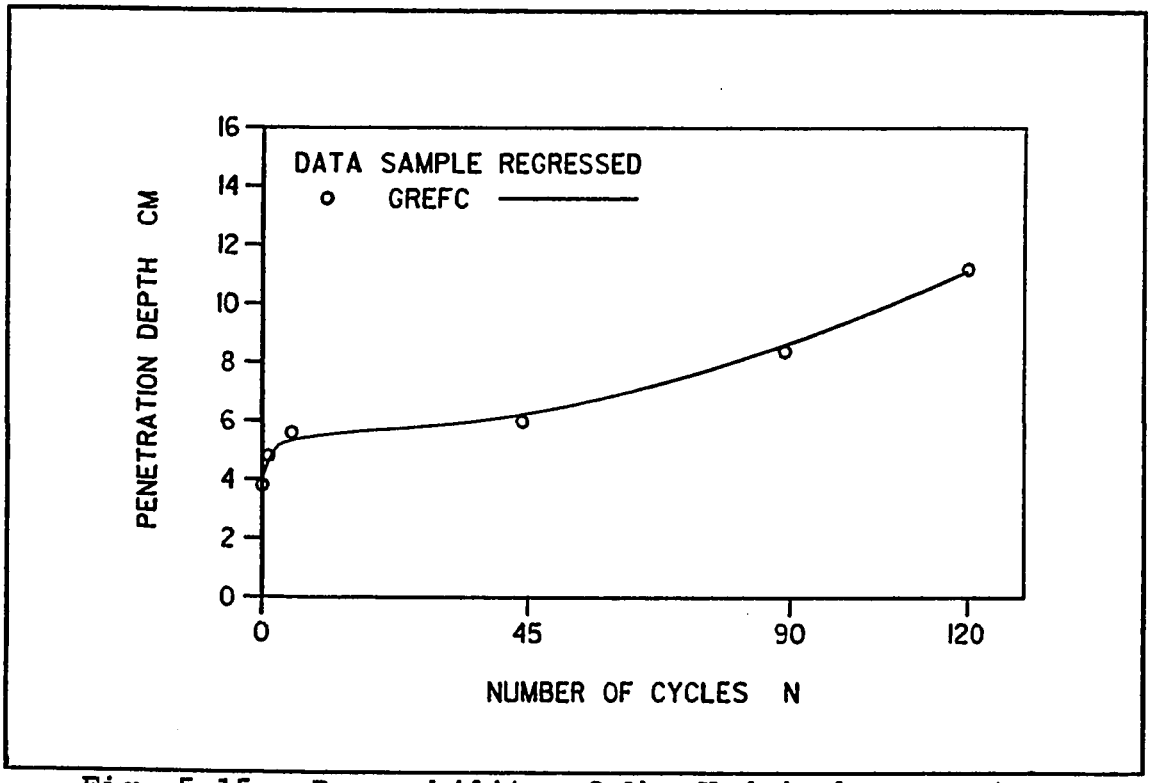

Fig. 5.15 : Permeability of Abu-Hadriyah concrete showing the rate after 1 and 5 cycles

Table 5.7 : Permeability of cast concrete

Group ID	Spec. No.	Permeability after Thermal Cycling					
		0	1	5	45	90	120
GREFC	1	3.7	4.5	5.5	5.5	7.8	10.5
	2	3.9	5.2	5.3	6.4	8.8	11.6
	Avg.	3.8	4.9	5.4	6.0	8.3	11.1
GRYDC	1	4.0	---	---	5.0	7.4	10.5
	2	5.5	---	---	5.8	7.0	11.7
	Avg.	4.8	---	---	5.4	7.2	11.1
GJDHC	1	6.0	---	---	8.0	12.3	11.7
	2	7.5	---	---	8.8	10.6	11.7
	Avg.	6.8	---	---	8.4	11.5	11.7
GSMXC	1	4.5	---	---	7.8	12.2	15.5
	2	4.5	---	---	10.0	13.0	15.1
	Avg.	4.5	---	---	8.9	12.6	15.3
GSPLC	1	3.5	---	---	4.2	5.8	7.4
	2	3.0	---	---	3.4	5.8	7.5
	Avg.	3.3	---	---	3.8	5.8	7.5
GLTXC	1	1.2	---	---	1.5	3.6	4.2
	2	2.0	---	---	3.0	4.6	5.0
	Avg.	1.6	---	---	2.3	4.1	4.6

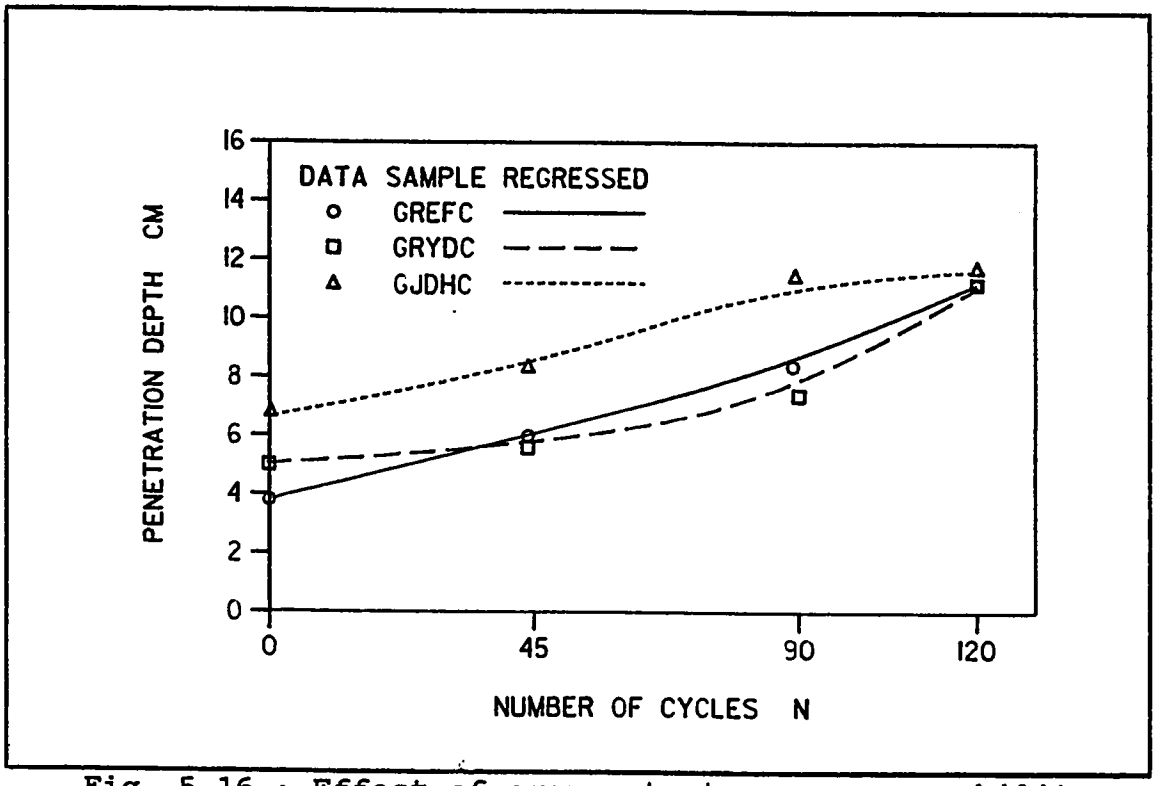

Fig. 5.16 : Effect of aggregate type on permeability

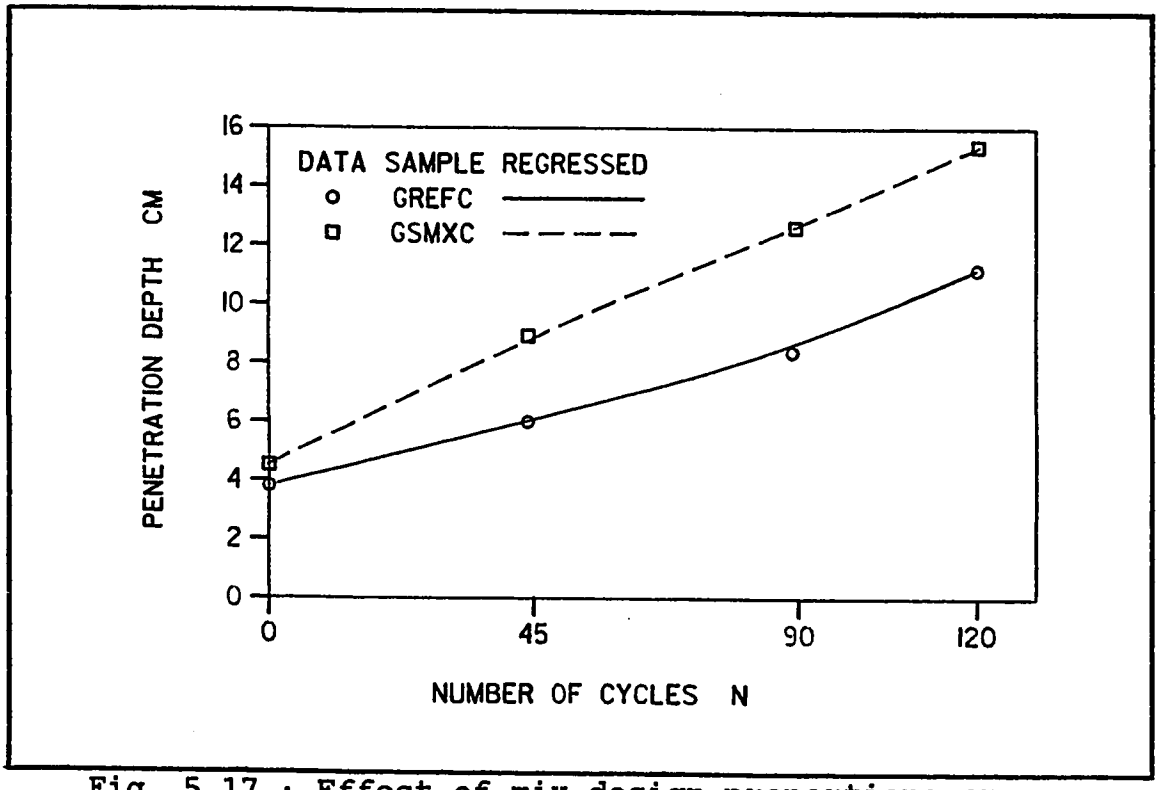

Fig. 5.17 : Effect of mix design proportions on permeability

Another factor that affects the permeability of concrete subjected to TICC environment is the mix design proportions (Fig. 5.17). Sandy mixes proved to be highly permeable in comparison to well proportioned mixes. This is obvious whilst comparing the permeability of the sandy mix concrete (GSMXC) with the reference concrete (GREFC), where on thermal cycling the rate of permeability increase was much higher than that of the well proportioned reference concrete mix. Therefore concretes containing high percentages of fines deteriorate faster than well proportioned concretes, especially in TICC environment where the coefficient of thermal expansion of quartzitic sand plays a great role in speeding up the deterioration process.

Presence of admixtures in the mix prove to be of great benefit where permeability is concerned (Fig. 5.18). As shown in the figure both admixture concretes, latex (GLTXC) and super plasticizer (GSPLC) showed the lowest initial permeability values and the least rates of increase. The reference concrete (GREFC) showed values about 40 percent higher than those of the admixture concretes. Therefore admixture concretes possess better resistive characteristics that retard the TICC damage.

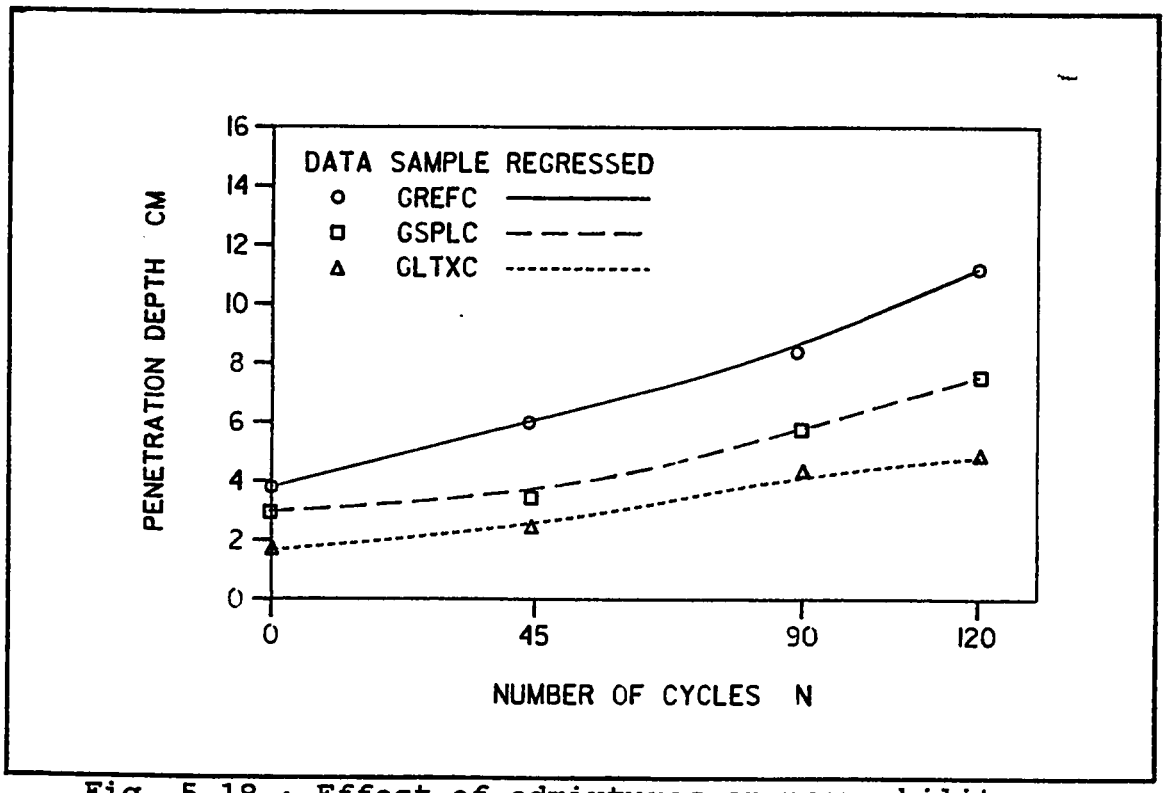

Fig. 5.18 : Effect of admixtures on permeability

Table 5.8 : Permeability of cored concrete

Group ID	Curing Method	Permeability (cm)		Percent Increase
		Uncycled cubes	Naturally cycled cores	
GC	Good	7.0	13.9	98.6
	Bad	10.0	14.5	45.0
GS50	Good	4.0	6.5	62.5
	Bad	7.4	7.5	1.4
GS45	Good	3.8	4.6	21.1
	Bad	4.2	6.8	61.9
GS40	Good	3.6	5.5	52.8
	Bad	5.5	6.0	9.1

Curing Method :

1. Good : Covered by burlap and watered twice daily for the first 7 days then left uncovered for 21 days more.

2. Bad : Covered by burlap and watered once on the first day then left uncovered for 27 days more.

5.1.4 Coefficient of Thermal Expansion

This portion deals with the investigation of the coefficient of thermal expansion of the three different types of aggregates used in the mixes. The coefficient of thermal expansion of both Riyadh aggregate and Riyadh concrete were calculated (Fig. 5.19 & 5.20) to be the slopes of the strain-temperature curves over the temperature range from 20 to 100 degrees Celsius. The coefficient of thermal expansion of Riyadh concrete was determined to be $7.96x10^{-6}$ per degree Celsius, while that of Riyadh aggregate was $7.54x10^{-6}$ per degree Celsius. All coefficients of thermal expansion of aggregates, hardened cement paste, concretes and quartzitic sand are presented (Table 5.9). As shown in the table there is a great difference between the coefficient of thermal expansion of the aggregate and the hardened cement paste for Abu-Hadriyah aggregate where both Riyadh and Jabal Dhahran aggregate show less incompatibility in thermal coefficients. Therefore Riyadh and Jabal Dhahran aggregate prove to be the most suitable local types of aggregate to be used in the Easten Province where due to its severe climatic conditions a TICC problem occurs. Riyadh aggregate is preferred rather than Jabal Dhahran aggregate due to its better soundness property as mentioned previously.

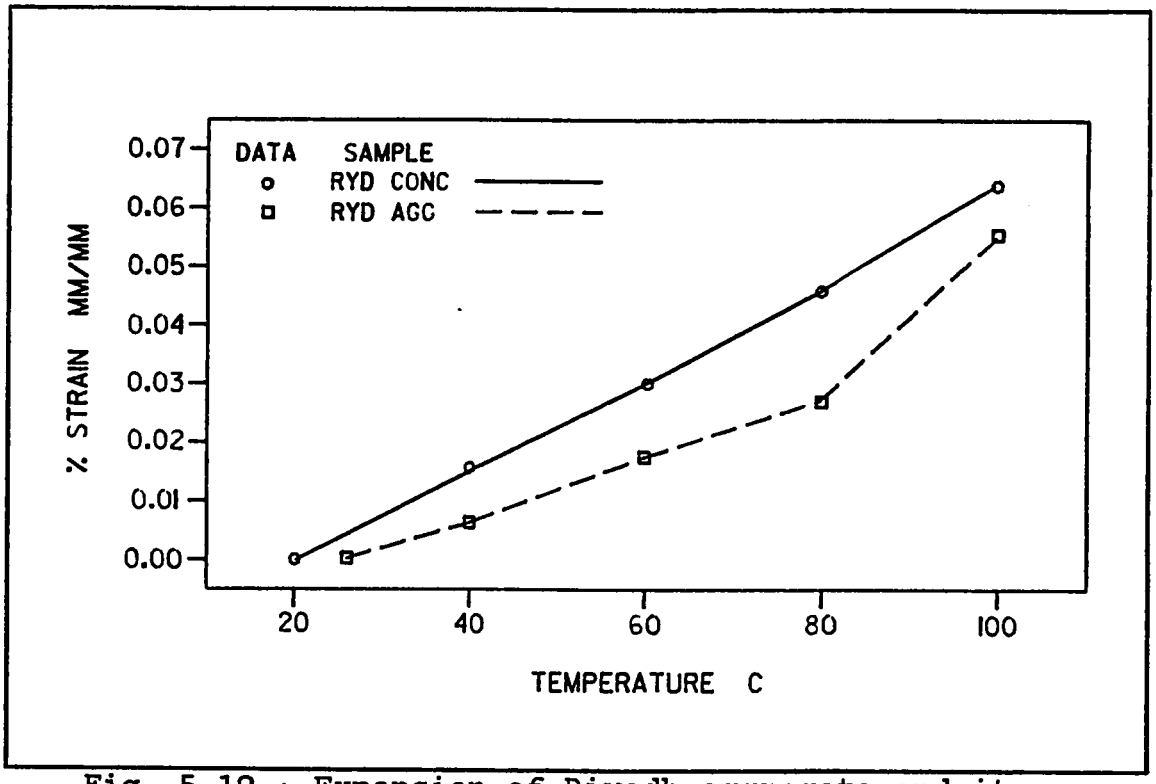

Fig. 5.19 : Expansion of Riyadh aggregate and its concrete while heating

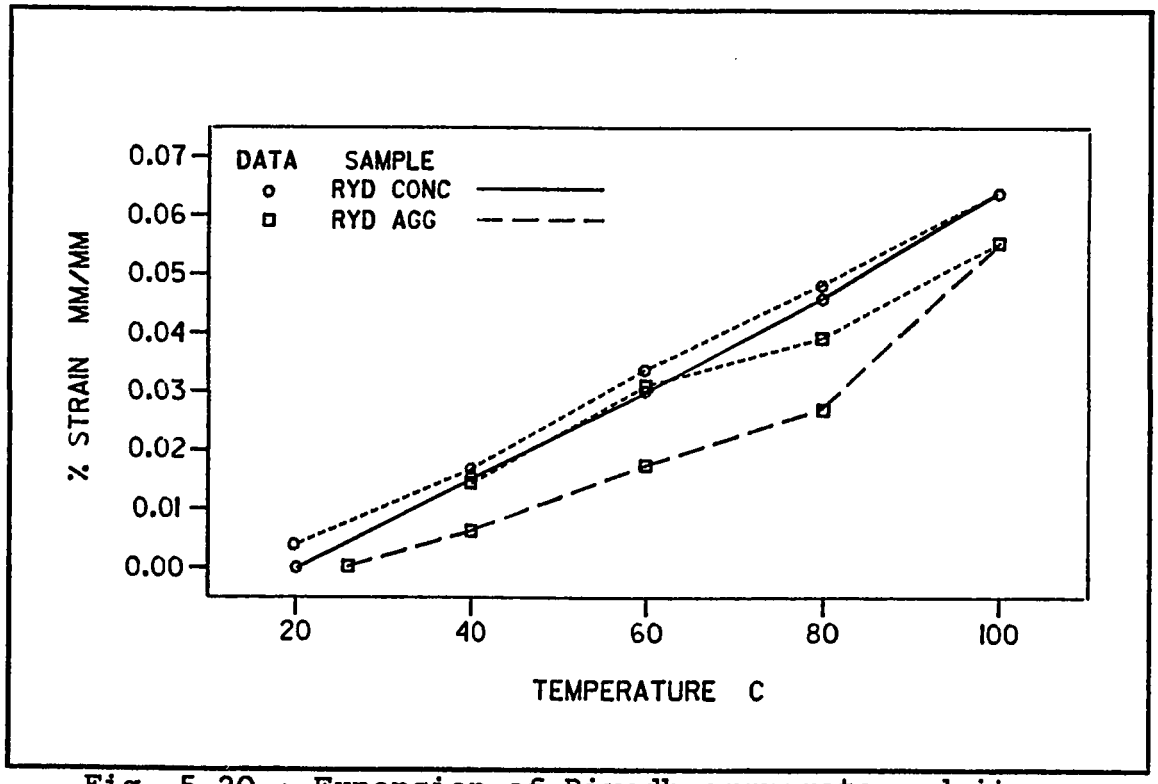

Fig. 5.20 : Expansion of Riyadh aggregate and its concrete while heating and cooling

Table 5.9 : Coefficient of thermal expansion

Concrete Component	Type (Origin)	Coefficient of Thermal Expansion CTE (mm/mm/^{o}C)
Coarse Aggregate	Abu-Hadriyah Riyadh Jabal Dhahran (Limestones)	$6.20x(10^{-6})$; {$11.76x(10^{-6})$} $7.54x(10^{-6})$; {$7.96x(10^{-6})$} $9.99x(10^{-6})$; {$13.20x(10^{-6})$}
Fine Aggregate	Dune Sand (Quartzitic)	* $7.00x(10^{-6})$ to $13.10x(10^{-6})$
Cement Paste	Portland Cement Type I	@ $9.00x(10^{-6})$ to $25.40x(10^{-6})$ # $10.20x(10^{-6})$ to $11.20x(10^{-6})$

Remarks :

{ } CTE of the aggregates concrete

* Values from reference 67

@ Values from reference 11

\# Values from reference 45

5.1.5 Compressive Strength

For completeness of results the compressive strength of the cast concrete groups (GREFC), (GRYDC), (GJDHC), (GSMXC), (GSPLC), and (GLTXC) was determined (Table 5.10). Also the compressive strength vs age curves were plotted (Fig. 5.21). Regarding the cored concrete groups (GC), (GS50), (GS45), and (GS40) under both good and bad curing, the 28-day compressive strengths were determined (Table 5.11).

Table 5.10 : Compressive strength of cast concrete

Group ID	Spec. No.	Compressive Strength at Age (KN)			
		14 days	28 days	42 days	56 days
GREFC	1	178.0	175.7	215.7	207.9
	2	169.0	173.7	208.4	202.3
	Avg.	173.5	174.7	212.1	205.1
GRYDC	1	153.2	148.8	217.8	238.2
	2	149.1	161.1	225.5	204.2
	Avg.	151.2	155.0	221.7	221.2
GJDHC	1	72.8	130.8	166.0	156.1
	2	107.0	117.8	160.0	168.9
	Avg.	89.9	124.3	163.0	162.5
GSMXC	1	95.6	117.2	152.5	124.1
	2	89.6	106.7	141.0	132.9
	Avg.	92.6	112.0	146.8	128.5
GSPLC	1	156.0	207.4	235.0	257.2
	2	177.9	215.0	241.0	227.5
	Avg.	167.0	211.2	238.0	242.4
GLTXC	1	178.0	200.8	204.5	256.5
	2	149.2	213.0	261.9	218.5
	Avg.	163.6	206.9	233.2	237.5

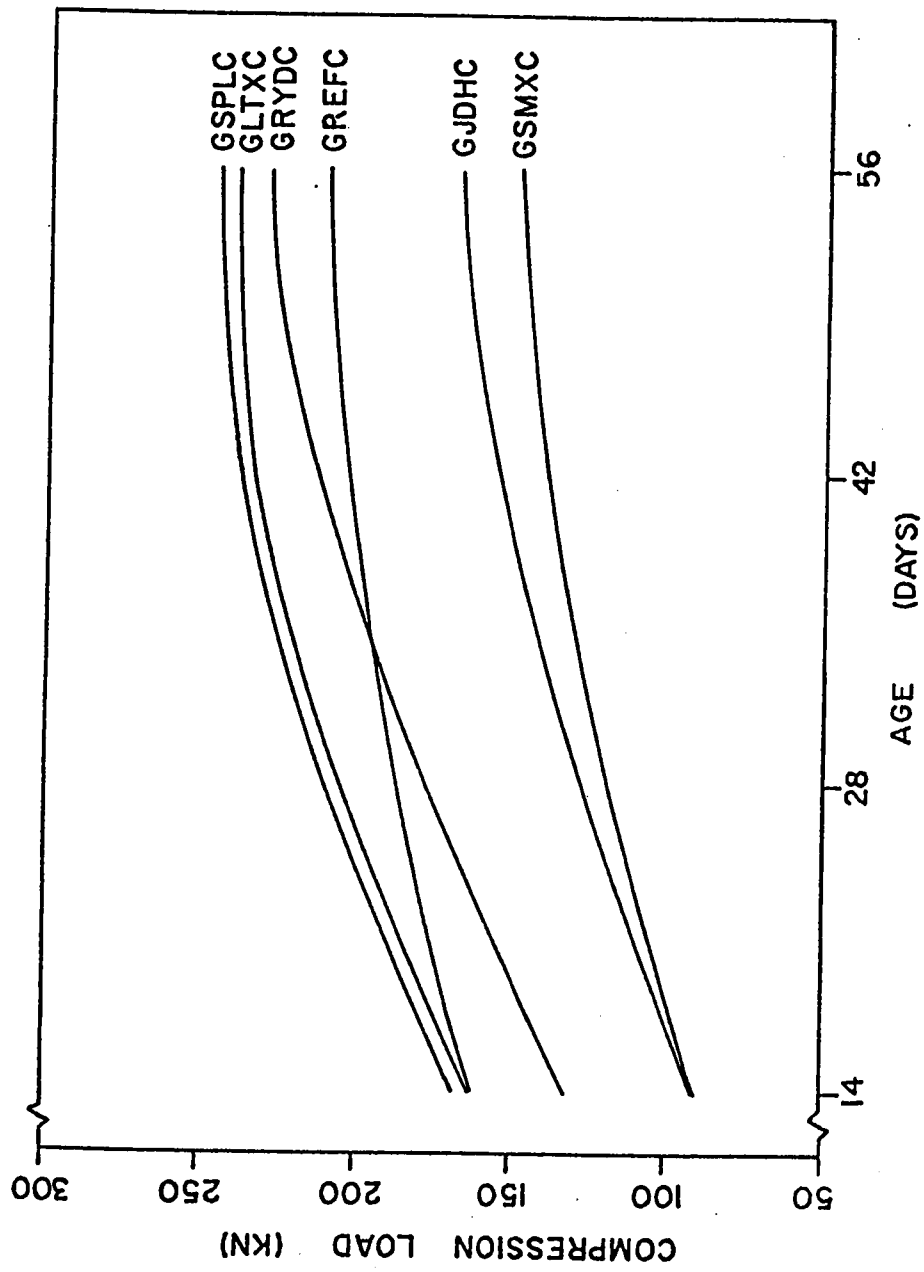

Fig. 5.21 : Compressive strength of the cast concrete groups

Table 5.11 : Compressive strength of cored concrete

Group ID	Curing Method	Spec. No.	Compressive Strength (KN)	
			At 28 Days	Average
GC	Good	1 2	124.9 124.6	124.8
	Bad	1 2	63.8 54.6	59.2
GS50	Good	1 2	143.5 146.0	144.8
	Bad	1 2	138.8 107.4	123.1
GS45	Good	1 2	194.3 182.7	188.5
	Bad	1 2	182.4 132.0	157.2
GS40	Good	1 2	212.6 219.9	216.3
	Bad	1 2	219.0 186.9	203.0

Curing Method :

1. Good : Covered by burlap and watered twice daily for the first 7 days then left uncovered for 21 days more.

2. Bad : Covered by burlap and watered once on the first day then left uncovered for 27 days more.

5.2 Discussion

Results of fracture toughness, modulus of rupture, and permeability increase for the cast concrete groups (GREFC), (GRYDC), (GJDHC), (GSMXC), (GSPLC), and (GLTXC) are presented (Table 5.12). It appears that results of permeability and fracture toughness are more sensitive to cracking (caused by TICC phenomenon) whereas the modulus of rupture values reveal some increase on cycling. This increase in the strength characteristic as measured by the modulus of rupture is due to further hydration of unhydrated cement at higher temperatures and loss of moisture within the concrete during the heat cycling process where concrete in a dry state possesses higher strength than that in a moist state. Similar increase in strength on thermal cycling was witnessed by many other researchers as Aronov, Zhukov, Dmitriev, Sergeeva, Walker et al, and Meyers {34}. Therefore it is more reliable to monitor fracture toughness and permeability values when predicting the level of damage caused by TICC phenomenon. Consequently the idea of introducing a so called toughness index and permeability index was developed (Table 5.13), where the toughness index was meant to be the fraction of the cycled fracture toughness with respect to the reference uncycled fracture toughness and the permeability index is the rate of increase in permeability per cycle.

Table 5.12 : Permeability increase, fracture toughness, & modulus of rupture

Group ID	Number of cycles										
	45 cycles			90 cycles			120 cycles			180 cycles	
	ΔP	F.T.	M.R.	ΔP	F.T.	M.R.	ΔP	F.T.	M.R.	F.T.	M.R.
GREFC	2.2	-33.0	46.4	4.5	-7.8	51.3	7.3	-18.5	38.4	----	----
GRYDC	0.6	47.0	2.8	2.4	42.2	1.1	6.3	-5.9	11.2	----	----
GJDHC	1.6	-48.0	-6.3	4.7	-18.6	13.7	4.9	-17.8	13.4	-26.7	-23.0
GSMXC	4.4	-61.0	-19.7	8.1	-47.5	-6.3	10.8	-55.6	-12.5	----	----
GSPLC	0.8	xxxx	10.9	2.5	-0.1	15.9	4.2	-2.7	5.3	----	----
GLTXC	0.7	7.4	-5.4	2.5	27.1	-4.3	3.0	-14.2	2.1	-32.0	-3.3

ΔP :Permeability increase (cm)
F.T.:Fracture Toughness (%)
M.R.:Modulus of Rupture (%)

Similar increase in strength (M.R. & Comp. St.) up to 120 cycles was stated by; Aronov, Zhukov, Dmitriev, Sergeeva, Walker et al and Meyers {34}

Table 5.13 : Fracture and permeability indices

Group ID	Toughness index Kt					Permeability index Kp (mm/cycle)		
	45 cyc	90	120	180	210	45 cyc	90	120
GREFC	0.84	0.78	0.74	----	----	0.49	0.50	0.61
GRYDC	1.47	1.42	0.94	----	----	0.13	0.27	0.53
GJDHC	0.88	0.80	0.74	0.60	----	0.36	0.52	0.41
GSMXC	0.58	0.42	0.36	----	----	0.98	0.90	0.90
GSPLC	xxxx	0.99	0.97	----	----	0.11	0.28	0.35
GLTXC	1.14	1.14	1.00	0.58	----	0.16	0.28	0.25
GSRTC	1.02	0.82	0.51	----	----	----	----	----
GSWDC	0.98	0.92	0.86	0.68	1.00	----	----	----

Toughness index $$Kt = \frac{G_{IC} \text{ cycled}}{G_{IC} \text{ reference}}$$

Permeability index $$Kp = \frac{(P \text{ cycled} - P \text{ reference}) \quad (mm)}{\text{Number of cycles} \quad (cycles)}$$

For applying these indices in proctoring the deterioration of structures, certain limits should be defined after which the structure may be considered unfit regarding its durability, especially in an environment conducive to corrosion. Improvement in concrete designs for TICC environment may be achieved by taking into consideration a durability criterion along with the conventional strength criterion during the design process.

Considering each of the variables, aggregate type, mix design proportions, support restraint, successive wetting and drying, and addition of admixtures, the following subsections deal with the effect of each on the TICC deterioration phenomenon.

5.2.1 Aggregate Type

Riyadh and Jabal Dhahran aggregate were found to be two good types of local aggregates used in the eastern province where climatic conditions are severe and presence of high incompatibility in coefficients of thermal expansion of aggregate and concrete may cause a great durability problem. The coefficient of thermal expansion of the aggregate and the hardened cement paste for both are close in value hence the intensity of the TICC environment is less in nature. Abu-Hadriyah aggregate showed a greater incompatibility problem where the difference between the coefficient of

thermal expansion of its aggregate and the hardened cement paste was the greatest. Another thing was the rate of increase in its permeability was the greatest. Therefore Abu-Hadriyah aggregate is the least suitable type of aggregate to be used in a TICC environment. Riyadh aggregate is considered the most suitable due to the fact that its soundness properties are much better than those of Jabal Dhahran aggregate. In addition, the initial permeability of Jabal Dhahran concrete does not meet the requirements of DIN. So Riyadh aggregate is more preferred than Jabal Dhahran aggregate when used in a TICC environment.

5.2.2 Mix Design Proportions

Difference in the coefficients of thermal expansion of both fine and coarse aggregates are mainly caused due to the difference in origin of both the fine and coarse aggregates used in the mix. In this work the fine aggregate used was quartzitic sand while the coarse aggregates were limestone in nature. This variation in the coefficients of thermal expansion causes a TICC problem which increases in intensity when the mix possesses a low coarse to fine aggregate ratio. It has been shown that sandy mixes are highly more vulnerable to the TICC deterioration phenomenon than well proportioned mixes.

5.2.3 Support Restraint

Presence of initial prestress in a concrete structure subjected to a TICC environment proves to aggravate the damage where tensile stresses build up from two sources, the original prestress and the stress resulting from TICC. Therefore it is highly recommended to reduce the incompatibility as much as possible since all structures are designed to withstand stresses. This may be achieved by using the proper type of aggregate that has a coefficient of thermal expansion close to that of the cement paste and the fine aggregate. A more practical approach would be to use admixtures that have been shown to neutralize to an extent TICC related damage.

5.2.4 Successive Wetting and Drying

Alternate wetting and drying showed a beneficial effect on concretes under TICC environment, where values of modulus of rupture and fracture toughness exhibited improvement over the spectrum of thermal cycles considered. This is due to the further hydration of unhydrated cement at higher temperatures in the early cycles, together with continuous autogeneous healing. Another reason may be due to the effect of moisture on the coefficients of thermal expansions of the concrete components. Results are oscillatory in nature, mainly due to the varying moisture content of the samples.

5.2.5 Admixtures

Admixtures such as latex and super plasticizers prove to be very beneficial to concrete subjected to TICC environment. Fracture toughness, modulus of rupture, and permeability all show noticeably better resistance to TICC related deterioration. These admixtures greatly delay the damaging process where permeability values were found to be more than 50 percent less than reference concrete for any number of thermal cycles N. Both the initial permeability and the rate of permeability increase were reduced considerably in the two mixes with admixtures. Naturally cycled, superplasticized concrete showed extremely good results where the permeability values of superplasticized concrete were reduced to about one third those of reference non-superplasticized concrete. This means that super plasticizers aid to a great extent the delay of TICC related damage.

CONCLUSIONS AND RECOMMENDATIONS

1. The effect of TICC related damage on a key durability parameter, permeability, has been established both from testing samples in a laboratory environment as well as in an exposure site.
2. In view of several factors beneficial to strength characteristics in young, moist concrete, monitoring of such characteristics may be misleading in interpretation of TICC damage. This is particularly true in the early phase of the cycling regime, where strength was found to be relatively insensitive to TICC damage. By contrast, fracture toughness showed greater sensitivity to such damage. However, permeability measurements exhibited greatest sensitivity to TICC damage showing significant increase within five thermal cycles.
3. Riyadh and Jabal Dhahran aggregate have proved to be more suitable than Abu-Hadriyah aggregate when used in a TICC environment. However Jabal Dhahran aggregate showed to be unsuitable from its soundness point of view, therefore Riyadh aggregate is the most suitable in an overall selection. Jabal Dhahran aggregate is not recommended to be used in a TICC environment due to its high initial permeability that exceeds the DIN standards.

4. Presence of in-situ stress appears to aggravate the TICC damaging process, hence care should be taken in the selection of a thermally compatible aggregate to be used in severe climatic conditions as those prevailing in the Eastern Province of Saudi Arabia. This component needs to be studied further in more details.
5. High fine to coarse aggregate ratio mix proportions, together with fine and coarse aggregate from different origins, aggravates the TICC phenomenon. This confirms a hypothesis of Venecanin based on a theoretical three component model for concrete {14}.
6. The most beneficial effect was exhibited by the use of admixtures as latex and super plasticizer. Both mixes showed the least permeability values. They also exhibited toughness indices that were very close to unity after 120 cycles. Loss in modulus of rupture was maintained at a minimum due to presence of admixtures.
7. Regarding naturally cycled concrete, TICC was shown to be the cause of excessively increased permeability values. Again the use of super plasticizer admixture kept the level of deterioration down to approximately a third. Permeability values of super plasticized cycled concrete were 30 percent those of the control uncycled concrete without admixture.
8. Further studies should be conducted in greater details on the use of admixtures to reduce TICC related damage.

9. Modification in the existing codes for the Eastern Province are recommended as follows :

   (i) Specifications must be stated for acceptable CTE values of coarse and fine aggregates to minimize impact of TICC damage.

   (ii) Recommend acceptable permeability index for design concrete mix for use in important structures such as bridge decks and airport runways. The permeability index is preferred to toughness index because of the ease of measurement and its greater sensitivity. Strength indices for TICC related damage can be misleading.

   (iii) Should aggregate availability be restricted to those with low CTE, such projects should use admixtures as latex and super plasticizer to help improve TICC performance.

REFERENCES

1. Rasheeduzzafar, F.H. Dakhil, and A.S Al-Gahtani, "Deterioration of Concrete Structures in the Environment of the Middle East", ACI Jour., p-13, Jan. 1984

2. L.H. Tuthill, S.D. Venecanin, and authors Rasheeduzzafar, F.H. Dakhil, and S.A. Al-Gahtani, Discussion of "Deterioration of Concrete Structures in the Environment of the Middle East", ACI Jour., p-646, Nov. 1984

3. P.G. Fookes, and L. Collis, "Problems in the Middle East", Concrete, Vol.9, No.7, p-12, July 1975

4. W.H. Johnson, and W.H. Parson, "Thermal Expansion of Concrete Aggregate Materials", National Bureau of Standards Jour., Vol.32, p-101, March 1944

5. W.H. Johnson, and W.H. Parson, "Factors Affecting the Thermal Expansion of Concrete Aggregate Materials", ACI Jour., Proc. Vol.40, No.5, p-457, April 1944

6. J.H. Griffith, "Thermal Expansion of Typical American Rocks", Bulletin No.128, Eng. Experiment Station, Iowa State College, Ames, p-1, 1936

7. J.C. Pearson, "A Concrete Failure Attributed to Aggregate of Low Thermal Coefficient", ACI Jour., Proc. Vol.38, No.1, p-29, Sept. 1941

8. F.B. Hornibrook, H.S. Meissner, R.B. Young, B. Kellam, R.E. Davis, M.O. Withey, M.A. Swayze, C.G. Walker, F.V. Reagel, T.F. Willis, and author J.C Pearson, Discussion on "A concrete failure attributed to aggregate of low thermal coefficient", ACI Jour., Proc. Vol.38, No.6, p-36, June 1942

9. S.D. Venecanin, "Influence of Thermal Incompatibility of Concrete Component or its Strength", Doctoral Disertation Beograd

10. S.D. Venecanin, "Deterioration of Concrete due to the Thermal Incompatibility of its Component", Proc. VI, Congress of Yogoslav Structure Engineers, Vol.T, p-369, 1978

11. S.D. Venecanin, "Stress in Concrete due to the Thermal Incompatibility of its Components." Int. Conf. Materials Science and Restoration, Tech. Akad Esslingen FRG, Proc. Vol. , p-93, Sept. 1983

12. S.D. Venecanin, "Experimental Study of Thermal Icompatibility of Concrete Composite", Third Int. Conf. on the Durability of Building Materials and Composite, Vol.III, p-510, Helsinki 1984

13. J.N. Deserio, "Thermal and Shrinkage Stressess - They Damage Structures", Designing for the Effect of Creep, Shrinkage, and Temperature in Concrete Structures, ACI Detroit, SP 27, p-43, 1971

14. S.D. Venecanin, "Analysis of Thermal Stress in Concrete when it is Heated as Nonhomogeneous Three-Component Composite Material", Symp. Innovation of Yogoslav Codes on Concrete, Materials and Composite Structures, Vol.III, p-97, 1980, Symp. of Yogoslav Society of Structural Engineers .

15. E.J. Callan, "Thermal Expansion of Aggregates and Concrete Durability", ACI Jour., Proc. Vol.48, p-485, Feb. 1952

16. D.L. Bloem, S. Walker, R.E. Glover, T.F. Willis, F.V. Reagel, and author E.J. Callan, Discussion of "Thermal expansion of aggregates and concrete durability", ACI Jour., Proc. Vol.48, p-504, Dec. 1952

17. S.I. Meyers, "Thermal Expansion Characteristics of Hardened Cement Paste and Concrete", Highway Research Board, Proc. Vol.30, p-193, 1950

18. R.E. Davis, "A Summary of the Results of Investigation Having to do with Volumetric Changes in Cements, Mortars, and Concretes due to Causes other than Stress", ACI Jour., Proc. Vol.26, No.4, p-407, Feb. 1930

19. H. Dettling, "The Thermal Expansion of Hardened Cement Paste, Aggregates, and Concrete", Bulletin No.164, Berlin, p-1, 1964, Also, Translation No.458, PCA Technical Information Dept., from SLA Translation Center, John Crerar Library, Chicago

20. S.I. Meyers, "Volume Change in Cement and Mortar", Concrete, p-16, August 1935

21. G.J. Verbeck, and W.E. Hass, "Dilatometer Method for Determination of Thermal Coefficient of Expansion of Fine and Coarse Aggregate", Highway Research Board (HRB), Proc. Vol.30, p-187, 1951

22. L.J. Mitchell, "Thermal Expansion Tests on Aggregates, Neat Cement, and Concretes", ASTM, Proc. Vol.53, p-963, August 1953

23. S.I. Meyers, "Thermal Coefficient of Expansion of Portland Cement", Inds. Eng. Chem., p-1107, August 1940

24. J.H. Emanuel, and J.L. Hulsey, "Prediction of the Thermal Coefficient of Expansion of Concrete", ACI Jour., Proc. Vol.74, p-149, April 1977

25. S. Walker, D.L. Bloem, and W.G. Mullen, "Effects of Temperature Changes on Concrete as Influenced by Aggregates", ACI Jour., Proc. Vol.48, No.8, p-661, April 1952

26. E.C. Higginson, and D.G. Kretsinger, "Prediction of Concrete Durability from Thermal Tests of Aggregate", ASTM, Proc. Vol.53, p-991, 1953

27. S.I. Meyers, "How Temperature and Moisture Changes may Affect the Durability of Concrete", Rock Products, p-153, August 1951

28. S. D. Venecanin, "Deterioration of Crushed Limestone Concrete of Bridges and Thermal Incompatibility of Concrete Components", Congress of Yogslav Structure Engineers, Symp. 85 ARSM-29 ,Dubrovink 23-26, April 1985 .

29. J.C. Pearson, "Supplementary Data on the Effect of Concrete Aggregate Having Low Thermal Coefficient of Expansion", ACI Jour., Proc. Vol.40, No.1, p-33, Sept. 1943

30. Rasheeduzzafar, F.H Dakhil, "Field Studies on the Durability of Concrete Construction in a High Chloride-Sulphate Environment", Int. Jour. of Housing Science, Vol.4, No.3, p-203, 1980

31. J.R. Crowder, "United Arab Emirates, Building Conditions and Materials", Builbing Research Establishment (BRE Report), Dept. of Environment, 1983

32. A.J. Al-Tayyib, Rasheeduzzafar, and A.I Al-Mana, "Deterioration of Concrete Structures in the Gulf States", First Int. Conf. of Deterioration and Repair of Reinforced Concrete in the Arabian Gulf, Proc. Vol.1, p-27, 1985

33. H.E. Ashton, and P.J. Sereda, "Environment, Microenvironment and Durability of Building Materials", Durability of Building Materials, p-3, 1982

34. S.A. Mironov, E.N. Malinskyi, and M.M. Vakhitov, "Durability Assessment Criterion for Concrete Exposed to Dry Hot Climate Conditions", Durability of Building Materials, Vol.1, No.1, p-3, 1982

35. "Concrete in Hot Countries", STUVO Dutch member group FIP, P.O. Box 3011, 5203 DA, Hetoggenbosh, Netherland

36. A.M. Neville, "Properties of Concrete", Pittman, London, 1973

37. S.D. Venecanin, " Influence of Temperature on the Deterioration of Concrete in the Middle East ", Concrete, London, Vol. 11, No. 8, p-31, August 1977

38. P.G. Fookes, and L. Collis, "Aggregates and the Middle East", Concrete, London, Vol.9, No.11, Nov. 1975

39. P.G. Fookes, and L. Collis, "Cracking and the Middle East", Concrete, London, Vol.10, 1976

40. S.D. Venecanin, "Influence of Thermal Incompatibility of Concrete Components on its Durability of Concrete Pavements ", Proc. of Modern Achievements in Designing, Construction and Maintenance of Concrete Pavements Portoroz-Yogoslavia, p-9, Oct. 1985

41. S.D. Venecanin, "Durability of Composite Materials Influenced by Different Coefficients of Thermal Expansion of Components", Proc. Durability of Building Materials and Components, ASTM STP 691, 1980, International Conference on Durability of Building Materials and Components, Ottawa, Canada, p-179, August 1978

42. D.R.J. Owen, and A.J. Fawkes, "Engineering Fracture Mechanics Numerical Methods and Applications", Pinesidge Press Ltd.,Swansea, 1983

43. D. Broek, "Elementary Engineering Fracture Mechanics", Delft Univ. of Tech., Noordhoff International Publishing Leyden, Netherlands, 1974

44. R.M. Caddell, "Deformation and Fracture of Solids", Univ. of Michigan, Prentice Hall Inc., Englewood Cliffs, New Jersey, 1980

45. M.M. Muse, "Durability and Thermal Incompatibility of Concrete Components made from Local Materials in the Arabian Gulf Countries", M.S. Thesis, King Fahd University of Petroleum and Minerals, Dhahran, Saudi Arabia, 1988

46. W.D. Biggs, "The Brittle Fracture of Steel",McDonald and Evans, 1960

47. W.E. Anderson, "An Engineer Views Brittle Fracture History", Boeing Rept., 1969

48. C. Gurney, and J. Hunt, "Quasi-Static Crack Propagation", Proc. Roy. Soc. London, A299, p-508, 1967

49. D.S. Dugdale, "Yielding of Steel Sheets Containing Slits", Mech. Phys. Solids Jour., Vol.8, p-100

50. G.I. Barenblatt, "The Mathematical Theory of Equilibrium Cracks in Brittle Fracture", Adv. App. Mech., Vol.7, p-55

51. A.A. Wells, "Unstable Crack Propagation in Metals, Cleavage and Fast Fracture", Symp. of Crack Propagation, Cranfield, p-210, 1961

52. A.A. Wells, "Application of Fracture Mechanics at and beyond General Yield", British Welding Res. Ass. Rept., M13/63, 1963

53. J.A. Begley, and A.D. Landes, "A Comparison of the J-Integral Fracture Criterion with the Equivalent Energy Concept", in "Progress in Flow Growth and Fracture Toughness Testing", ASTM STP 536, p-246, 1973

54. H. Tada, "The Stress Analysis of Cracks Handbook", Del Research Corporation, 1973

55. A.A. Griffith, "The Phenomena of Rupture and Flow in Solids", Phil. Trans. Roy. Soc. of London, A 221, p-163, 1921

56. A.A. Griffith, "The Theory of Rupture", Proc. Inst. Int. Congress Appl. Mech., p-53, 1924

57. C.E. Inglis, "Stresses in a Plate due to the Presence of Cracks and Sharp Corners", Proc. Inst. Naval Architects, 55, p-219, 1913

58. C. Gurney, and K.M. Ngan, "Quasi-Static Crack Propagation in Nonlinear Structures", Proc. Roy. Soc. London, A325, p-207, 1971

59. C. Gurney, and Y.W. Mai, "Stability of Cracking", Eng. Frac. Mech., 4, p-853, 1972

60. M. Wecharatana, and S.P. Shah, "Slow Crack Growth in Cement Composites", Structural Div. Jour., Proc. ASCE, Vol.108, No.ST6, p-1400, June 1982

61. M. Wecharatana, and S.P. Shah, "Double Torsion Test for Studying Slow Crack Growth of Portland Cement Mortar", Cement and Concrete Research, Vol.10, p-833, 1980

62. G.J. Verback, "Hardened Concrete, Pore Structure", ASTM Sp. Tech. Publication, No.169, p-136, 1955

63. L.E. Copeland, and J.C. Hayes, "The Determination of Non-Evaporable Water in Hardened Portland Cement Paste", ASTM, Bul. No.194, p-70, Dec. 1953

64. "Specifications of the German Standard Code (DIN 1048)", Fedral Republic of Germany

65. "Annual Book of the American Standards for Testing and Materials, (ASTM Standards)", 1916 Race Street, Philadelphia, PA 19103, 1986

66. "Final Report of the National Bridge Deck Cracking Project", King Abdul Aziz City for Science and Technology (KACST), King Fahd University of Petroleum and Minerals (KFUPM), 1986

67. J.H. Griffith, "Thermal Expansion of Typical American Rocks", Bulletin No.128, Engineering Experiment Station, Iowa State College, Ames, p-1, 1963

CURRICULUM VITA

Personal Details

Full Name	:	LOUAY ABDEL-RAZEK ABOUL-NOUR
Nationality	:	Egyptian
Birth Date	:	January 4, 1964
Religion	:	Muslem
Sex	:	Male
Languages	:	Arabic and English
Address	:	14 Mohammed Mustafa Hamam St., First District, Nasr City, Cairo, Egypt (Tel. 604999)

Qualifications

- G.C.E. (General Certificate of Education), University of London, London, 1979

- B.Sc. Civil Engineering Department (GPA 3.96/5.00), King Abdul Aziz University (KAAU), Jeddah, Saudi Arabia, 1984
  Senior Project Title : Structural Analysis and Design of Folded Plates (Supervisor Prof. Dr. W.M. El-Dakhakhni)

- M.Sc. Civil Engineering Department (GPA 3.00/4.00), King Fahd University of Petroleum and Minerals (KFUPM), Dhahran, Saudi Arabia, 1988
  Master Thesis Title : Fracture and Permeability Characteristics of Thermally Degraded Concrete (Supervisor Assoc. Prof. Dr. M.H. Baluch)

Professional Career

- Abdallah Kamel Consultant Office, Jeddah, Saudi Arabia, Two months training on International Makkah-Madina Highway Project, Summer 1982

- Zuhair Fayez Architectural Office, Jeddah, Saudi Arabia, Two months training on Saleh Kamel Cornich Palace Project, Summer 1983

- Group Leader and Research Assistant for Transportation Survey, Makkah-Jeddah International Highway, Shemaissy Parking Station, Hajj Research Center, King Abdul Aziz University (KAAU), Jeddah, Saudi Arabia, Hajj season 1402 (1982)

- Research Assistant for Transportation Survey, Pilgrimage City of King Abdul Aziz International Airport, Hajj Research Center, King Abdul Aziz University (KAAU), Jeddah, Saudi Arabia, Hajj season 1403 (1983)

- Group Leader for Geo-Economic Sociological Survey of Old Districts of the City of Jeddah, Organized and Sponsored by the College of Engineering and the College of Arts, King Abdul Aziz University (KAAU), Jeddah, Saudi Arabia, Fall 1984

- Research and Teaching Assistant in Civil Engineering Department, King Fahd University of Petroleum and Minerals (KFUPM), Dhahran, Saudi Arabia, (from 1984 to 1988)
  Assisted in the following Applied Engineering Courses :
  Engineering Graphics
  Statics and Mechanics
  Concrete Technology and Materials
  Structural Analysis I & II
  Reinforced Concrete I & II

Computer Knowledge

- Computer Languages :
  BASIC and FORTRAN

- Familiar With :
  Personal Computers
  Main Frame IBM 370
  Interactive Computer Graphics VAX 2